Design and Simulation of Adaptive Low Speed Electro Pneumatic Frontal Impact Absorption System for Crossover Vehicles

By

kaleab Ameneshewa

A THESIS SUBMITTED TO

THE DEPARTMENT OF MECHANICAL SYSTEMS AND VEHICLE ENGINEERING

SCHOOL OF MECHANICAL CHEMICAL AND MATERIALS ENGINEERING

Presented in the Partial Fulfillment of the Requirements for the Award of the Degree of Master of Science in Automotive Engineering

Office of graduate studies

ADAMA SCIENCE AND TECHNOLOGY UNIVERSITY

ADAMA; ETHIOPIA

JUNE 2020

Design and Simulation of Adaptive Low Speed Electro Pneumatic Frontal Impact Absorption System for Crossover Vehicles

By

kaleab Ameneshewa

Advisor: Ramesh Babu Nallamothu (PhD)

A THESIS SUBMITTED TO

THE DEPARTMENT OF MECHANICAL SYSTEMS AND VEHICLE ENGINEERING

SCHOOL OF MECHANICAL CHEMICAL AND MATERIALS ENGINEERING

Presented in the Partial Fulfillment of the Requirements for the Award of the Degree of Master of Science in Automotive Engineering

Office of graduate studies

ADAMA SCIENCE AND TECHNOLOGY UNIVERSITY

ADAMA; ETHIOPIA

JUNE 2020

DECLARATION

I hereby declare that the work which is presented in the thesis entitled “design and simulation of adaptive low speed electro pneumatic frontal impact absorption system for crossover vehicles” in partial fulfillment of the requirements for the award of the degree of Master of Science in automotive engineering is an authentic record of my own work carried out from October 2018 to February 2020 under the supervision of Ramesh Babu Nallamothu (PhD), Department of Mechanical system and vehicle Engineering, at Adama science and technology university, Ethiopia. Any portion embodied in this thesis has not been submitted by me for the award of any other degree or diploma. All relevant sources of information used in this thesis have been acknowledged.

Name	Signature	Date
Kaleab Ameneshewa		
(Candidate)	_____	_____

This is to certify that the above statement made by candidate is correct to the best of my knowledge and belief. This thesis has been submitted for examination with my approval.

Name	Signature	Date
Dr. Ramesh Babu Nallamothu		
(Advisor)	_____	_____

We the undersigned members of the board of examiners of the final defense by Kaleab Ameneshewa Nigussie have read and evaluated his thesis entitled '' Design and Simulation of Adaptive Low Speed Electro Pneumatic Frontal Impact Absorption System for Crossover Vehicles'' and examined the candidate. This is therefore to certify that the thesis has been accepted in partial fulfillment of the degree of master of science in Automotive Engineering.

Name	Signature	Date
Name of student		
Advisor		
External Examiner		
Internal Examiner		
Chair Person		
Head of Department		
School Dean		
Post graduate Dean		

DEDICATION

This paper is dedicated to my family to their continuous and inspirational support through all of my studies.

ACKNOWLEDGEMENT

My first special thank is to the Almighty God for everything he made on me.

I must express my very profound gratitude to my advisor Dr. Ramesh Babu Nallamothu (Ph.D.) Mechanical Systems and Vehicle Engineering Department, Adama science and technology University, Ethiopia. His great inspiration helps and the guide in the right direction was very nice.

I would like to express my deepest thanks to my parents for providing me with unfailing support and continuous encouragement throughout my years of study and through the process of researching and writing this thesis. This accomplishment would not be possible without them.

Finally, I would like to acknowledge my friends for their understanding and help.

TABLE OF CONTENTS

contents **page**

LIST OF TABLES

LIST OF FIGURES

NOMENCLATURE

EA	Energy Absorption
FEA	Finite Element Analysis
SAE	Society of Automotive Engineers
MR	Magneto-Rheological
VIP	Vehicle Impact Protection
V	Volume [m^3]
P	Pressure [Pa]
m	Mass [kg]
A	Area [m^2]
l	Length [m]
Z	Deflection [m]
F	Force [N]
ls	Surge pipe length [m]
ds	Surge pipe diameter [m]
A_e	Effective area [m^2]
v_{bo}	Initial air bag volume [m^3]
v_{ro}	Initial reservoir volume [m^3]
k_{aux}	Auxiliary reservoir stiffness
K_{ez}	Elastic stiffness
$C_{z\beta}$	Velocity over the damper
Kt	Loss factor due to flow in the surge pipe
Cs	Damping caused by flow in surge pipe
mb	Mass resting on the air bag [kg]
g	Gravitational constant [m/s^2]
Ae	Effective area of the air bag [m^2]
P_a	Atmospheric pressure [N/m^2]
R	Specific gas constant, R= Cp - Cv, [J/kg K]
T	Absolute temperature [K]

ABSTRACT

Vehicle frontal low-speed impact causes vehicle frontal component damage and driver injuries. In the conventional vehicle frontal impact protection system, the frontal foam and reinforcing bar reduce the amount of damage and the degree of injuries. It is the fact that heavier opponent needs stiffer structure and lighter opponent needs less stiff structure but those structural components behave similarly in every crash situation, this clearly shows that if the frontal impact protection system behaves adaptively it can fulfill the requirements in both situations. This work deals with the usage of the controlled pneumatic actuator as a low speed and adaptable impact absorber in the vehicle frontal-impact absorption system to create dynamic behavior of impact absorber and achieve sufficient damping during the event of a crash. In this work air spring, the dynamic property is simulated using ABAQUS simulation software, and all-controlling electrical and electro-pneumatic components behavior is animated by using both PROTEUS 8 PROFESSIONAL and ARDUINO and the comparisons is done with the mechanical impact absorber. The result of electro-pneumatic shows a sufficiently good agreement with the physical parameter taken and the controlled system able to execute and take action within 15 microseconds, which is less than the impact duration for low-speed frontal crash and stiffer air spring column is maintained when the severity of the crash is higher by comparing speed and distance between cars and less stiff air spring column is maintained when the severity of the crash is minimum. Finally, it is found that adaptive impact absorption system has the ability to respond for different crash scenario's with in the speed range between 1kph up to 50kph while the mechanical crash absorber takes an impact happened between 18kph up to 43kph.

Keywords: Vehicle frontal protection system, Frontal collision, Air spring, Ultrasonic sensor, Microcontroller

CHAPTER ONE

INTRODUCTION

This chapter consists of the background of the study, statement of the problem, general and specific objectives, the significance of the study, beneficiaries, scope, and organization of the study.

1.1. Background

In the design of an automobile, the most important task is to minimize the occurrence and consequences of automobile accidents. Automotive safety can be improved by "active" as well as "passive" measures. Active safety refers to a technology that assists in the prevention of a crash. Passive safety includes all components of the vehicle that help to scale back the aggressiveness of the crash event. Crash protection priorities are directly proportional to the speed of the car when the crash occurs: at speeds up to 15 km/h, the main goal is to minimize repair costs, at speeds between 15 and 40 km/h, the first aim is to protect pedestrians; at speeds over 40 km/h, the most important concern is to guarantee occupant protection (Ostrowski et al., 2007). The term “Crash Management System” is usually wont to describe the structural module consisting of the bumper and therefore the related attachments which hook up with the longitudinal beams of the car. Front bumpers are connected to the front chassis rail by a separate deformation element ("crash box"). Energy absorbers are loaded in compression or tension also because the bumper moves from a designed outer position toward the vehicle body and is operative to soak up the energy of the impact. (Sakhare et al., 2017).

Pneumatic actuators are devices they use controlled compressed air to create mechanical motion. It gives both linear movement and angular rotation with a simple and continuously variable operational speed of the car. And also, can be used as impact absorbers by controlled restricted flow (Meghana et al., 2016).

1.2. Statement of the problem

In Ethiopia from the year 2010 to 2014 out of the total 14,263 injuries to the road users 5,420 injuries are during low speed accidents. For accidents happened at 50kph 4% are injuries accident, 6.1% are serious accidents and 8.2% are fatal accidents. According to the study there is 10% chance of fatality outcome when the impact is at 30kph in the pedestrian and cyclist impact. In order to increases the pedestrian safety softer frontal impact absorber is required. crash at the speed below 50kph the frontal parts of the vehicle such as radiators, fans, intercoolers and system elements are the second components to take the crash energy after the front structural elements such as bumper fascia, energy absorption foam, reinforcing bars and crash boxes, to protect this elements the crash box and front structural components has to take the impact energy but this structural elements are designed to specific ranges of speed which is the high and low range of low speed impact abortion. But for better protection of the vehicle components the instantaneous speed crash must be absorbed adaptively.

In automobile impact protection system crash protection priorities vary with speed and at different speed range different stiffness improves characteristics of impact absorbers. Energy absorbers currently used in vehicle impact absorption systems are mechanical impact absorbers incapable of varying their stiffness for the different crash scenario but it is clear that a low-velocity crash requires less structural stiffness and high-velocity crash requires relatively high structural stiffness. For compatibility, it is necessary to have a stiffer structure in case of a heavy opponent and a softer structure in case of a lighter opponent and also less stiff front impact absorber increase pedestrian safety.

Most of the crash boxes are mechanical impact absorbers they didn't return to their original position and shape after impact. This plastic failure makes them to not use again as impact protection components.

1.3. Objectives

1.3.1. General Objective

The general objective of this thesis is to design and simulate adaptive low speed electro pneumatic frontal impact absorption system for crossover vehicle.

1.3.2. Specific Objectives

The specific objectives are:

- To design and select pneumatic, and electro-mechanical components
- To select the appropriate position and location on the vehicle for optimum performance of the air spring.
- To prepare part and assembly drawings of the system using solid works software and
- To simulate the effectiveness of the system

1.4. Significance of the study

The significance of the thesis work is the following

- It improves pedestrian safety
- Reduces deceleration pulse because it minimizes impact energy transferring to occupant compartment
- It safeguards under hood components during animal strike and low speed collision
- It makes impact absorber reusable after low speed impact

1.5. Beneficiaries

Auto makers, pedestrians, vehicle owners, and researchers.

1.6. Delimitation (Scope)

In higher speed collision the kinetic energy of the impact is high, and the function of impact absorber is not visible so this thesis is limited to design and simulation of absorber at low-speed impact.

1.7. Organization of the study

This thesis is organized in the following chapters.

Chapter One: **Introduction**, includes background of the project, statement of the problem, specific and general objectives, and significance of the project, beneficiaries, and scopes of the project.

Chapter Two: **Literature Review,** includes the reviewed journals, principles and types of collisions and governing formulas.

Chapter Three: **Materials and Methods**, contains methods, design and analysis of air spring, materials, and simulation.

Chapter Four: **Result and discussion**, includes mechanical and electrical simulation result, and comparison with mechanical crash box.

Chapter Five: **Summary, Conclusion and Recommendation**

CHAPTER TWO

LITERATURE REVIEW

This chapter consists of introduction, literature review, Collision Types, mass and stiffness parameters, damping parameters, rubber properties and manufacturing process and, electrical components and working principle.

2.1. Introduction

The number one concern for drivers and passengers is safety. Automotive safety can be improved by "active" as well as "passive" measures. Active safety refers to a technology that assists in the prevention of a crash. Passive safety features are a system that does not do any work until it is called to action. This feature becomes active during accidents and works to minimize damage and reduce the risk of injuries during times of impact. This system includes seat belts, airbags, and the construction of the vehicle. Frontal construction (Vehicle passive energy absorption system) plays an important role during a frontal crash for both the passengers and vehicle frontal component safety. To do so the frontal structure of the vehicle (bumper system) includes an impact absorption unit to absorb the impact generated during a frontal collision.

Surviving a crash is all about kinetic energy. When the human body is moving, it has a certain amount of kinetic energy. After the crash, when it come to a complete stop, it will have zero kinetic energy. To minimize the risk of injury, you would like to remove the kinetic energy as slowly and evenly as possible. Figure 2.1 shows the basic automotive impact absorption system.

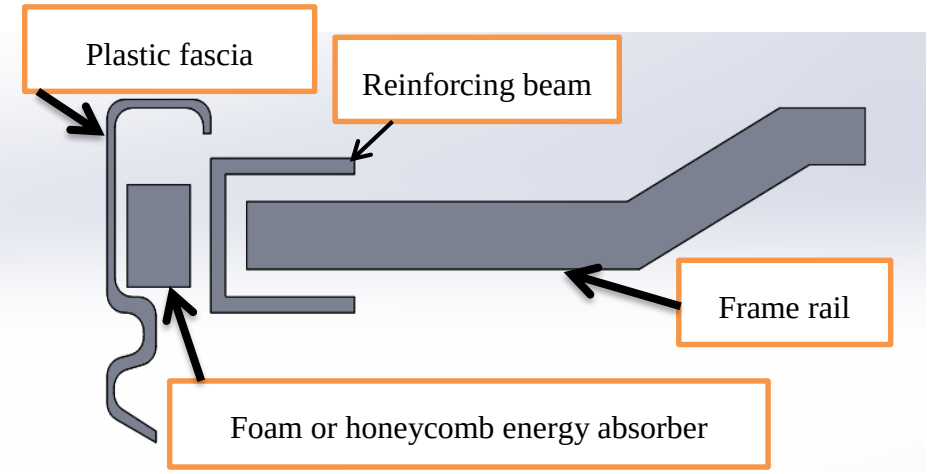

Figure 2.1 Conventional frontal impact absorption system

2.2. Literature review

Sakhare (2017) analyzed chassis impact in real life, frontal collision in which a vehicle runs front to front is considered and the crash is plastic. In collisions among multiple vehicles the crush energy absorbed by each vehicle determines the crash Severity for that vehicle. Finally, the study finds the full and one third collision of vehicle in two cases and find how much energy absorbed on both vehicles and its parts attached with chassis.

Ostrowski et al. (2007) studied about adaptive crashworthiness of front-end structure of motor vehicles. The aim of this research is to present a new concept of adaptive crashworthiness system. Main objectives of the proposed system are to predict, control and adjust the impact characteristics to various conditions by decreasing the pre-designed crushing stiffness of the vehicle frontal deformation zone. According to the initial pre-crash parameters (velocity, mass, stiffness and overlap) the prospective system can select proper crushing force. In most basic approach each absorber has two levels of the crushing stiffness – high and low. De-stiffening feature is driven by pyrotechnic detachable connectors integrated in the frontal car structure, which can be destroyed causing disconnection of selected structural members, excluding them from the energy dissipation process. Pyrotechnical stiffness control can be activated in a very short time, sufficient to act during typical road accidents. Among other things, the presented idea can be used to solve mass compatibility problems. Results presented in this paper show that adaptive frontal structure can help in crash performance optimization.

Meghana et al. (2016) studied about impact analysis of bumper and car chassis frame due to frontal collision for different materials namely aluminium alloy (6061), stainless steel, structural steel and carbon epoxy 2 and total deformation is observed. The strength of the component is determined by identifying the segment or part that the crack will occur or where the concentration of stress is high when force is attached in front of the component. From above result we are concluding that carbon epoxy material is more reliable for car bumper. It's having low deformation and low mass compared to other materials that are used.

Devi et al. (2014) design and simulate crash box in car, in the design of automobile almost important task is to minimize the occurrence and consequences of automobile accidents. There are many existing technologies like airbags, seatbelts etc., which are still not that effective. And now, here is another trail in the process and it is Crash box. Absorbing the kinetic energy that drops

from a high speed to zero after the crash is the key in this case. In this report, attention is focused upon finding an optimum cross-sectional shape of a crash box to ensure high capability for energy absorption without crash bead. And finally, a new design scheme of cross-sectional shape of a crash box was proposed.

Sharma et al. (2016) made design optimization of vehicle components for full frontal crash. Vehicular passive energy absorption plays an important part during frontal crash for passenger safety. Optimization of the frontal components is the key to increasing energy absorption due to large parameters. A full-frontal crash of Volvo V40 model has been done in this project using ANSYS Explicit Dynamics module. Simplified geometry to represent major energy absorption mechanism of the individual components involved in frontal crash have been modeled on ANSYS modeler and analyzed under standard test conditions. The components considered for optimization are bumper cover stiffener, energy absorber, and bumper cross-beam and chassis longitudinal member. MOGA and NLPQL implemented in ANSYS is utilized to optimize the geometries for individual components to give maximum energy absorption. The optimized geometry of each component was finally assembled together and analyzed again in under the same conditions.

Nasiruddin et al. (2017) reviewed energy absorption of automotive bumper beam, energy absorption during an impact is very important in automotive bumper system. Bumper beam is one of the main parts in bumper system which is used as protection for passengers and frontal compartment of a car during impact. This paper is carried out in order to determine the factors that affecting energy absorption of automotive composite bumper beam.

Balamurugan et al. (2017) studied about design of shock absorber for car front bumper. Automotive designs with economy, safety and aesthetics have been a great challenge to design engineers. Automobile bumper subsystem is the front and rear structure of the vehicle that has the purpose of energy absorption during low velocity impact. This Project deals with the idea of Hydraulic shock absorber using bumper in the front overhang of the four-wheeler, which reduces the loss and deformation of the vehicle during the accident. It includes Hydraulic fluids and shock absorber spring as an active component in the Impact reducing system. This Project model built using the CATIA V5 R20 Software. But in this paper the shock absorbing unit is mechanical impact absorber.

Jain et al. (2016) presented about the proof of concept design of a novel 4-stage collision energy absorption system mounted in the front overhang of passenger cars such as the regular sedan and hatchback segments with a seating capacity of five. The four stages comprise of a conventional bumper, magneto-rheological (MR) damper, open coil helical spring, and a shear plate assembly. During collision, a large amount of force will be transmitted in a very short duration, causing huge damage compared to gradual loading. In this work, a novel system is proposed for reduction of shock and impact in case of a frontal collision.

Ghasemnejad et al. (2008) discussed about crashworthiness of thin-walled corrugated crash box in axial crushing. In this paper the crashworthiness capabilities of thin-walled corrugated crash boxes in axial crushing relative to flat sidewall boxes from the same material are investigated. In order to achieve this, various design of corrugated aluminum alloy 6060 temper T4 crash boxes were chosen and their axial crushing behavior under impact loading was studied by developing a theoretical model based on Super Folding Element theory and by conducting finite element analysis using LS-DYNA in ANSYS. From the theoretical and FE analysis the crush force efficiency, the specific energy absorption and the frequency and amplitude of fluctuation of the dynamic crush force of the corrugated crash boxes were calculated and the results were compared with the reference corrugated model. It was shown that the corrugated crash boxes have advantages of a lower initial collapse force, a lower crush force fluctuation frequency and amplitude relative to a flat sidewall box. But the crash box after impact never used again.

Nagel et al. (2002) showed energy absorption and performance of a vehicle impact protection system. Current developments include initial review and selection of suitable Energy Absorbing (EA) mechanisms for use in the VIP, physical testing is being used to assess the energy absorbing capacity of the EA mechanisms under quasi- static and dynamic loading. Finite Element (FE) simulations are being used to validate such tests and compare the behavior of these mechanisms in a frontal impact. This paper present research's having passive impact absorbers and discuss the findings.

Nunes (2017) discussed about multi-objective design optimization of a frontal crash energy absorption system for a road-safe vehicle, this work focused on the development of an aluminum structure of this type, aiming for an optimized design, within the design parameters available for the vehicle project in which it is included. A Finite Element Analysis (FEA) model of the frontal

energy absorption structure for frontal impact is developed and validated with a quasi-static compression experimental procedure. A multi-objective optimization process, that can be adaptable to the future needs of the project, is developed. Several changes in the geometry are tested, focusing on specific deficits in the performance of the structure. Through this process, a robust and adaptable FEA model is achieved and a compilation of the influence of several parameters on the impact performance is obtained. The optimized structure shows a significant performance improvement in the event of a frontal collision and, according to the established limits, it is expected to satisfy the legal values of safety in the tests carried out by the responsible entities. The energy absorption unit never used again after impact.

Jie et al. (2014) discussed influence of material properties on automobile energy-absorbing components crashworthiness in cities traffic jam, automotive accident often occurs to low-speed and behind or angle collisions. No attention is paid to the low speed crashed for no personnel injury. Therefore, it is quite necessary to study the technical problems of the car involved in low velocity impact. In low velocity impact accident, the automobile energy absorbing component is expected to be collapsed with absorbing crash energy prior to other body parts so that the damage of the main cabin frame is minimized and passengers may be saved. The automobile energy-absorbing component equipped at the front end of car, is one of the most important automotive parts for crash energy absorption. The automobile energy-absorbing component (a kind of thin walled metal tube) at low velocity impact was studied, and material properties on automobile energy -absorbing components crashworthiness were proposed. However, the energy absorption unit is not adaptable for different crash scenario.

Chen et al. (2015) discussed vehicle front structure energy absorbing optimization in frontal impact energy absorption performance is one of the most important indexes in the vehicle safety during impact. Research on the car frontal structure energy performance and structure optimization was conducted in this paper. Whole vehicle model was established by Hyper Mesh and simulated in LS-DYNA. Simulation results indicated that modification was need for the original structure to meet requirement. Based on simplified whole vehicle model, orthogonal design optimization was implemented, including bumper cross beam material (A), bumper cross beam thickness (B), energy absorber groove distance (C), and front longitudinal beam groove number (D), with 3 levels for each factor. The best option was B3D1A3C3 was gained by using range analysis and integrated

balance method. Simulation results showed that both front and total energy absorption were improved. The optimized structure increased front energy absorption to 51.1%, which can meet the industry requirement. Effect of the system on Pedestrian safety didn't studied.

Griskevicius (2007) adaptive crashworthiness of front-end structure of motor vehicles presented, the aim of this research is to present a new concept of adaptive crashworthiness system. Main objectives of the proposed system are to predict, control and adjust the impact characteristics to various conditions by decreasing the pre-designed crushing stiffness of the vehicle frontal deformation zone. According to the initial pre-crash parameters (velocity, mass, stiffness and overlap) the prospective system can select proper crushing force. In most basic approach each absorber has two levels of the crushing stiffness – high and low. De-stiffening feature is driven by pyrotechnic detachable connectors integrated in the frontal car structure, which can be destroyed causing disconnection of selected structural members, excluding them from the energy dissipation process. Pyrotechnical stiffness control can be activated in a very short time, sufficient to act during typical road accidents. Among other things, the presented idea can be used to solve mass compatibility problems. Results presented in this paper show that adaptive frontal structure can help in crash performance optimization, by adjusting system properties to the various conditions of impact scenario. Decrease of the front-end crash stiffness of a striking vehicle and extension of the crushing distance can decrease occupant risk through limited side intrusion and improved deceleration pulse shape, comparing to passive systems. However, system response for instantaneous velocity is not considered and analyzed.

Woo et al. (2007) discussed frontal crash mitigation using MR impact damper for controllable bumper and performance characteristics of a magnetorheological (MR) impact damper for controllable bumper in vehicle systems. Recently, several mechanisms are proposed in order to minimize the injury of vehicle occupants during frontal collision. One of the promising candidates is the MR fluid which undergoes significant instantaneous reversible changes in material characteristics when subjected to a magnetic field. Using this salient property, a new type of MR impact damper is devised in this work. The proposed damper is integrated with bellows to induce the flow motion and the motion is operated under flow mode. The field-dependent damping force is evaluated by computer simulation with various conditions. The lower speed head-on collision stiffness of MR flued didn't improve pedestrian's safety.

Deshmukh et al. (2006**)** showed adaptive energy-absorbing materials using field-responsive fluid-impregnated cellular solids. Adaptive materials with rapidly controllable and switchable energy-absorption and stiffness properties have a number of potential applications. We have developed, characterized and modeled a class of adaptive energy-absorbing systems consisting of nonlinear poroelastic composites wherein a field-responsive fluid, such as a magnetorheological fluid or a shear-thickening fluid, has been used to modulate the mechanical properties of a cellular solid. The mechanical properties and energy-absorbing capabilities of the composite are studied for variations in design parameters including imposed field strength, volume fraction of the field-responsive fluid within the composite and impact strain rates. The total energy absorbed by these materials can be modulated by a factor of 1- to 50-fold for small volume fractions of the fluid (∼15%) using moderate magnetic fields varying from 0 to 0.2 T. A scaling model is also proposed for the fluid–solid composite mechanical behavior that collapses experimental data onto a single master curve. The model allows optimization of the composite properties in tune with the application requirements. Potential application areas are discussed with emphasis on applicability in impact-absorbing headrests and cushioned assemblies for energy management. The lower speed head-on collision stiffness of MR flued didn't improve pedestrian's safety.

Witteman et al. (1999) studied the necessity of an adaptive vehicle structure to optimize deceleration pulses for different crash velocities. To minimize injury to the occupants, the frontal vehicle structure must absorb much more energy in the first deformation phase in case of a high-speed collision. Depending on the crash situation an intelligent system must regulate the structure stiffness yielding additional energy absorption by means of friction. Concept ideas are mentioned to achieve different crash pulses at different crash velocities within the available deformation length. An independent search for optimal deceleration pulses at several crash velocities is necessary, because the usually found structure-based pulses are not obviously the optimal pulses for minimal injury to the occupants. Therefore, in this paper the more interesting case of the reverse question is answered: which crash pulse gives the lowest injury levels with an already optimized restraint system, instead of finding the optimized restraint system for a given crash pulse. For this research, a method is described in which a numeric model of an interior and a FEM dummy has been used to find the levels of the injury criteria. To compare the results of different crash pulses, an overall severity index has been used. From a described research an optimal pulse has been found after several considered pulse variations at a crash speed of 56 km/h. This pulse, used as example,

gives as it seems much lower injuries. During the first 18 cm deformation length the deceleration level must be high, then a low deceleration interval is required, and at the end (dummy is restrained by belt and airbag) the deceleration must be high again. Also, for other crash velocities, pulses are mentioned with adapted pulse characteristics for optimal results. And also

He discussed possibilities to design an adaptive vehicle structure that can change the stiffness real time for optimal energy absorption in different crash situations. It is necessary to have a stiffer structure in case of a heavy opponent and a softer structure in case of a lighter opponent. And Friction is found as the best controllable way for adaptable energy absorption. In a proposed new concept design the right amount of energy could be absorbed by means of friction generated by hydraulic brakes on two rigid backwards moving beams. In case of an offset or oblique crash a mounted cable system moves the missed beam backwards. With this new intelligent design with interactive control, an optimal vehicle deceleration pulse can be possible for each crash velocity independent on the struck car position.

Campos et al. (2015) studied steel energy absorption system for heavy quadricycles and nonlinear explicit dynamic analysis of its behavior under impact by FEM. Current knowledge of the behavior of heavy quadricycles under impact is still very poor. One of the most significant causes is the lack of energy absorption in the vehicle frame or its steel chassis structure. For this reason, special steels (with yield stresses equal to or greater than 350 MPa) are commonly used in the automotive industry due to their great strain hardening properties along the plastic zone, which allows good energy absorption under impact. This paper presents a proposal for a steel quadricycle energy absorption system which meets the percentages of energy absorption for conventional vehicles systems. But these steel structure cannot be used for low speed impact absorption.

2.3. Collision Type

Collision type is the most important factor governing vehicle performance since it determines how the two car's structures will interact. For this reason, collision type will have a modifying influence on the effect of other parameters such as geometry and stiffness. For example, the effective global stiffness of a vehicle changes significantly from a full-frontal impact to frontal offset impact. In this example, the differences in effective stiffness between the two collision types are attributed to

the specific structures used for energy absorption and the modes by which they fail (Devi et al. 2014).

There are five major types of motor vehicle collisions

1. Head-on
2. Rear-end
3. Lateral
4. Rotational
5. Roll-over

2.3.1. Head on collision

The vehicle has hit a utility pole in the center of the car. The impact point stopped its forward motion, but the rest of the car continued forward until the energy was absorbed by the bending of the car. Head on collision is shown in figure 2.2.

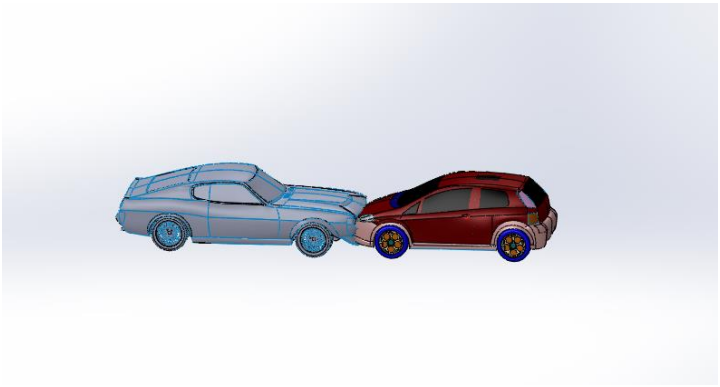

Figure 2.2 Head-on collision

2.3.2. Rear Impact

Rear-impact collisions occur when a slower-moving or stationary vehicle is struck from behind by a vehicle moving at a faster rate of speed. Figure 2.3 shows the rear impact.

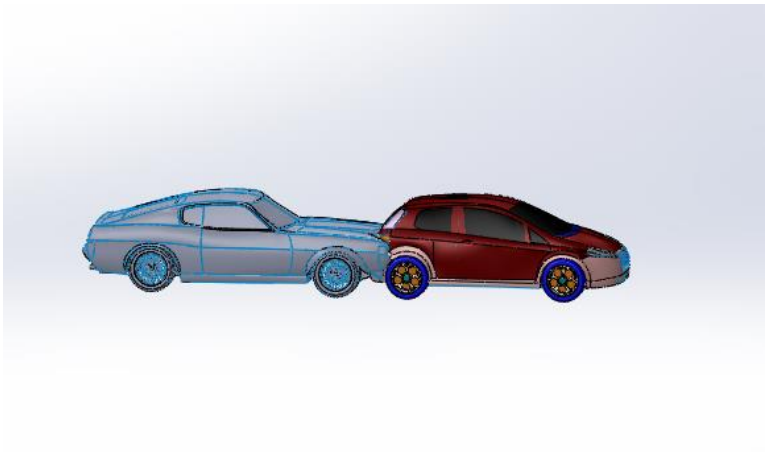

Figure 2.3 Rear end impact

2.3.3. Lateral Impact

Lateral-impact mechanisms come into play when the vehicle is involved in an intersection collision or when the vehicle veers off the road and impacts sideways utility pole, tree, or other obstacle on the roadside. Figure 2.4 shows the lateral impact.

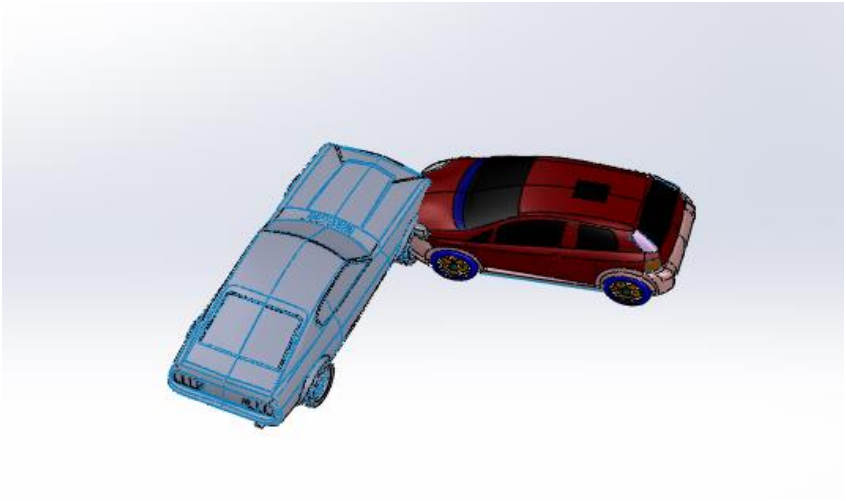

Figure 2.4 Lateral Impact

2.3.4. Rotational Impact

Rotational-impact collisions occur when one corner of a vehicle strikes an immovable object, the corner of another vehicle, or a vehicle moving slower or in the opposite direction of the first vehicle. The rotational impact is shown in figure 2.5.

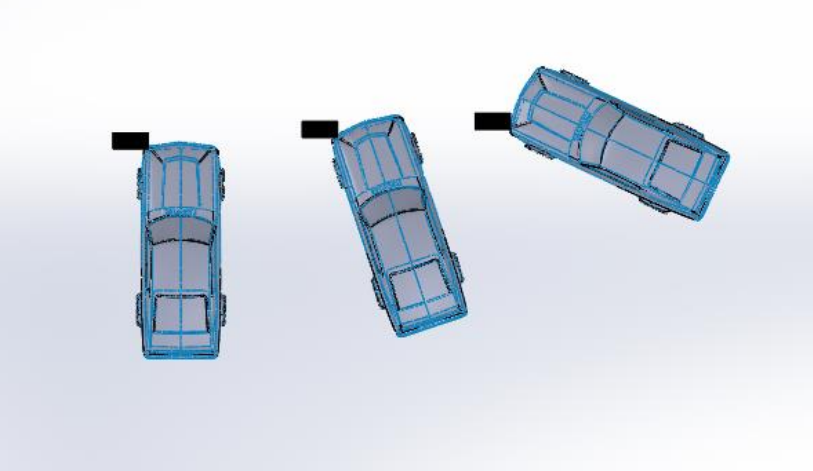

Figure 2.5 Rotational Impact

2.3.5. Rollover

During a rollover, a vehicle may undergo several impacts at many different angles, as may the unrestrained occupant's body and internal organs figure 2.6 shows the rollover crash.

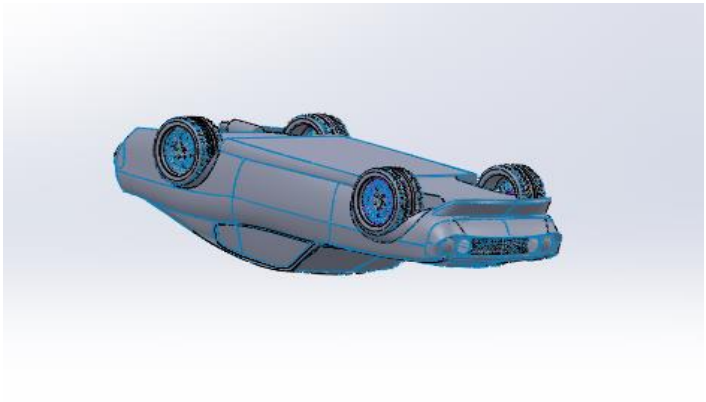

Figure 2.6 Rollover

2.4. Geometry

Car structures are designed to perform a multitude of functions as well as good crashworthiness. As a consequence, car fronts often have local areas of stiff structure within a much larger area of weaker structure. Due to this lack of stiffness uniformity it is usual in a car to car frontal impact, for the stiff parts of one vehicle to penetrate the weaker parts of the other. This may result in penetration fork effect or over-ride, since in these situations the vehicle's energy absorbing structure is ineffectively used; higher occupant compartment intrusions are often observed.

2.5. Mass and Structural Stiffness

The effects of mass and mass ratio on injury risk have been studied for many years and dominate the literature on compatibility. There is plenty of evidence that in car to car impacts the risk of injury in the heavier car is lower than that in the lighter car

Stiffness and mass parameters of air spring

The elastic stiffness of air spring and mass

$$K_{ez} = \left(\frac{1}{\frac{p_0 A_{e^2} n}{V_{b0}+V_{r0}} + P_g \frac{dA_e}{dz}} + \frac{1}{K_{aux}} \right)^{.-1} \quad (2.1)$$

Where: -

K_{ez} is stiffness for elastic part N/m

P_0 is the initial pressure

A_e is the effective area of the air bag (m^2)

d_s is the surge pipe diameter (m)

z is deflection

n is the polytrophic constant.

K_{aux} stiffness of auxiliary spring

V_{bo} is initial air bag volume

V_{ro} is initial reservoir volume

$$K_{vz} = \left(\frac{1}{\frac{p_0 A_{e^2} n}{V_{b0}} + P_g \frac{dA_e}{dz}} + \frac{1}{K_{aux}} \right)^{.-1} - K_{ez} \quad (2.2)$$

Where: -

K_{vz} vertical stiffness N/m

K_{ez} is stiffness for elastic part N/m

P_0 is the initial pressure

A_e is the effective area of the air bag (m^2)

d_s is the surge pipe diameter (m)

z is deflection

n is the polytrophic constant.

K_{aux} stiffness of auxiliary spring

V_{bo} is initial air bag volume

V_{ro} is initial reservoir volume

$$M= 1_s A_s P\left(\frac{A_e}{A_s}\frac{V_{r0}}{(V_{b0}+V_{r0})}\right)^2 \quad (2.3)$$

Where: -

M is mass(kg)

l_s is the surge pipe length (m)

A_e is the effective area of the air bag (m^2)

P pressure (N/m^2).

V_{bo} is initial air bag volume

V_{ro} is initial reservoir volume

2.6. Damping of air spring

The pneumatic spring is a column of confined gas in a container designed to utilize the pressure of the gas as a force medium of the spring. The compressibility of the gas provides the desired elasticity. The spring rate is the result of a change in the effective area and the change in gas pressure as the spring is deflected. The gas pressure varies with the speed and magnitude of deflection; for a unit of deflection, the pressure and therefore, the spring rate will be different for isothermal, adiabatic, or polytropic processes. To absorb the impact in the pneumatic system is about creating throttle flow. In the air damping, there are two pressure chamber one is equal to the air spring internal pressure and the other is at atmospheric pressure. Assume two chambers are connected through a throttle valve, The Damping is carried out by the change of the total air volume V and the damping by the throttle flow from one chamber to another through the valve. The desired dissipated energy is not caused by the air internal friction in the valve but only down to the valve.

$$C_s = \frac{1}{2}. P_0 .K_t A_s, \text{ if } \beta \text{ is } 2. \quad (2.4)$$

Where: -

C_s is damping caused by the flow in the surge pipe

k_t is the total sum of the loss coefficients in the surge pipe

P_0 is the initial pressure

2.7. Manufacturing process of rubbers

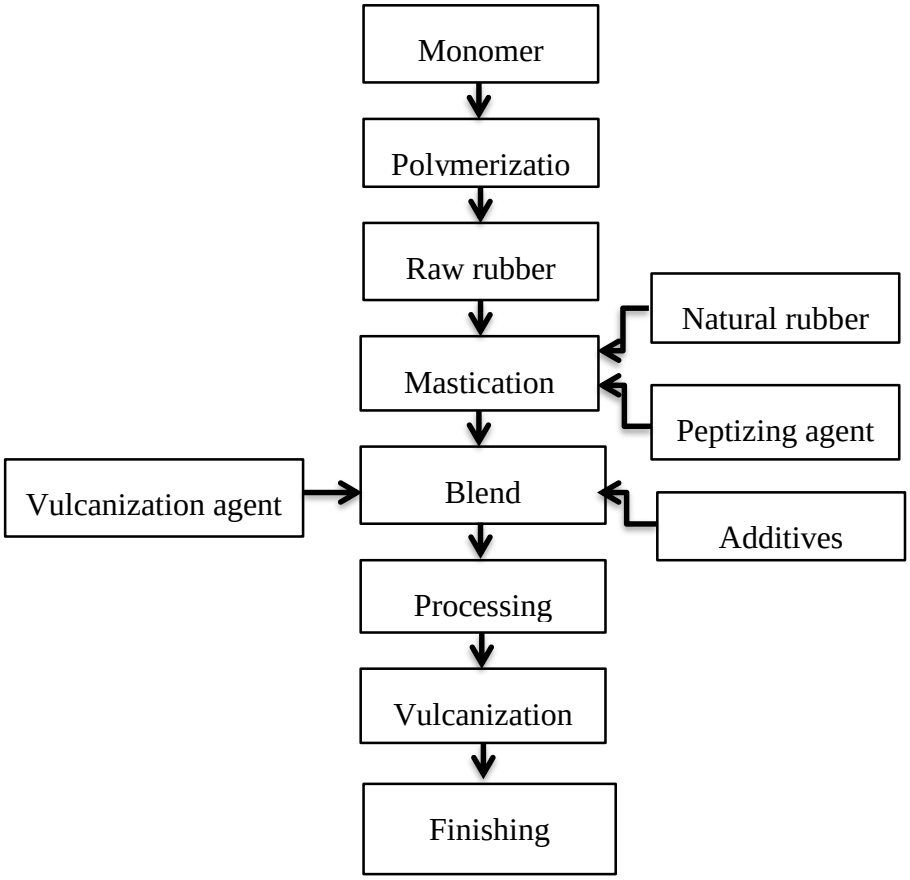

Figure 2.7 Manufacturing process of rubbers

As indicated in figure 2.7 The manufacturing process of synthetic rubber starts with the manufacturing raw rubber. The first step in this process is polymerization. This is a chemical reaction in which small molecules (monomers) are joined together to form large molecules (polymers).

Natural rubber is collected in ready polymerized form. Thus, the manufacturing process of natural rubber starts by mastication. Mastication is a process in which molecules are physically or chemically shredded to make mixing and processing easier. Mastication makes the rubber softer.

Most synthetic rubbers do not need mastication because they are made of shorter molecules. A peptizing agent prevents reactions between the broken chains.

Additives may be for instance fillers and vulcanization agents. The purpose of additives is to improve properties or process ability. Rubbers can be processed in many ways (e.g. by compression molding, injection molding and extrusion). During the process or after it the rubber is vulcanized (cross-linked), due to which rubber elasticity and dimensional stability appear. After processing and vulcanization, the rubber product often has to be finished e.g. by cutting.

2.8. Behavior of elastomers

The predominant property of elastomers is elastic recovery after deformation in compression or tension. Even after stretching an elastomer to many times its original length, under ideal circumstances it will return after removal of the tension to its original shape and length. In addition, elastomers are characterized by great toughness under static or dynamic stresses, by better abrasion resistance than that of steel, by impermeability to air and water and in many cases by high resistance to swelling in solvents and attack by chemicals. Like many other polymers, Elastomers show viscoelastic properties, which nowadays can be tailored for numerous special applications, e.g. tyres, vibration and shock isolation and damping. These properties are exhibited over a wide temperature range and are retained under various climatic conditions and in ozone-rich atmospheres.

Rubbers are also capable of adhering to most other materials, enabling different hybrid constructions. By joining elastomers to metals, components which combine the elasticity of elastomers with the rigidity of metals can be achieved. The force that induces the recovery of deformed rubber is dependent on the entropy of the rubber material.

2.9. General properties of elastomers

The property profiles of elastomers depend mainly on the choice of the particular rubber, the compound composition, the production process and the shape and design of the product. Moreover, the type of loading, e.g. whether it is static or dynamic, strongly influences elastomer properties. Satisfactory properties can be obtained only by proper compounding of elastomers with chemicals and additives, and by subsequent vulcanization in appropriate conditions. Depending on the type and amount of rubber chemicals and additives in a compound, and depending on the degree of

vulcanization, a given rubber can yield vulcanize with considerably different properties with respect to hardness, elasticity or strength.

2.9.1. Thermal expansion

The degree of thermal expansion of different rubbers varies considerably depending e.g. on the elastomers and fillers and their properties in the rubber compound. Generally speaking, the linear thermal expansion coefficient of elastomeric materials is five 5 to 20-fold compared with e.g. that of steels. Consequently, the heat shrinkage of molded elastomer products can be several percent.

2.9.2. Hardness

The hardness of rubber is determined and measured based on the protrusion depth of a standardized body under well-defined conditions. Hardness measurement is one of the most frequently measured properties of rubbers. Hardness is commonly quantified using the IRHD or Shore 0 to100 scales. The hardness of a conventional elastomeric product is around 50 to 70 IRHD.

2.9.3. Tensile properties

In order to obtain tensile material properties, it is customary to define the stress which is required for a certain deformation, strain. Frequently, the stress values corresponding 100 or 300 % deformation are chosen to describe tensile stiffness (s 100 or s300 modulus). The modulus at the early stage of the tensile test is called Young's modulus. The stress at the breaking point of the sample is defined as tensile strength (MPa) and the breaking deformation compared to the original length is defined as elongation at break (%). The values of the tensile strength of rubbers and thermoplastic elastomers are taken as satisfactory/good on the range 7 to15 MPa, and as excellent when the values are over 15 MPa. The values of elongation at break vary in the range 300 – 1000 %.

2.9.4. Modulus of elasticity

As mentioned above, the force is measured which corresponds to a certain strain and is calculated to correspond to the original cross-sectional area. This stress value is a measure of the stiffness of a rubber sample and one of the most important measures for the evaluation of vulcanizes. The stress value is often called modulus. The statistical mechanical theory of rubber elasticity gives the following equation for the force and stress:

$$\sigma = \left(\frac{\rho RT}{M_c}\right)\left(\lambda^2 - \frac{1}{\lambda}\right) \quad (3.1)$$

Here R is general gas constant, T is the absolute temperature, Mc is the number average molar mass of the chain segments between the cross-links of rubber, l is the relative elongation (L/Lo) and r is the density.

The modulus

$$\left(\frac{\rho RT}{M_c}\right) \quad (3.2)$$

Shows that tension increases with rising temperature and an increasing degree of cross-linking (decreasing Mc), In addition, the stress depends on deformation speed and the form of the deformed body. The shape of the body is typically described by shape factor S.

2.9.5. Tear strength

Tear strength is defined as the resistance force which a rubber sample, modified by cutting or slitting, offers to the propagation of the tear. A multitude of test specimen configurations have been presented for tear test.

The force (kN) requires to tear the sample divided by the thickness (m) of the sample is defined as the value of tear strength. Also, the tear energy - which is largely independent of sample geometry, has gained importance in material evaluation.

The values for the tear strength of elastomeric materials with good tear properties are in the range 50-100 kN/m, and values over 100 kN/m are excellent. Natural rubber is one of the best elastomers in this respect.

2.9.6. Permanent set, relaxation and creep

Permanent set is a measure of the viscous behavior of elastomers. The set can be either of the compression or tension type.

The compression set CS, and also the tensile set, is given at constant deformation by the relation,

$$CS = \frac{h_0 - h_2}{h_0 - h_1} \quad (3.4)$$

Where h_o is the initial height of the sample before deformation, h1 is the height during deformation and h2 the height a certain time after deformation. Frequently, the samples are stored in the compressed state at an elevated temperature in order to simulate the requirements of gasket materials where changes due to aging effects play a role.

Relaxation and creep express the time dependence of the stress or the deformation. During the relaxation test the strain is kept constant and the change in stress is monitored, while during the creep test the stress is kept constant and the time dependent strain is measured. The stronger the viscous component, the more pronounced relaxation or creep is.

2.9.7. Abrasion resistance

Abrasion resistance describes the durability of materials under wearing conditions. Most rubbers have exceptionally good abrasion resistance, which is a consequence of the ability of rubbers to creep over the irregularities of the wearing counterpart in sliding. Good wearing resistance is typically achieved with vulcanized general-purpose rubbers, NR, IR, SBR and BR. In an environment exposed to oil, polychloroprene (CR) and nitrile rubber (NBR) are the rubbers with best abrasion resistance. Buthyl and ethylene-propylene rubbers, on the other hand, have the best abrasion resistance at elevated temperatures.

2.9.8. Resilience and hysteresis

The ratio of stored, reversible energy in deformation to dissipated energy is termed resilience. Resilience can be easily evaluated using modern dynamic mechanical analyzers. Since the mechanical energy dissipated during dynamic loading is transformed into heat due to molecular friction, the viscous component may be measured directly by monitoring the increase in heat in the sample (heat build-up).

The energy dissipation property of rubbers is often called also internal dampening or hysteresis loss. The hysteresis loss of rubbers depends quite strongly on temperature and loading amplitude, and is typically of the order of 5to 40 %.

2.9.9. Electrical properties

Most general-purpose elastomers like natural rubber (NR) and a variety of synthetic elastomers (e.g. SBR, IR, BR, EPDM, IIR, and MQ), exhibit very low electrical conductivity and are therefore suitable as electrical insulating materials.

2.9.10. Chemical endurance

Some fluids can cause big volume changes in rubbers which derive from the infiltration of the fluid into the macromolecules (swell) or from the dissolving of rubber ingredients in the fluid (shrinkage). Water, acids and bases may also bring about some hydrolysis in certain rubbers, leading to impairment of tensile properties. Nitric acid and concentrated hydrochloric acid react with most rubbers and leads them to deteriorate.

2.9.11. Ozone and weathering resistance

A deformed rubber with strained parts often becomes cracked outdoors because the double bonds of macromolecules are broken by oxygen, ozone or electromagnetic radiation. Adding anti-aging agents, such as waxes, antioxidants and anti-ozonants, can at least partially prevent such damage.

2.9.12. Dynamic properties

Elastomers are viscoelastic materials. It means that part of the deformation is recovered after the load is removed and part of the deformation is permanent. Dynamic properties of elastomers depend on temperature, type frequency of loading and amplitude of deformation. Also shape of the product effects on dynamic properties.

2.9.13. Natural Rubber (NR)

Natural rubber can be isolated from more than 200 different species of plants. Commercially significant source of natural rubber is Hevea Brasiliensis. Natural rubber is obtained from latex, which is the emulsion of cis-1,4-polyisoprene and water. Latex is obtained from the tree by tapping the inner bark and collecting the latex in cups. A stabilizing agent, such as ammoniac, can prevent too early coagulation. The operating temperature range for NR is -55...+70 °C.

Advantages of NR

- Good process ability
- Excellent elastic properties

- Good tensile strength
- High elongation
- Good tear resistance
- Good wear resistance
- Little dissipation factor - low heat build-up in dynamic stress
- Excellent cold resistance
- Good electrical insulator
- High resistance to water and acids (not to oxidizing acids)

Disadvantages of NR:

- Poor weather and ozone resistance
- Restricted high temperature resistance (short-time maximum temperature 100°c)
- Swelling in oils and fuels: low oil and fuel resistance
- Unsuitable for use with organic liquids in general (even though vulcanization considerably improves swelling resistance), the major exception being low molecular weight alcohols

Applications:

- Tires (60 - 70%)
- Tubes, conveyor belts and v-belts
- Coatings
- Gaskets
- Latex products
- Footwear
- Adhesives

2.10. Steel

Steel is an alloy consisting mostly of iron, with carbon content between 0.2% and 2.1% by weight, depending on the grade. Steel contains less carbon than cast iron (2.1% to 4%), but considerably more than wrought iron (less than 0.08%). Basic carbon steels are alloyed with other elements, such as chromium and nickel, to increase certain physical properties of the metal. Steel can be machined, welded, and forged, all to varying degrees, depending on the type of steel.

Steels and other metals are classified based on method of manufacture, method of shaping, method of heat treatment, properties, intended use, and chemical composition.

In addition, certain steels and other metals are often referred to by trade names. Probably the most reasonable way to classify steels is by their chemical composition. Steels that derive their properties primarily from the presence of carbon are referred to merely as “steels” or sometimes as “plain carbon steels.” Steels that derive their properties primarily from the presence of some alloying element other than carbon are referred to as “alloys” or “alloy steels.”

2.11. Air spring control

2.11.1. Ultrasonic sensor

Ultrasonic sensors are a type of sensors used to measure the distance of an object from the point the sensor is placed. Ultrasonic waves are sounds with frequencies higher than 20 kHz which is not heard by humans. The theory on the principle of measuring the reflection time.

The transducer in ultrasonic sensor releases a wave pulse and receives back the reflection (echo).

Ultrasonic sensor has two modules those are transmitter module and receiver module.

Features of ultrasonic sensor

- Colors didn’t influence detection

Unlike photo electric sensors this type of sensor can detect an object without being influenced by colors. Even if the object is transparent the sensor is capable of sensing it.

- Detecting objects over a wide area

These types of sensor can able to detect reflection from a wider area than photoelectric sensor, so they can check a wide area all at the same time.

- None contact detection

This sensor detects an object without physical contact so there will be no mechanical damage in sensing object.

The distance of an object can be calculated by using

$$d=\frac{t*c}{2} \quad (3.5)$$

Where: -

d=distance of an object

t=time delay between wave emission and echo reception

c=ultrasonic sound velocity (m/s)

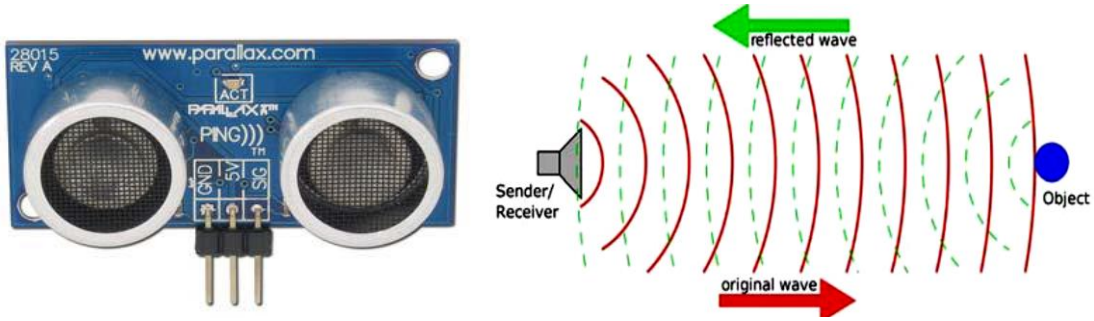

Figure 2.8 Ultrasonic sensor (www.paraliax.com)

- Ultrasonic sensor working principle

As shown in figure 2.8 & 2.9 first the sensor sends 20 kHz sound which is not heard by human by its ultrasonic speaker and wait to measure the time it takes the echo to return to its ultrasonic microphone, when the sensor detects the echo with its ultrasonic microphone it changes that high signal back to low. The time measurement is how long it took the released sound to reflect back to the receiving module.

The ultrasonic pulse is generated using a piezoelectric transducer and echo reflected by the ground is received by another piezoelectric transducer. Both the pulse transducer and receiver are mounted close to each other to make up the measuring head.

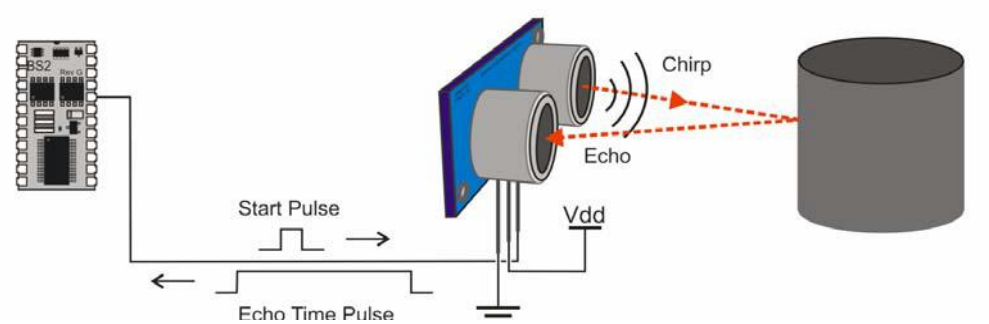

Figure 2.9 Ultrasonic sensor working principle (www.paraliax.com)

$$u(D) = \sqrt{(k * T_f)^2 * u^2(V_s) + (k * V_s)^2 * u^2(T_f)} \quad (3.6)$$

2.11.2. Pressure sensor

Pressure is one of the most important physical parameters in fluid operation, and it is the force exerted on a unit of area.

Working principle

An electronic pressure sensor relies on a physical reaction to applied pressure, then measuring the resulting proportional change electronically. Commonly used phenomena include changes in capacitance, or changes in ohmic resistance of a strain gauge or piezoelectric element, which are proportional to the magnitude of the deflection when pressure is applied.

Mainly there are two types of pressure sensor those are

- Capacitive pressure sensor and
- Piezoresistive pressure sensor

Capacitive pressure sensor

This type of pressure sensor works based on measurements of capacitance from two parallel plates. The capacitive pressure transducer relies on capacitance change produced by deflection of the membrane, which alters the capacitor geometry. The various components of the is shown in the figure 2.10.

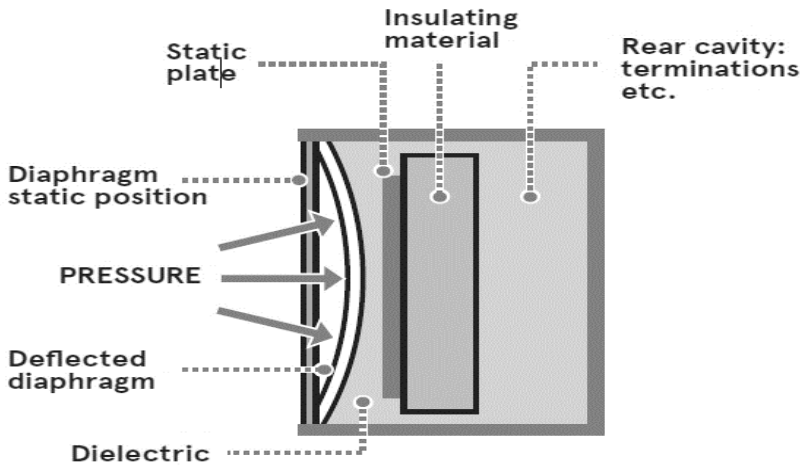

Figure 2.10 Capacitive pressure sensor (www.fierelectronics.com)

$$c = \frac{\varepsilon A}{d} \tag{3.7}$$

Where: -

A = area of plates

d = distance between two plates

Because of the above working principle the response of these types of pressure sensors is none linear; to compensate this external processor is required.

Piezoresistive pressure sensor

As indicated in figure 2.11 these types of pressure sensor work based on Piezoresistive properties of silicon and other materials such as si, Ge, and metals. Piezoelectric sensors use an element made of a material which generates electrical energy when they are under strain, such as quartz or tourmaline. Crucially, they only produce energy when the pressure changes, and are therefore suitable only for dynamic pressure measurements. They are also susceptible to shock and vibration.

Piezoresistivity is caused by two factors

1. Geometry deformation
2. Resistivity changes

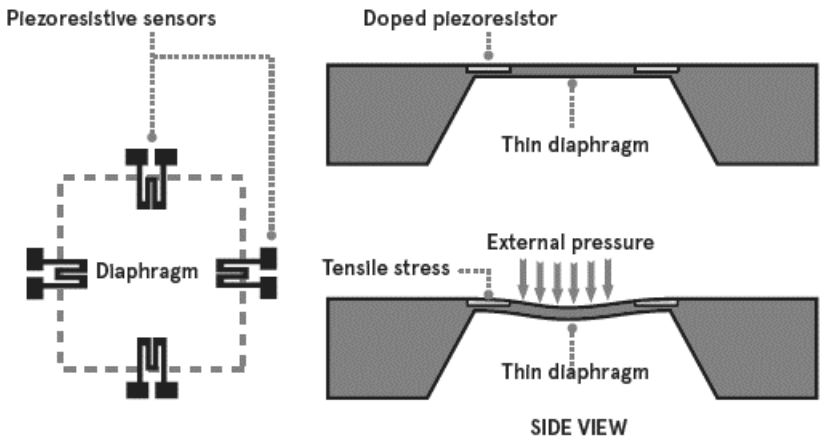

Figure 2.11 Piezoresistive pressure sensor (www.blog.first-sensor.com)

Voltage output or sensor signal is the product of input voltage and alter in resistance.

$$V_{out} = I_{in} * \Delta R \qquad (3.8)$$

As you see within the above picture constant Source Bridge is employed to urge linear output and it shows how the sensing elements of a bridge-type pressure sensor are attached to a versatile diaphragm.

Basic working rule

- Basic working rule

A pressure sensor converts changes in pressure of a gas or a liquid into an electrical signal by means of a pressure sensing device, and generates an analog output proportional to the pressure or a switching output which operates at the specific pressure.

Pressure is sensed by mechanical elements like plates, shells, and tubes that are designed and constructed to deflect when pressure is applied. This is often the essential mechanism converting pressure to physical movement. Next, this movement must be transduced to get an electrical or other output. Finally, signal conditioning could also be needed, counting on the sort of sensor and therefore the application.

- Sensing Elements

The main sort of sensing elements are Bourdon tubes, diaphragms, capsules, and bellows. The Bourdon tube is a sealed tube that deflects in response to applied pressure. All except diaphragms

provide a reasonably large displacement that's useful in mechanical gauges and for electrical sensors that need a big movement

- Terms utilized in pressure sensing

Transducer is a device in pressure sensing unit which converts one physical quantity into another physical quantity. Figure 2.12 shows the working principle of pressure sensor.

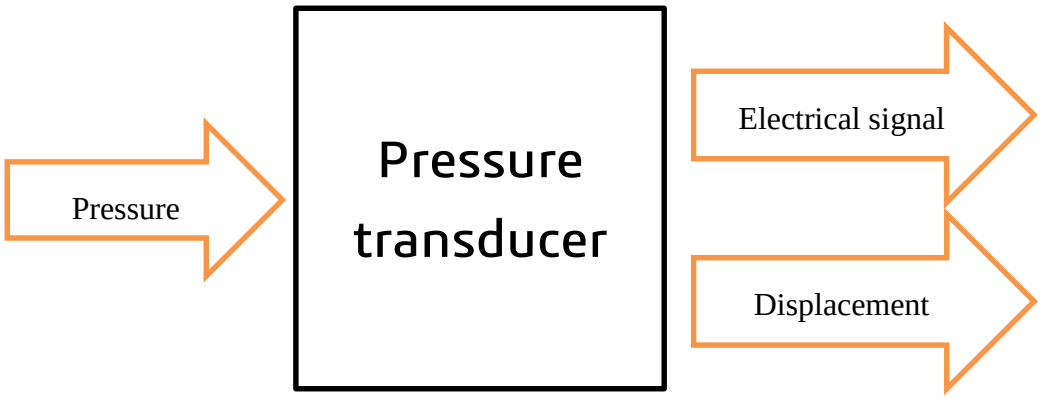

Figure 2.12 Pressure sensing

Absolute Pressure: - is that the pressure of a vessel located in a complete vacuum usually determined by adding 14.7 to the gauge pressure.

Absolute pressure= gauge pressure + atmospheric air pressure.

Adiabatic Process: -all the calculation variables, volume, pressure, and temperature, change with none heat transfer (not often a real-life situation).

Atmospheric Pressure: -The average air pressure measured at sea level, so normally accepted to be 14.7 pounds per sq. in. (psi) or 101352.9 Pascal.

Constant Volume: -with Airflow Process. Volume and temperature constant, pressure changes.

Gauge Pressure: - Gas pressure of the vessel, which is above atmospheric pressure usually measured by a Bourdon tube gauge in pounds per Sq. in. (psi).

Differential pressure-is the difference between two pressures.

2.11.3. Speed sensor

The speed sensor uses the variable reluctance magnetic sensing principle, and there for the cylindrical permanent core with a coil wire wound around it mounted on stationary hub carrier; axle housing or back plate produces a magnetic flux which overlaps the rotating exciter ring. The exciter could also be of the tooth ring or rib slot ring type attached to the rotating driveshaft. Varity of teeth or slots are arranged radially which with the speed rotation of the road wheal determine the frequency of the signal transmitted to the electronic control unit, because the wheel and exciter revolve the teeth and gaps or ribs and slots of the exciter undergo the magnetic flux of the sensor. The coil wrapped round the magnetic cone senses the changing intensity of magnetic flux because the teeth or rib undergo the flux line then an alternating voltage is induced with the coil, whose frequency is proportional to the speed of rotating wheel. The voltage is transmitted to the control unit whenever the road wheels are rotating no matter whether the brakes are applied and various components are indicated in the figure 2.13.

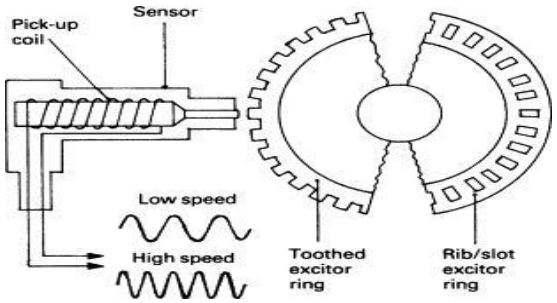

Figure 2.13 Speed sensor (www.banggod.com)

Basically, there are two sort of speed sensor

1. Inductive sensor
2. Hall effect sensor

Inductive sensor

Inductive sensor also referred to as magnetic pickup sensor during the operation work because of inductive effect, the sensor coil is producing the oscillating voltage. When the trigger wheel with the teeth passes in closer distance to the pole pin of the sensor the magnetic flux surrounding the coil induce state change and the components are shown in the figure 2.14.

Sensor construction

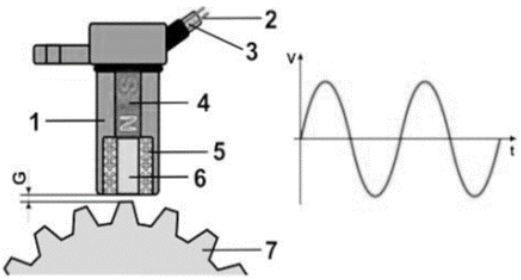

1. sensor housing
2. Output wires
3. Coaxial coated protection
4. Sensor Permanent magnet
5. Inductive coil
6. Pole pin trigger wheel
7. Trigger wheel

Figure 2.14 Inductive sensor (www.baumer.com)

- Hall effect sensor

As shown in figure 3.15 the Hall Effect sensor uses the very fact that a magnetic field generates a voltage within a hall element. Its level is independent of its rates of change. The sensor includes the magnet and dual hall element. With the profile passing by, the magnetic flux varies thereby creating the signal voltage within the hall element.

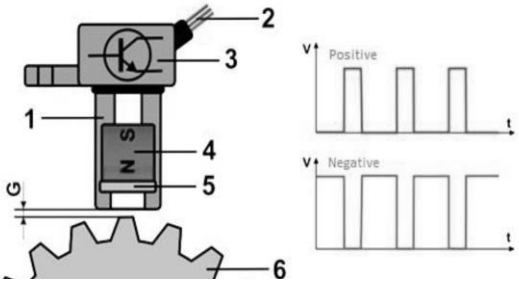

1. sensor housing
2. Output wire
3. Integrated electronics
4. Sensor Permanent magnet
5. Hall effect device
6. Trigger wheel

Figure 2.15 Hall Effect sensor (www.baumer.com)

2.11.4. Quick exhaust (release) valve

Quick exhaust valves work by providing a rapid exhaust of controlled air, it's going to be mounted as one unite of in combine with the control valves. The seal inside quick release valve is formed like a bat wing. When atmospheric pressure is shipped to the cylinder, it hits the rear side of the seal and pushes the front side against the exhaust port. This seals it off and allows air to enter the cylinder. When the control valve is shifted, the bat wing design of the seal begins to catch the exhausting air and shifts itself over to dam off the primary inlet. This enables all the exhaust air to right away dump out the exhaust port. The on and off situation and sectional view is indicated in figure 2.16 & 17.

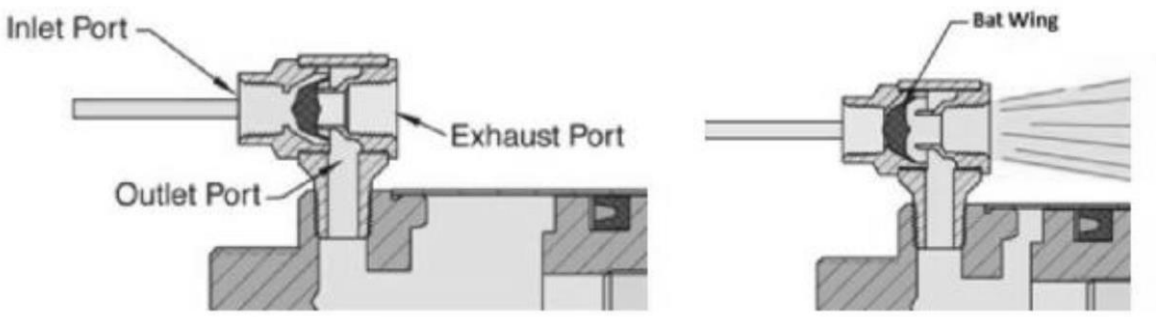

Figure 2.16 Quick exhaust valves (www.clippared.com)

To control the quantity of exhausted air from the system solenoid operated variable diameter valve is employed. solenoid operated variable diameter valve is like a check valve the air passes through variable diameter port, the quantity of air passes through the valve is directly proportional to the diameter and therefor the shape of the port. The diameter of the valve is controlled by linear motor plunger plugged in to the valve port.

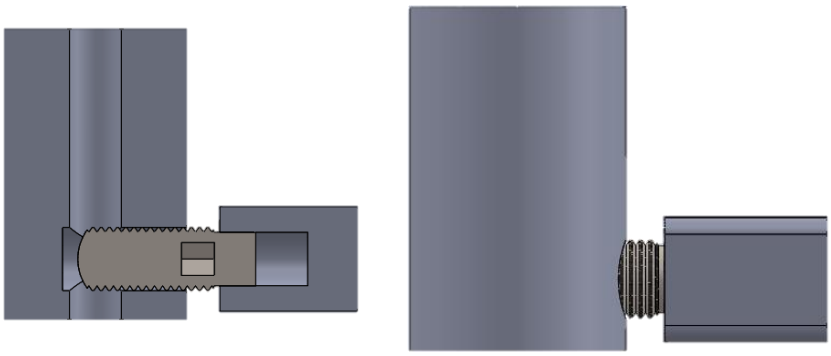

Figure 2.17 Solenoid operated quick exhaust valve

2.12. Summary of the review

From the researches its observed that astrowski et ai. (2007) shows adaptive crashworthiness of front end structure of a motor vehicle but the study focuses only on high and low crash stiffness's.

Witteman (1999) showed possibilities to design the adaptive vehicle structure that can change the stiffness real time for optimal energy absorption in different crash situations but the system control is by means of friction generated by hydraulic brakes on two rigid backwards moving beam.

Concept design of a noval 4-stage collision energy absorption system Jain et al. (2016) mounted in the front passenger car the study is done in the sedan car and used MR damper but the system is not active and controllable.

adaptive crashworthiness of front-end structure of motor vehicles Griskevicius (2007) Main objectives of the proposed system are to predict, control and adjust the impact characteristics to various conditions by decreasing the pre-designed crushing stiffness of the vehicle frontal deformation zone. However, the instantaneous velocity response of the system is not analyzed.

CHAPTER THREE

MATERIALS AND METHODS

This chapter includes methods, design and simulation, selection of materials, physical properties modeling and simulation of air spring, modeling of air spring using abaques and mounting location.

3.1. Methods

The methodology followed in achieving the set objectives, includes various stages as briefly described below. It is shown in the form of a flowchart in figure 3.1.

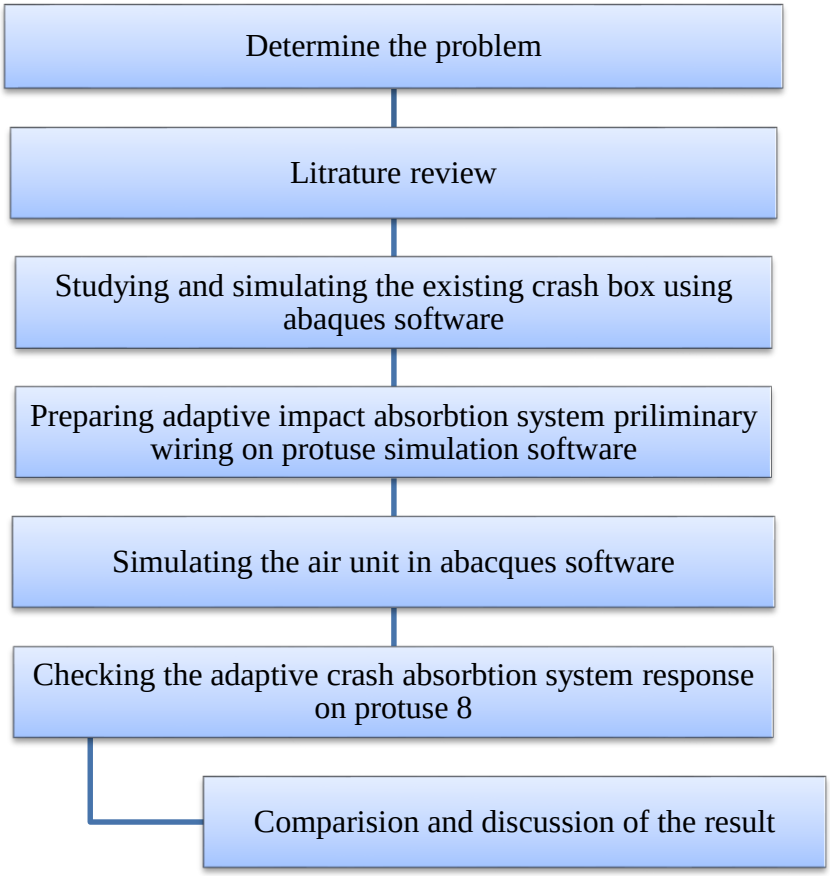

Figure 3.1 Methods

3.1.1. Literature review

Literature survey of the existing impact absorption system and the previous works done related to impact absorption system is the key step of the methodology which helps in gaining enough

knowledge and helps in understanding the current status of the research in the field and identifying the research gap existing.

3.1.2. Methods of Data Collection

The necessary data for the impact absorption system is collected by the following methods.

- By visiting concerned automobile industries and interaction with resource persons in vehicle design
- By visiting various websites in the area of vehicle design & dynamic analysis, SAE and other publications

3.1.3. Design and simulation

After reviewing the literature, design, and simulation of the system components was carried out. During the conceptual design process, a black box approach was used, which helps me to study a variety of mechanisms and select the appropriate design path by considering different criteria. Once the efficient design path was determined the design of individual parts of the mechanism was done so that the system can perform its function well. After accomplishing the design of parts; simulation of the system was done using solid works software.

3.2. Selection of materials

The materials available to engineers for structural applications embrace a particularly wide selection of properties. Generally, materials classified into three families as follows:

- Metals & alloys
- engineering ceramics & glasses
- engineering polymers & elastomers

3.2.1. Engineering polymers & elastomers

3.2.1.1. *Elastomers*

Elastomers are all amorphous, except at high strains, which tend to order the molecules of the material. Polyisoprene, natural rubber (NR) has good abrasion resistance, but low resistance to heat, ozone and oil (willem et al., 2005).

Air springs are pneumatic actuator made of natural rubber. Air springs make use of the fact that air has elastic or springiness when compressed and integrating directional control valves, sensing unit and controller makes them device having different stiffness by attaining different air pressure inside. This property allows them to use in front end collision energy absorber (willem et al., 2005). The parameters of rubber are shown in the table 3.1.

Table 3.1 Rubber property

Material	**Parameters**	**Value of parameters**
Rubber	Density	1e-009
	Mooney rivline parameters c01	80
	Mooney rivline parameters c10	80
	TEMP	25

3.2.1.2. Low-Carbon Steels

From all the different types of steels, those produced in the greatest quantities fall within the low-carbon classification. These generally contain less than about 0.25 wt. % C and are unresponsive to heat treatments intended to form martensite; strengthening is accomplished by cold work. Microstructures consist of ferrite and pearlite constituents. As a consequence, these alloys are relatively soft and weak but have outstanding ductility and toughness; in addition, they are Machin able, wieldable, and, of all steels, are the least expensive to produce. Typical applications include automobile body components, structural shapes (I-beams, channel and angle iron), and sheets that are used in pipelines, buildings, bridges, and tin cans.

When strength is not a major concern, low-carbon steels are good choices because they are easy to handle (draw, bend, punch, swage, etc.) and fairly inexpensive. Surface hardness can be improved by a process called carburizing which involves heating the alloys in a carbon-rich atmosphere.in this thesis low carbon steel (AISI 1020) is used for air spring lower and top structural plates.

AISI 1020 is a low hardenability and low tensile carbon steel with Brinell hardness of 119 – 235 and tensile strength of 410-790 MPa. It has high machinability, high strength, high ductility and good weldability. It is normally used in turned and polished or cold drawn condition. Due to its low carbon content, it is resistant to induction hardening or flame hardening. Due to lack of

alloying elements, it will not respond to nitriding. However, carburization is possible in order to obtain case hardness more than Rc65 for smaller sections that reduces with an increase in section size. Core strength will remain as it has been supplied for all the sections. Alternatively, carbon

3.2.1.3. Chemical Composition

The chemical composition of AISI 1020 steel is:

Element Content

Carbon - C 0.17 - 0.230 %

Iron - 99.08 - 99.53 %

Manganese - Mn 0.30 - 0.60 %

Phosphorous - P ≤ 0.040 %

Sulfur- S ≤ 0.050 %

3.2.1.4. Physical Properties

The physical properties of AISI 1020 steel are:

Physical Properties	**Metric**
Density	7.87 g/cc

3.2.1.5. Mechanical Properties

The mechanical properties of AISI 1020 steel are shown in table 3.2.

Table 3.2 Mechanical Property of AISI 1020

Mechanical Properties	**Metric**
Elongation at Break (in 50 mm)	36.5 %
Modulus of Elasticity (Typical for steel)	200 GPa
Bulk Modulus (Typical for steel)	140 GPa
Tensile Strength Ultimate	394.72 MPa
Tensile Strength, Yield	294.74 MPa

Poissons Ratio	0.290
Shear Modulus (Typical for steel)	80.0 GPa

Table 3.3 property table for mild steel

Material	Density	Young's modulus	Poisson's ratio
Mild steel	7.85e-9	200000	0.26

Mild steel is a carbon steel with a maximum of about 0.25% carbon and it's also known as low carbon steel and mild steel is used for a crash box.

3.2.1.6. Applications

AISI 1020 steel is used in case hardened condition and finds use in the following components:

- Axles
- General engineering parts and components
- Machinery parts
- Shafts
- Camshafts
- Gudgeon pins
- Ratchets
- Light duty gears
- Worm gears and
- Spindles

3.3. Modeling and simulation of air spring

Air springs are rubber or fabric actuators that support and contain a column of compressed gas. They are used as pneumatic actuators and vibration isolators. Unlike the conventional pneumatic cylinders, they have no pistons, dynamic seals, and piston rods. This behavior makes them better suited to handle off-center impacts.

Air springs make use of the fact that air has elastic or springiness when compressed. Due to the overall construction air springs are virtually noise-free.

Their spring constant is often increased as increasing the compressed gas pressure inside the chamber.

3.3.1. Types of air spring models

From the several types of air spring models the followings are the majors.

- NISHIMURA
- VAMPIRE
- SIMPAC
- GENSYS

GENSYS

GENSYS air spring model fully describe all parameters of air spring. This air spring model is three-dimensional and can describe lateral, longitudinal and vertical behavior of the air spring. The model is described for three effects elasticity, friction and viscosity and not, like the other models, for the behavior in the different physical parts of the air spring system. The vertical model has a nonlinear damping

NISHIMURA

This types of air spring model are used to model orifice damping and flow resistance through the pipe.

VAMPIRE

This types of air spring model are used for a damping coefficient less than 50Ns/m. in this model the mass related to air mass of surge pipe and relative acceleration is considered.

SIMPAC

In this model the main concern is to represent the influence of air in the main volume.

3.3.2. Terms in air spring

- ***Assembly***

Assembly of air spring includes the flexible member like rubber body, top plate and bottom plate.

- ***Assembly volume***

Air spring assembly volume is working volume exclusive of any external working volume.

- ***Compression stroke***

Compression stroke in air spring is reduction in height from the normal design height in its operation.

- ***Design load***

This is the normal maximum static load the air spring expected to support.

- ***Design height***

The overall height of the air spring

- ***Effective area***

Effective area is the actual working area perpendicular to the output force of air spring. It is not the diameter of the air spring.

- ***Reservoir volume***

Reservoir volume is any working volume located externally from the air spring assembly but functioning with air spring.

3.3.3. Construction of air spring

Air spring incorporates a carefully designed rubber and fabric bellows that contain a column of compressed air. The rubber itself does not provide force or support load the column of air spring does this when the air spring is inflated according to the load required of it. They are highly engineered elastomers with specifically designed metal end closures. The construction of air spring is shown fin figure 3.2.

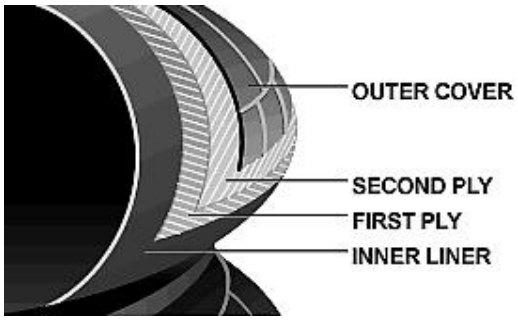

Figure 3.2 Construction of air spring, April 2005 <http://www.bearing-service.ru>.

A standard two-ply air bellows is made up of four layers

- An inner layer of calendared rubber.
- A first ply of fabric reinforced rubber.
- A second ply is a fabric reinforced rubber with the cords with specific bias angle.
- An outer cover of calendared rubber.

For the design and modeling of air spring the dimensional and mass parameters are taken from the vehicle specifications and by measuring the actual cashbox space on the vehicle. The overall dimension of air spring is given below in figure 3.3.

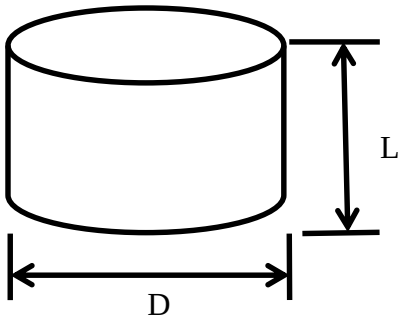

Figure 3.3 Air spring dimension

m is mass of the car

D is diameter of air spring

L is length of the column

l_s is the surge pipe length (m)

d_s is the surge pipe diameter (m)

A_e is the effective area of the air bag (m^2)

V_{bo} is initial air bag volume

V_{ro} is initial reservoir volume

Mass of the car M=2000kg

Low speed =30km/hr.=8.33m/s

D=100 mm

L=70 mm

l_s=2.1 m

d_s=0.038 m

A_e=0.018 m^2

V_{bo}=0.0219 m^3

V_{r0}=0.2198 m^3

K_{aux}=2250000 N/m

A_s=0.001134 m

During an impact volume of air spring is reduced which confine the molecules more closely together result in increasing of pressure and also temperature. The gas pressure inside the air spring varies with the speed and magnitude of deflection for a unit of deflection.

$$P_g = \frac{F}{A_e} \qquad (3.3)$$

$$F_{avg} = -\frac{\frac{1}{2}mv^2}{d} \quad (3.4)$$

F_{avg}=-0.5 x 2000 x 8.33^2/0.3

F_{avg}=231kN

$$P_g = \frac{F}{A_e}$$

P_g = 12.9MPa

From different types of air spring method GENSYS air spring model fully describe all parameters of air spring. This air spring model is three-dimensional and can describe lateral, longitudinal and vertical behavior of the air spring. The model is described for three effects elasticity, friction and viscosity and not, like the other models, for the behavior in the different physical parts of the air spring system. The vertical model has a nonlinear damping, which depends on the velocity raised to β. The model of genesis air spring model is shown in the figure 3.4.

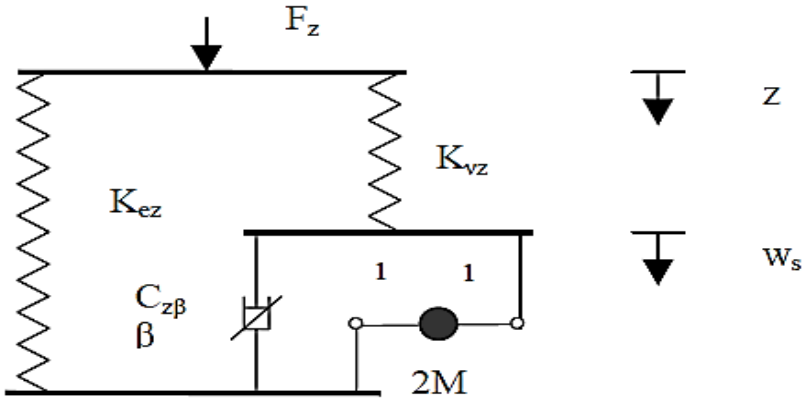

Figure 3.4 GENSYS air spring model

In this air spring model, there are seven vertical parameters to be determined to fully describe the vertical behavior of air spring.

- Friction damper $F_{fz,max,}$ z_2 (Nm)
- Nonlinear viscous damper $C_{z\beta}$, β (Ns^{β}/m^{β})

- Mass (2M) to describe the inertia of air in the surge pipe (kg)
- The elastic part is described by K_{ez} (N)
- The friction part is described by $F_{fz,max}$, z_2
- Viscous part is described by K_{vz} , $C_{z\beta}$,β and M.

Stiffness and mass parameters of air spring is shown the figure 3.5.

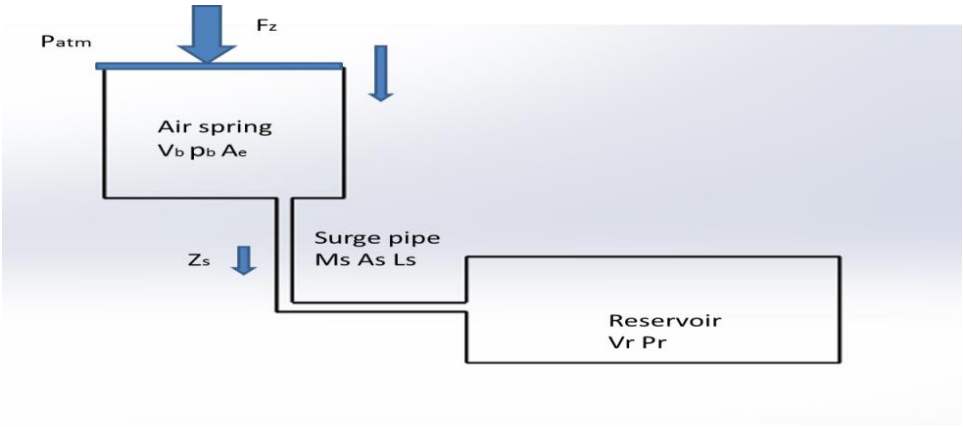

Figure 3.5 Stiffness and mass parameters of air spring

$$K_{ez} = \left(\frac{1}{\frac{p_0 A_{e^2} n}{V_{b0}+V_{r0}} + P_g \frac{dA_e}{dz}} + \frac{1}{K_{aux}} \right)^{.-1} \tag{3.5}$$

$$K_{ez} = \left(\frac{1}{\frac{12849796.3 * 0.0182 * 1.4}{0.0219 + 0.2198}} + \frac{1}{2250000} \right)^{.-1}$$

$$\underline{K_{ez} = 24089.5 N/m}$$

$$K_{vz} = \left(\frac{1}{\frac{p_0 A_{e^2} n}{V_{b0}} + P_g \frac{dA_e}{dz}} + \frac{1}{K_{aux}} \right)^{.-1} - K_{ez} \tag{3.6}$$

$$K_{vz} = \left(\frac{1}{\frac{12849796.3 * 0.0182 * 1.4}{0.0219}} + \frac{1}{2250000} \right)^{.-1} - 24089.5$$

$$\underline{K_{vz} = 213907.4 N/m}$$

The mass M can be found from the following expression,

$$M= 1_s A_s P\left(\frac{A_e}{A_s}\frac{V_{r0}}{(V_{b0}+V_{r0})}\right)^2 \quad (3.7)$$

$$M= 2.1*0.001134*163.8\left(\frac{0.018}{0.001134}\frac{0.2198}{(0.0219+0.2198)}\right)^2$$

$$\underline{M=81.3kg}$$

3.3.4. Damping of air spring

Damping parameters of air unite of the system is shown in figure 3.6 diagrammatically.

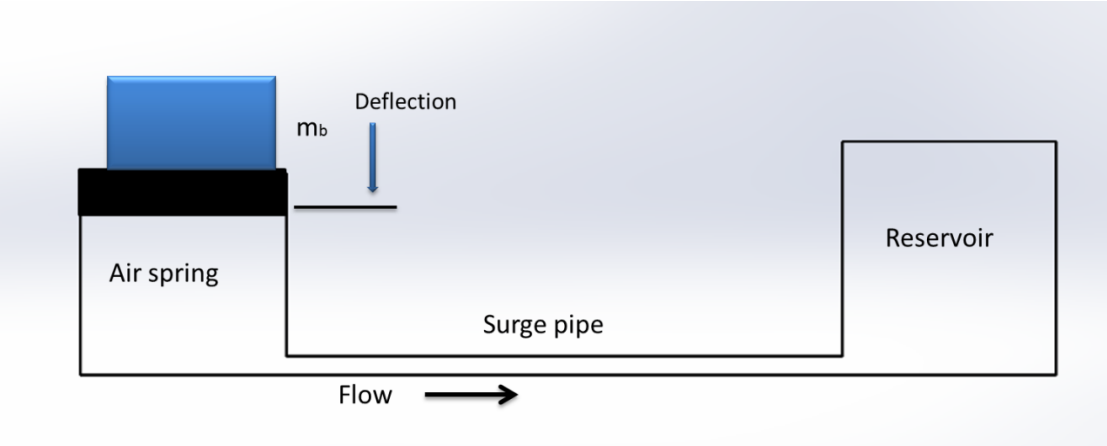

Figure 3.6 Simplified pneumatic impact absorber system

$$\frac{dp}{dz} = \frac{-\mathrm{p}.\gamma.\mathrm{V}^{(\gamma-1)}\frac{dV}{dz}}{V_{b0}+V_{r0}} = \frac{-\mathrm{p}.\gamma.\frac{dV}{dz}}{\mathrm{V}}$$

$$\Delta\mathrm{P} = -\frac{\mathrm{p}\gamma}{\mathrm{V}}.\Delta V$$

And the equilibrium internal absolute air pressure is

$$P_0 = \frac{m_b\, g}{A_e} + P_a \quad (3.8)$$

$$P_0 = \frac{81 * 9.81}{0.018} + 101325$$

$$\underline{P_0 = 1.45470\mathrm{MPa}}$$

Where

m_b, is the mass resting on the air bag (kg),

g is the gravitational constant (m/s^2),

A_e is the effective area of the air bag (m^2) and

P_a is the atmospheric pressure (N/m^2).

Change in air spring volume is

$$\Delta V_b = A_e \Delta z + \Delta q, \tag{3.9}$$

Δz is the deflection of the spring due to air compression.

A_e is the effective area of the air bag

Δq is the flow of air from the air bag to the reservoir.

The change in reservoir volume is

$$\Delta V_r = -\Delta q. \tag{3.10}$$

The flow of air from the air spring to reservoir is positive

When the flow of gas from air spring causes change in internal pressure

$$\Delta P_r = -\frac{\gamma p_0}{V_r}\Delta V_r = \frac{\gamma p_0}{V_r}\Delta q, \tag{3.11}$$

V_r is the reservoir volume

$\Delta P_b - \Delta P_r = P_0 w_f = P_0 \frac{1}{2} K_t z_s^2$, assume flow in the surge pipe can be considered as steady and incompressible

w_f is the work done by losses in the surge pipe (J/kg),

p_0 is the equilibrium air density (kg/m^3),

k_t is the total sum of the loss coefficients in the surge pipe and

z_s, is the average speed in the surge pipe (m/s).

Then the equilibrium air density is

$$P_0 = \frac{P_0}{\mathrm{RT}} \tag{3.12}$$

Where

R is the specific gas constant, $R=C_p-C_v$, (J/kgK) and

T is the absolute temperature (K).

The pressure loss in the surge pipe occurs due to the loss of energy in the fluid due to discharge port friction and turbulent eddies.

$K_t = k_{fr} + k_c$

Where

k_{fr} is the loss coefficient due to friction,

k_c is the loss coefficient due to contraction and

The loss work due to surge pipe friction can be determined from

$$w_f = \frac{1}{2} z_s^2 \frac{\mathrm{l}_s \mathrm{f}}{d_s} \tag{3.13}$$

Where

z_s the average speed in the surge pipe (m/s),

l_s is the surge pipe length (m)

d_s is the surge pipe diameter (m) and

f is the friction coefficient

Loss coefficient due to friction, k_{fr}, becomes

$$k_{fr} = \frac{\mathrm{l}_s \mathrm{f}}{d_s} \tag{3.14}$$

$$k_{fr} = 0.00053694$$

The friction coefficient depends on the Reynolds number (Re) and the relative roughness (k/D) and can be determined from the Moody diagram.

$$f = \frac{0.25}{\left[log_{10}\left(\frac{k}{3.7D} + \frac{5.74}{Re^{0.9}}\right)\right]}2 \quad (3.15)$$

$f = 0.018$

$K_t = k_{fr} + k_c + k_e$

$K_t = 0.00053694 + 0.5 + 1.0$

$K_t = 1.5005369$

The average speed, z_s, can be calculated using the continuity equation,

$p_s A_s z_s = pb\, A_e\, z$, if $Ps = p_b$, i.e. incompressible, then

$$z_s = \frac{A_e z}{A_s} \quad (3.16)$$

The force change over the surge pipe can be expressed as

$$\Delta F_S = A_s(\Delta p_b - \Delta p_r) = A_s P_0 \frac{1}{2} K_t z_s^2$$

$C_s = \frac{1}{2}.\, P_0\, .K_t\ A_s,$ if β is 2. (3.17)

$C_s = \frac{1}{2} * 145470 * 1.5005369 * 0.001134$

$C_s = 123.7222$N-S/M

$$M = 1_s A_s P\left(\frac{A_e}{A_s}\frac{V_{r0}}{(V_{b0} + V_{r0})}\right)^2 \quad (3.18)$$

$$m_s k_{wz^2} w_s = \frac{p_0\, {}_{nA_e}\, K_{wz}}{V_{b0}}(z - w_s) - C_s K_{wz}\,.^{1+\beta}\, w_s.^{\beta}$$

From the above two equations

$Mw_s = K_{vz}(z - w_s) - C_{z\beta}\,|w_s|^{\beta}\ \text{sing}(w_s)$

$$\frac{p_{0A_s}\ {}_{nA_e}\ K_{wz}}{V_{b0}} - C_s K_{wz}\,.^{1+\beta}\,|w_s|.^{\beta}\ \text{sign}\ (w_s)$$

And gives

$$C_{Z\beta} = C_s K_{wz} .^{1+\beta} = C_s \left(\frac{A_e}{A_s} \frac{V_{r0}}{(V_{b0} + V_{r0})}\right) .^{1+\beta}$$

The above equation shows that the relationship between nonlinear damping and damping in the serge pipe.

$$C_{Z\beta} = C_s \left(\frac{A_e}{A_s} \frac{V_{r0}}{V_{b0} + V_{r0}}\right) .^{1+\beta} \quad (3.19)$$

(If β is 2)

$$C_{Z\beta} = \frac{1}{2} . p . k_t . A_s \left(\frac{A_e}{A_s} \frac{V_{r0}}{V_{b0} + V_{r0}}\right)^3$$

$$C_{Z\beta} = \frac{1}{2} . 163.8 * kt * 0.001134 \left(\frac{0.018}{0.001134} \frac{0.2198}{0.0219+0.2198}\right)^3$$

$C_{Z\beta}$=kt 279.4 NS^2/m^2

3.4. Modeling of air spring using abaques

The air spring modeled in Abaqus is cylindrical in shape with inner diameter of 100 mm and 150mm outer diameter. The air spring has been idealized in model as consisting of two circular metal disks connected to each other via a rubber component. The lower disk has of radius of 70 mm and the upper disk has a radius of 72 mm. the disks are coaxial and are 70 mm apart.

The fluid cavity is modeled using the surface-based fluid cavity capability, to define cavity completely and insure proper calculation surface element are defined in three dimensional models along the bottom and top rigid disk boundaries of the cavity, even though no displacement element exists along those surfaces. Since Abaqus does not provide two-dimensional surface elements the rigid disk boundaries are modeled with structural elements rather than surface element within the model.

The rubber component is modeled as shell element, the circular top and bottom plates are modeled as rigid element.

3.4.1. Boundary conditions

- Fluid cavity inflated to a pressure at step one
- For Bottom plate- U1=U2=U3=UR1-UR2=UR3=0
- For top plate- U1=UR2=UR3=0

- For top plate –U3=UR1=UR2=0
- For top plate –U2=30cm
- Top plate and rubber body has tie contact
- Rubber body and bottom plate has tie at center are and surface to surface contact at the others (adjust slave surface to its initial position)
- Contact property between rubber body and bottom plate is rough
- Top plate is modeled as rigid body (adjust point to center of mass at start of analysis)
- Bottom plate is modeled as rigid body

3.4.2. Material property

The rubber is modeled as an incompressible moony Rivlin (hyper elastic) material with c10 = 80, c01 = 80, d1 = 0, and temp = 25 , and the steel is modeled as a linear elastic material with E = 210.0 GPa and v = 0.3. Table 3.4 shows the air spring materials and their parameters.

Table 3.4 Air spring materials

Material	Parameters	Value of parameters
Steel	Elastic modulus	2.1e+5 MPa
	Density	7.8e-9 t/mm^3
	Poisson ratio	0.3
Rubber	density	1e-009
	Mooney rivline parameters c01	80
	Mooney rivline parameters c10	80
	TEMP	25
Air	Gas constant	287 J/KgK
	Temperature	-273.15+25 K

- Loading

In the model the air spring is first pressurized to 12.9 MPa while holding the upper disk fixed. This pressure is applied at the cavity reference node. In this case air volume is adjusted automatically to fill the cavity.

While the air spring holding the pressure, the top plate is compressed to 30 cm in the negative y direction. Figure 3.9 shows the various components of air spring.

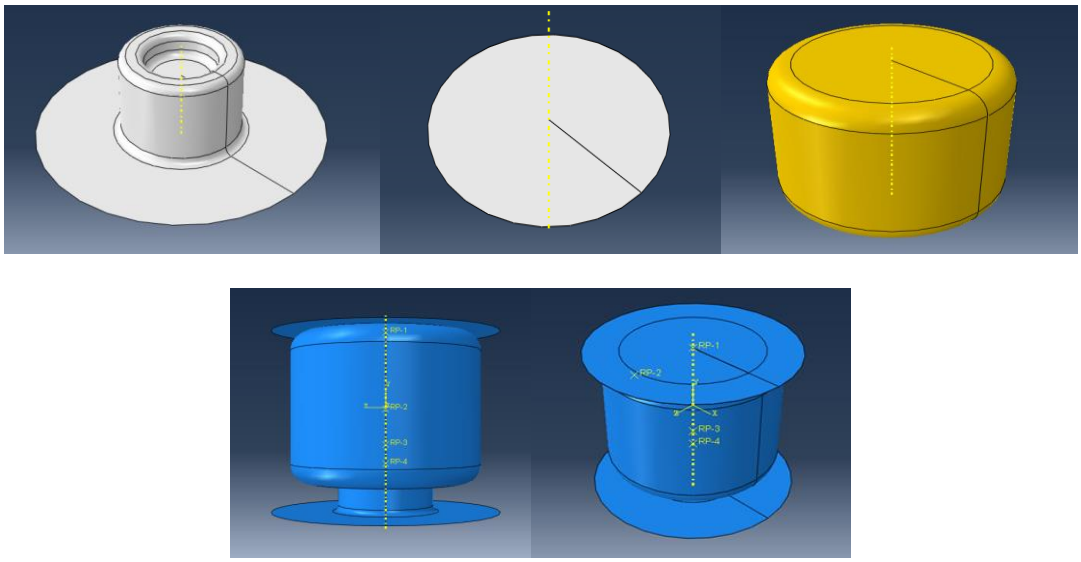

Figure 3.7 Air spring components and assembly

To make the designed air bellow functions adaptively during low speed collision it's important to mount the air spring at the end of front chassis rail. The vertical axis of the air spring should be perpendicular to the axis of rotation of the wheel for the optimum functioning of the air column unit. Figure 3.8 shows the mounting of air spring in the vehicle.

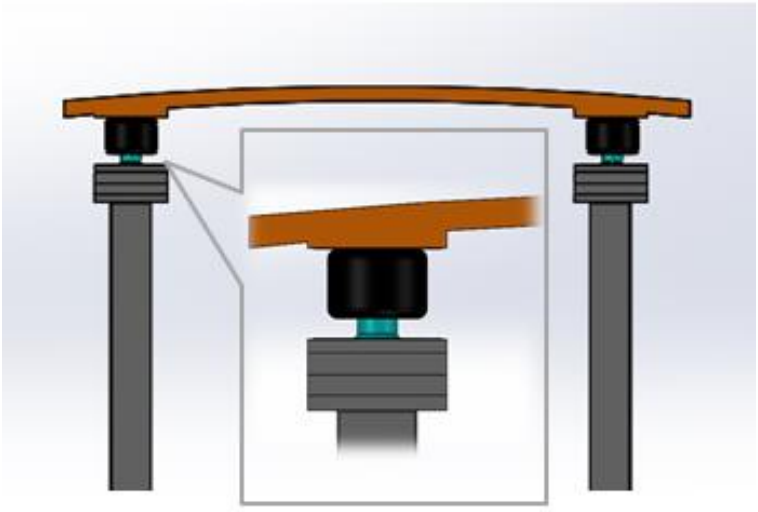

Figure 3.8 Air spring mounting between reinforcing bars and chassis rail

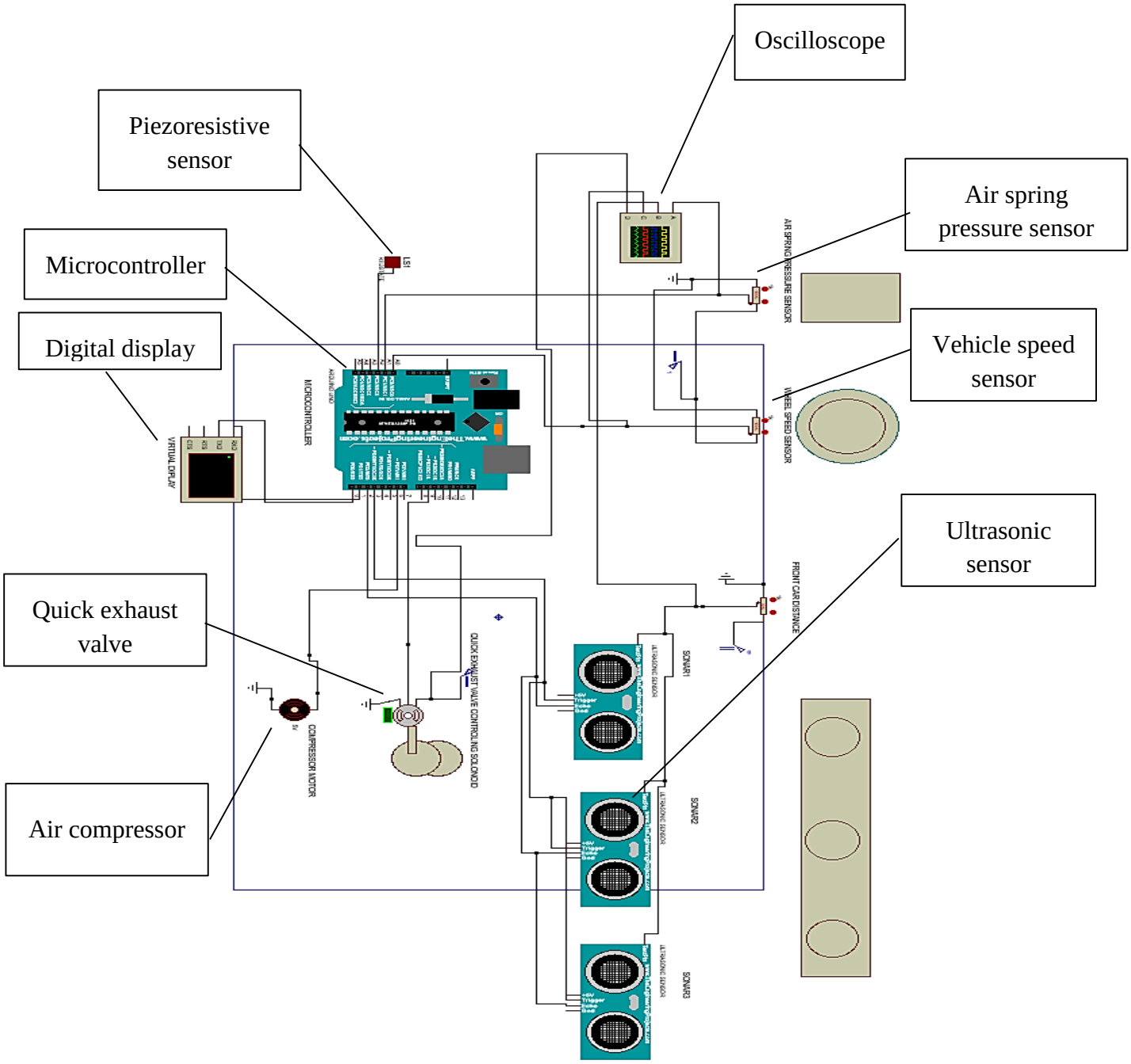

Figure 3.9 Overall circuit diagram

Figure 3.10 shows the overall circuit diagram of the system in the circuit the programmable microcontroller is used, in the microcontroller input pinpoints ultrasonic sensor, vehicle speed sensor, air spring pressure, and Piezoresistive sensor gives the input signal to the controller receiver section and the input signal is compared to the preset program in the processing section and the command is given to the actuators that are wired to the output pinpoints. The actuators used in the systems are quick exhaust valves and compressors.

CHAPTER FOUR

RESULTS AND DISCUSSION

4.1. Introduction

Speed has been identified as a key risk factor in road traffic injuries, influencing both the risk of a road crash as well as the severity of the injuries that result from crashes. Controlling vehicle speed can prevent crashes happening and can reduce the impact when they do occur, but a collision occurs unintentionally so building a system to reduce the consequence is important.

It is the fact that injuries and damages during a collision are directly proportional to the amount of kinetic energy generated during the motion of the vehicle, to minimize the risk of injury and damage, it is important to remove the kinetic energy as slowly and evenly as possible.

Kinetic energy is directly proportional to the mass and the square of the speed of the vehicle, so at a different speed, the vehicle will have a different amount of kinetic energy. To absorb these varying kinetic energy, it is important to develop an adaptive kinetic energy absorbing system to reduce injuries and damages that happen during the collision. The variation of braking distance with varying speed is given in table 4.1.

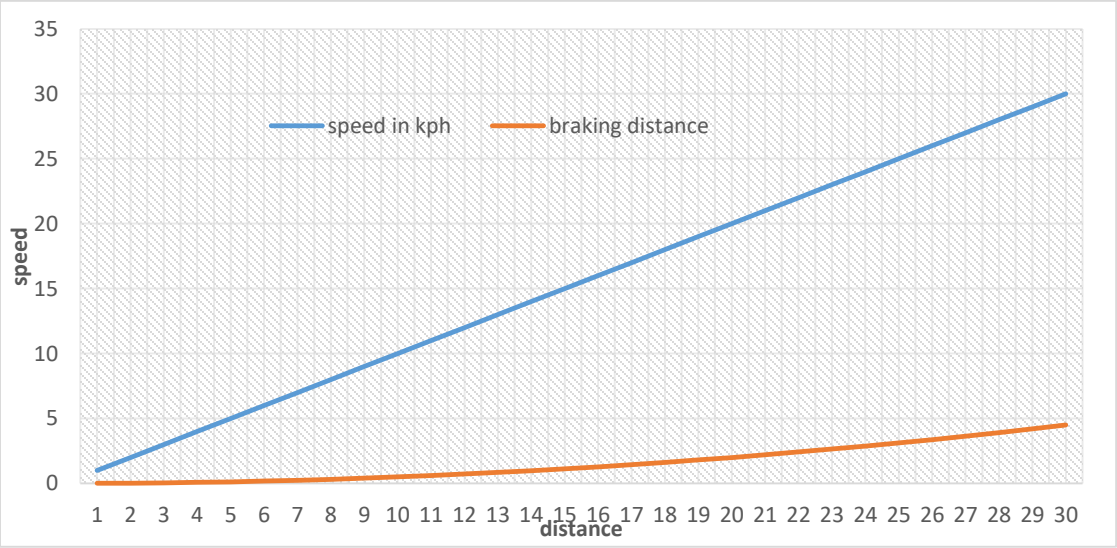

Figure 4.1 Speed and braking distance

Table 4.1 Speed and braking distance

speed in kph	constant	coefficient of friction	braking distance (m)
1	250	0.8	0.005
2	250	0.8	0.02
3	250	0.8	0.045
4	250	0.8	0.08
5	250	0.8	0.125
6	250	0.8	0.18
7	250	0.8	0.245
8	250	0.8	0.32
9	250	0.8	0.405
10	250	0.8	0.5
11	250	0.8	0.605
12	250	0.8	0.72
13	250	0.8	0.845
14	250	0.8	0.98
15	250	0.8	1.125
16	250	0.8	1.28
17	250	0.8	1.445
18	250	0.8	1.62
19	250	0.8	1.805
20	250	0.8	2
21	250	0.8	2.205
22	250	0.8	2.42
23	250	0.8	2.645
24	250	0.8	2.88
25	250	0.8	3.125
26	250	0.8	3.38
27	250	0.8	3.645
28	250	0.8	3.92
29	250	0.8	4.205
30	250	0.8	4.5

4.2. Shapes of air spring at different state

To fulfill the major requirements of adaptive impact absorption it is important to use controllable active elements. To achieve those requirements air spring is used, air spring is a dynamic element it contains top and bottom steel plates and rubber bodies, so combining compressed air and rubber body can make air spring column. By controlling the amount of air inside the rubber body we can able to vary the stiffness characteristics of air spring, this characteristic greatly supports the fact about heavier opponent needs stiffer structure and lighter opponent needs less stiffness. The symbols, deformed and original shape of air spring is shown in figure 4.2 a & b & 4.3.

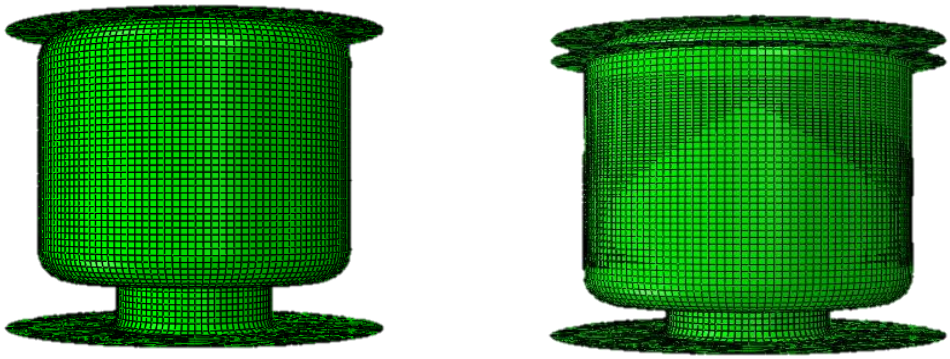

Figure 4.2 a. UN deformed shape of air spring b. deformed shape of air spring

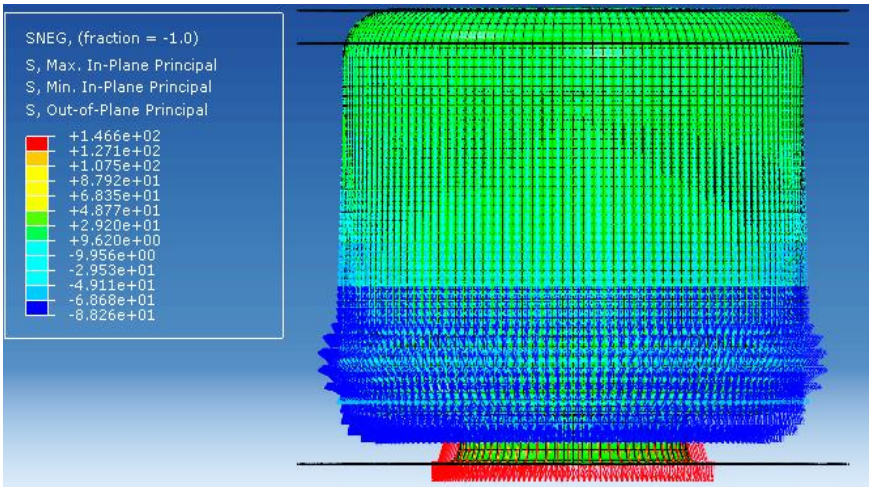

Figure 4.3 Symbols on deformed shape

In the simulation of air spring using Abaqus an incompressible moony Rivlin (hyper-elastic) material with c10=80, c01= 80, d1=0, and temp=25, and the steel with E=210.0GPa and v=0.3 is used. The following pictures show the material distribution in the model. The material orientations on-air spring is shown in figure 4.4. & 4.5.

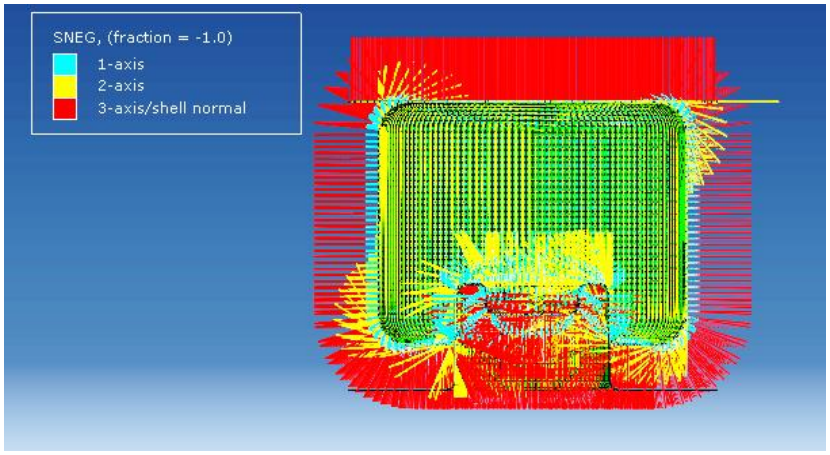

Figure 4.4 Material orientation on deformed shape sectional view

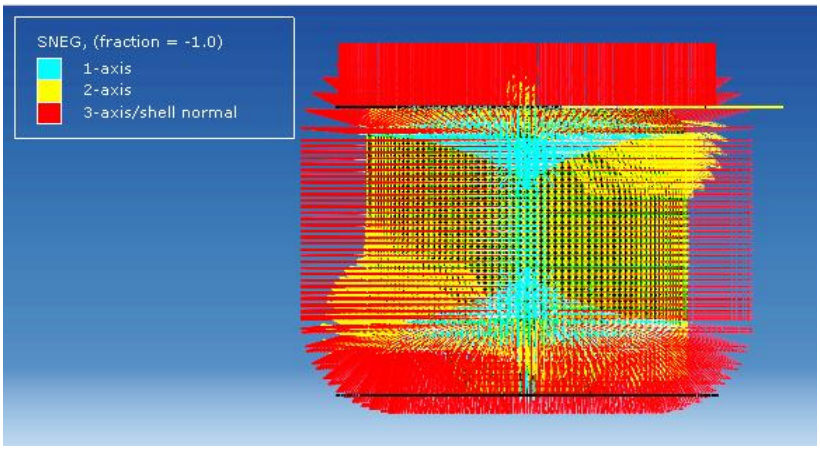

Figure 4.5 Material orientation on deformed shape

As indicated in figure 4.6 the von mises stress concentration on the inflated air spring when the spring is compressed about 30cm in the negative y-direction, and as the graph indicates the stress concentration is below the Tresca stress and we can say it is safe.

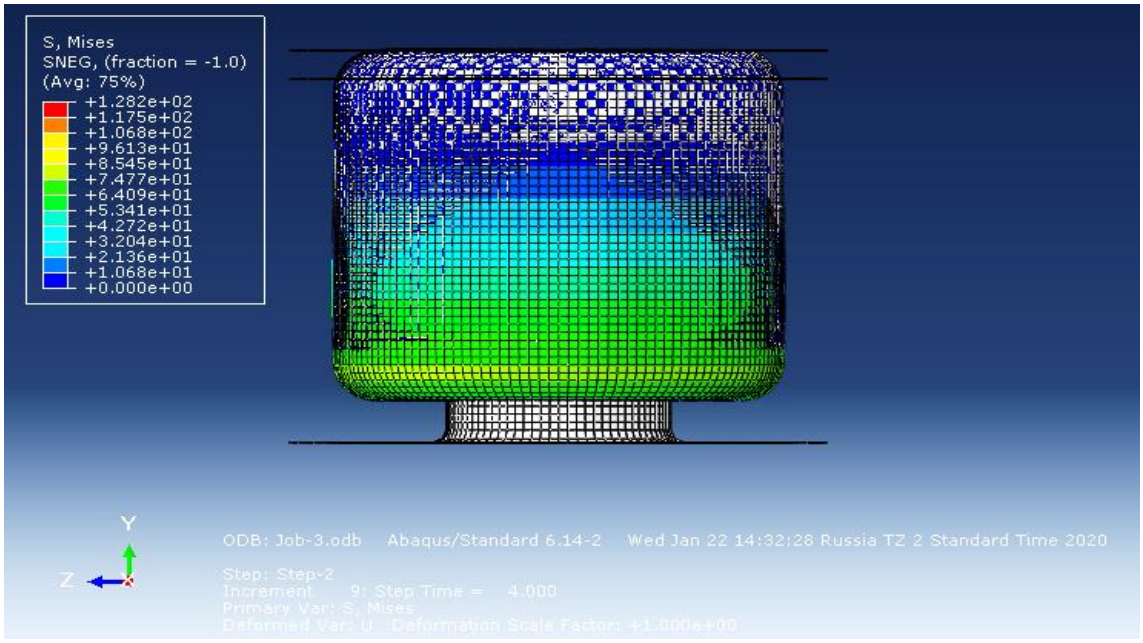

Figure 4.6 Stress contour on the air spring

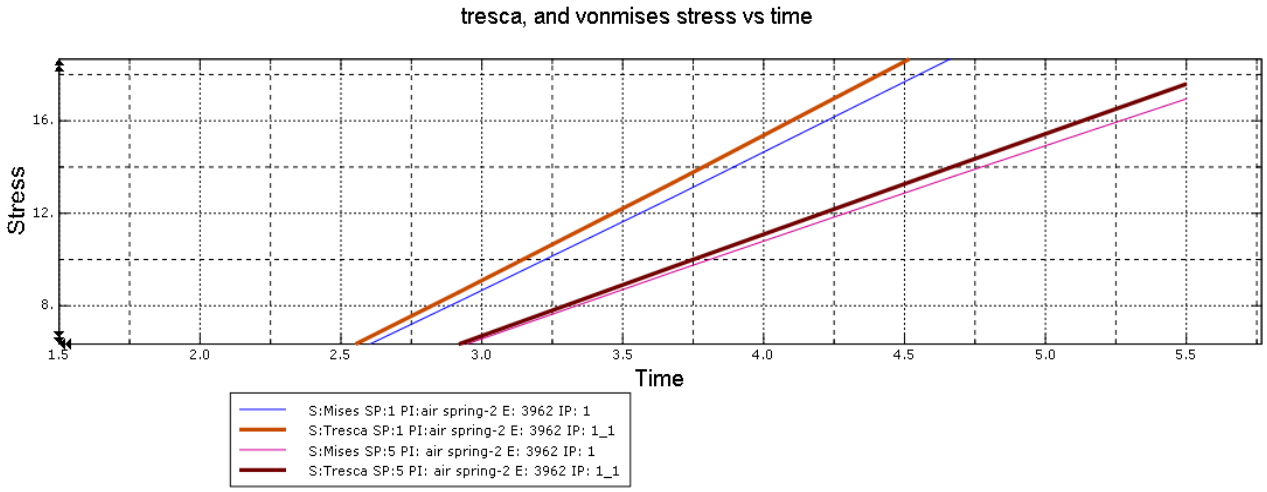

Figure 4.7 Von-mises stress

As the following graph in figure 4.7 shows all the stress components during the simulation of air spring lies below the Tresca line, so it's safe to use the air spring with this range which is proportional to the required range.

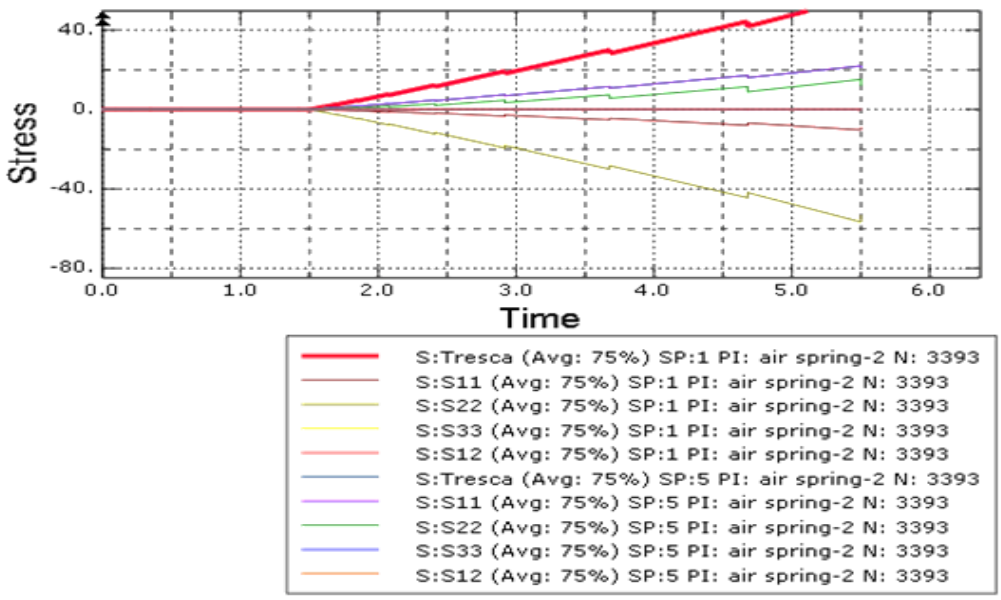

Figure 4.8 Stress components

As indicated in the parameter the air spring is first inflated to the required pressure level and then compressed in 30cm in the negative y-direction, so the graph shows the characteristics in both steps. The effective area of the air spring change is negligible; pressure is directly proportional to the applied force so as the compression force increases the pressure also increases. The varying time with stress is given in figure 4.9.

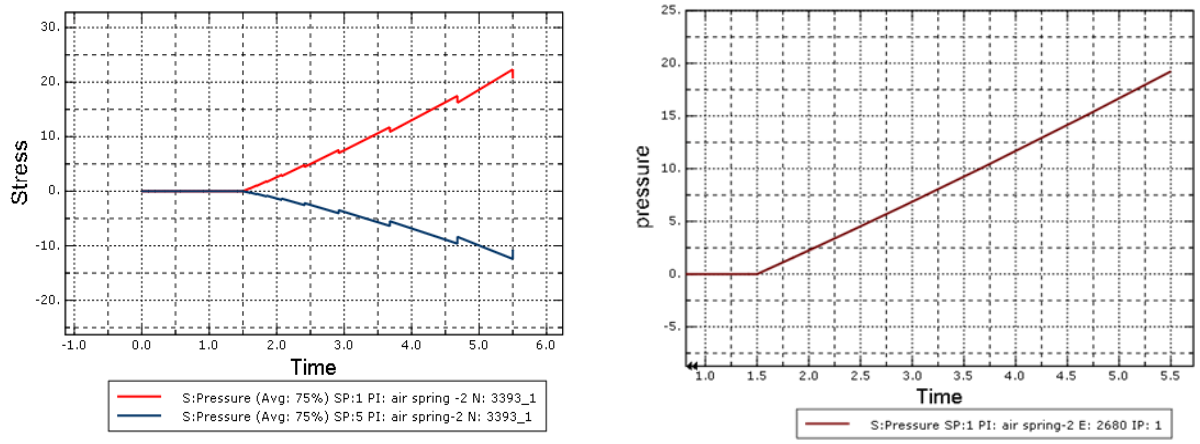

Figure 4.9 Pressure versus time

4.2.1. Spatial displacement

When the air spring is compressed to 30cm in the negative y-direction, the rubber body compressed in the same direction. The following result shows the magnitude and direction of displacement. Figure 4.10 shows displacement magnitude and symbols on air spring.

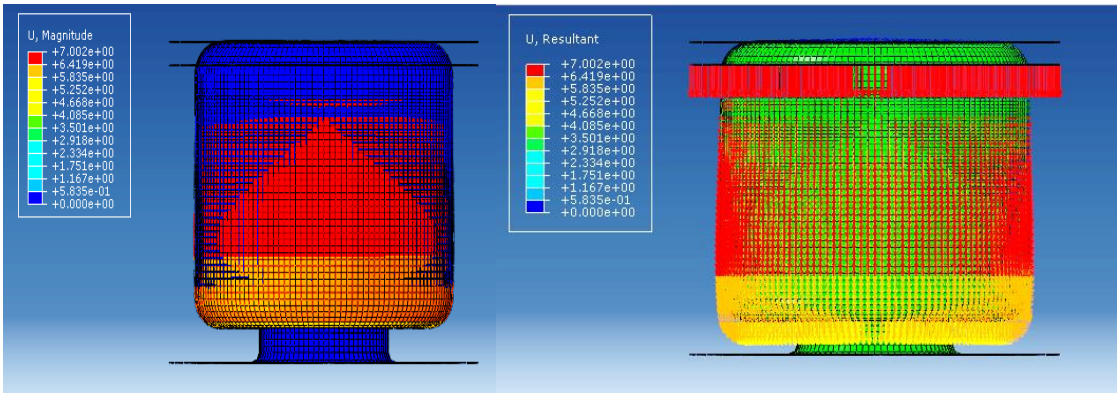

Figure 4.10 Magnitude and symbols on air spring

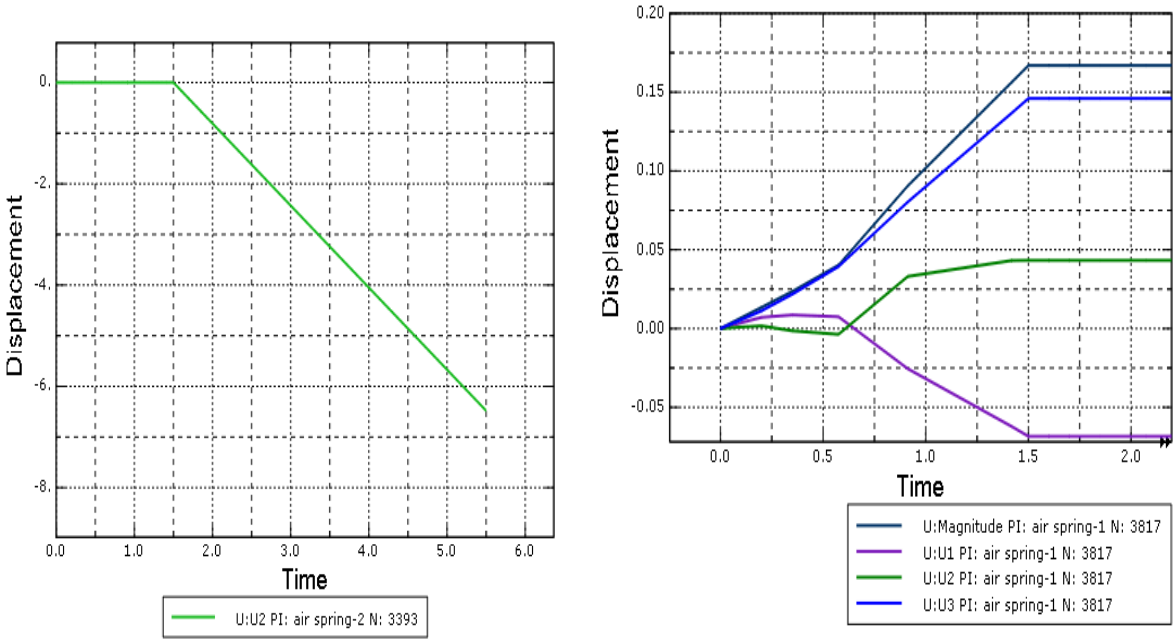

Figure 4.11 Displacement vs. time

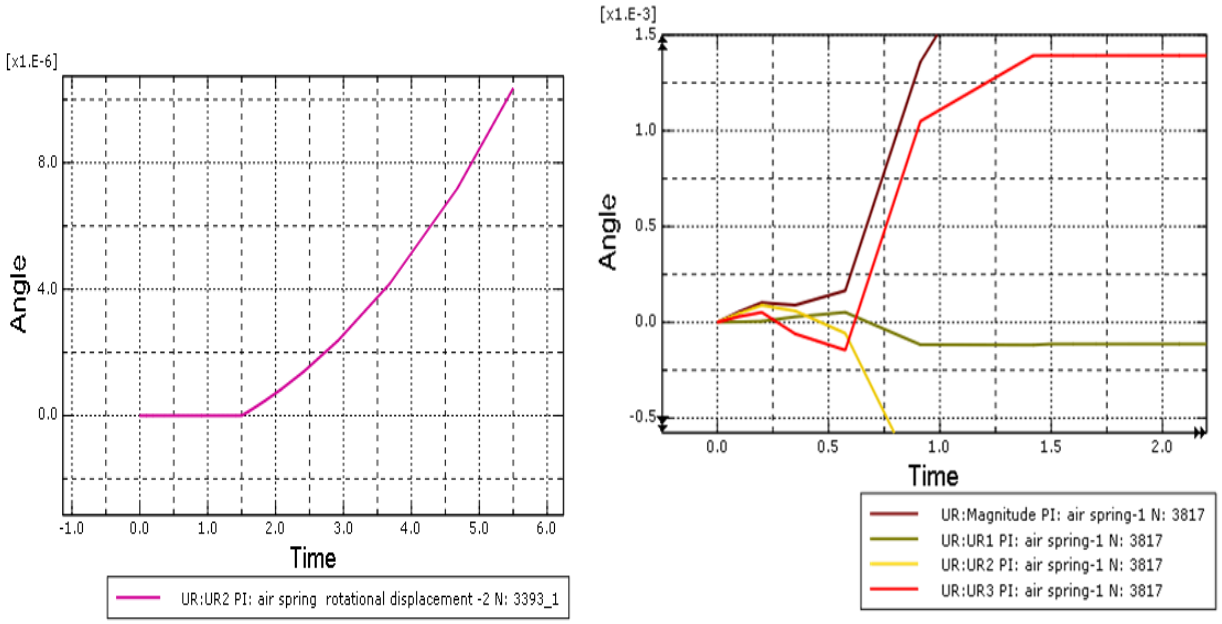

Figure 4.12 Rotational displacement vs. time

4.3. Crash box

The crash box is a mechanical element mounted between the front chassis rail and reinforcing bar. Here the crash box is simulated at a different speed to find out the operating condition as well the response to different opponent types. Figure 4.13 shows the response of the crash box at 11.94 m/s.

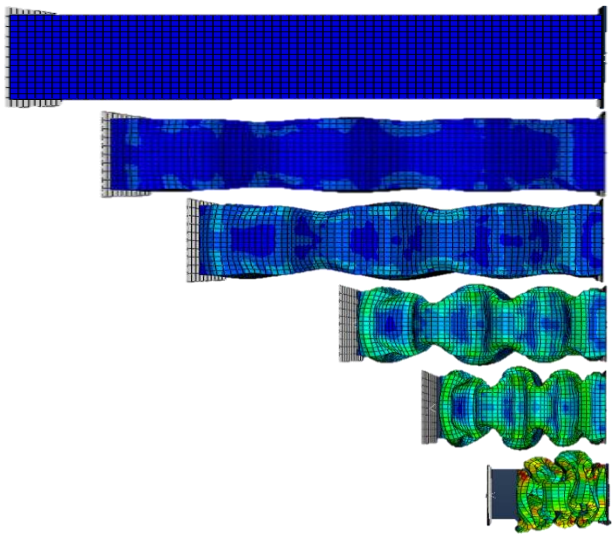

Figure 4.13 Mechanical crash box response at 11.94 m/s

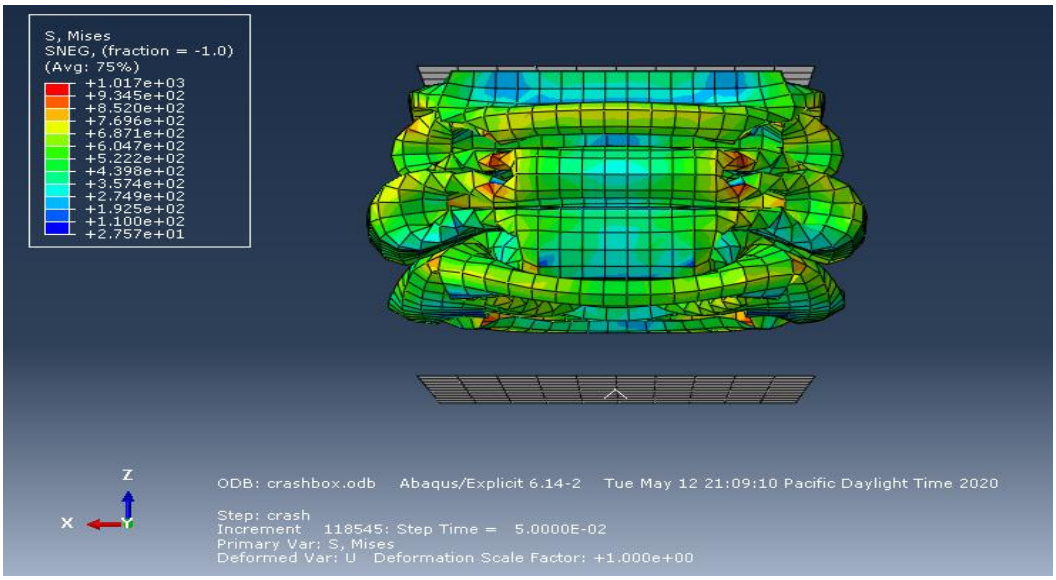

Figure 4.14 Stress contour on mechanical crash box

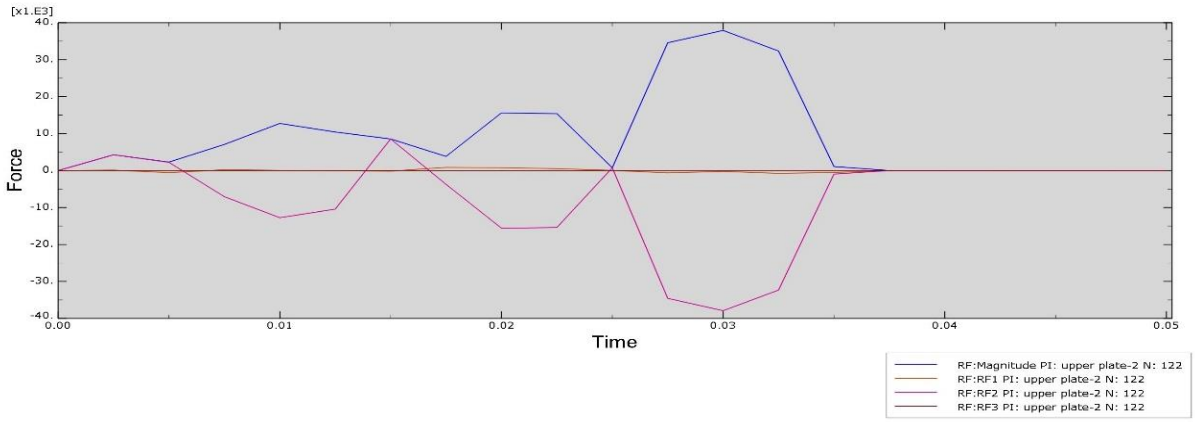

Figure 4.15 Force vs time at 11.94 m/s

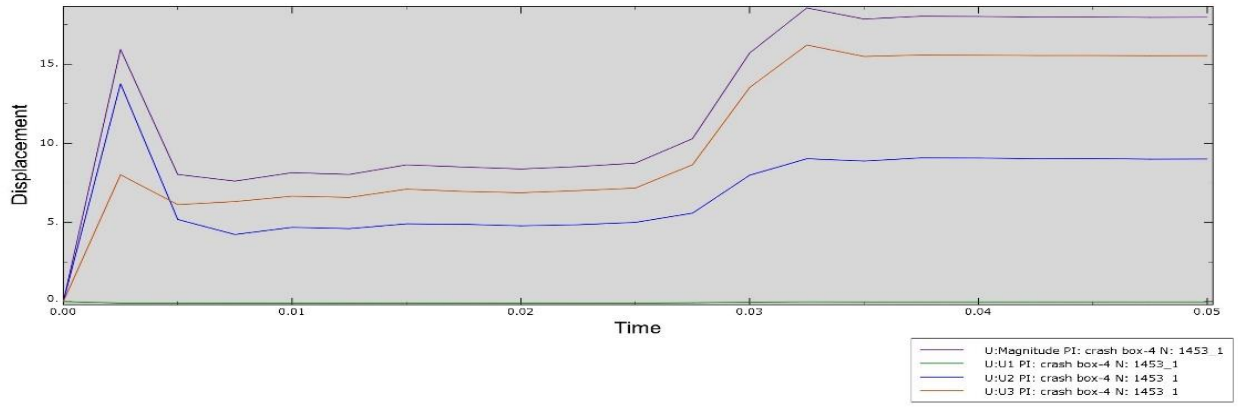

Figure 4.16 Displacement vs time at 11.94 m/s

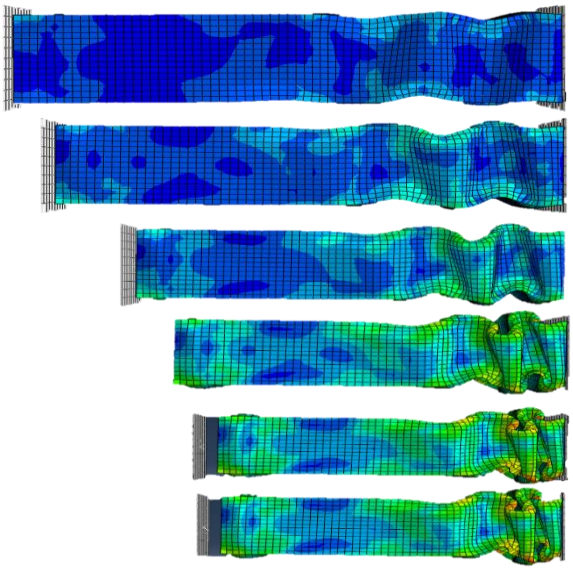

Figure 4.17 Mechanical crash box response at 10 m/s

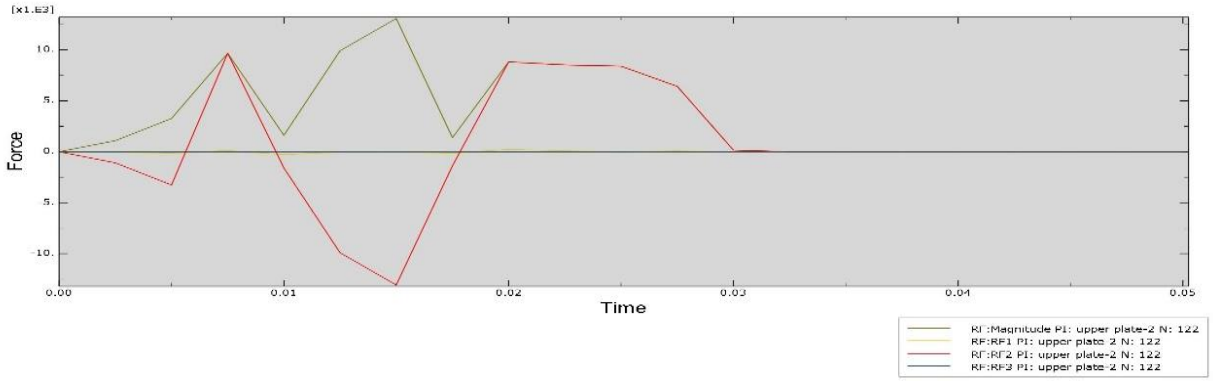

Figure 4.18 Force vs time at 10 m/s

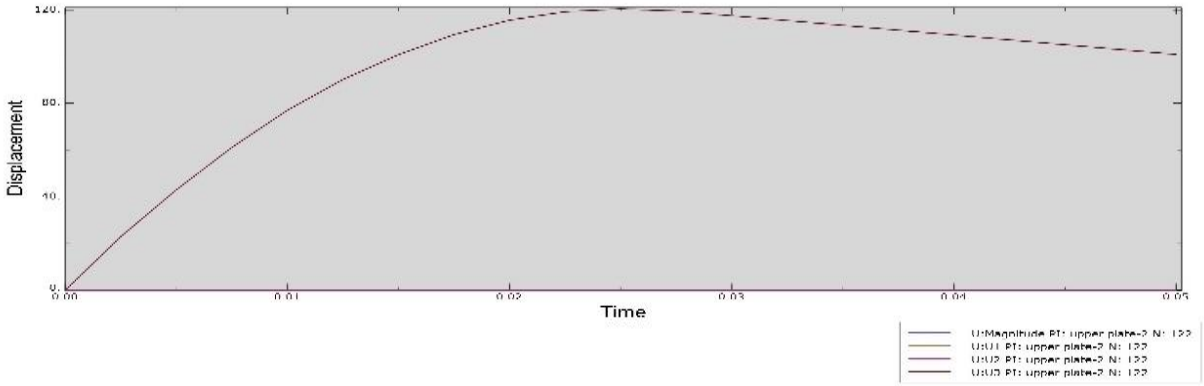

Figure 4.19 Displacement vs time at 10 m/s

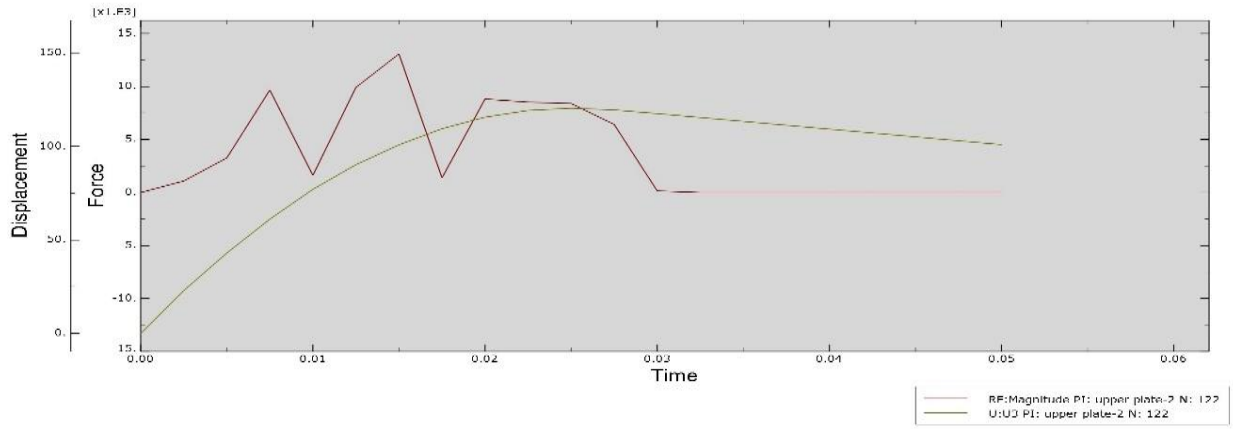

Figure 4.20 Relationship between force and displacement at 10 m/s

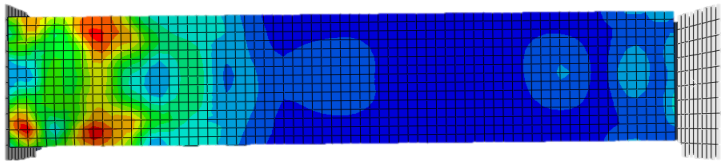

Figure 4.21 Mechanical crash box response at 7 m/s

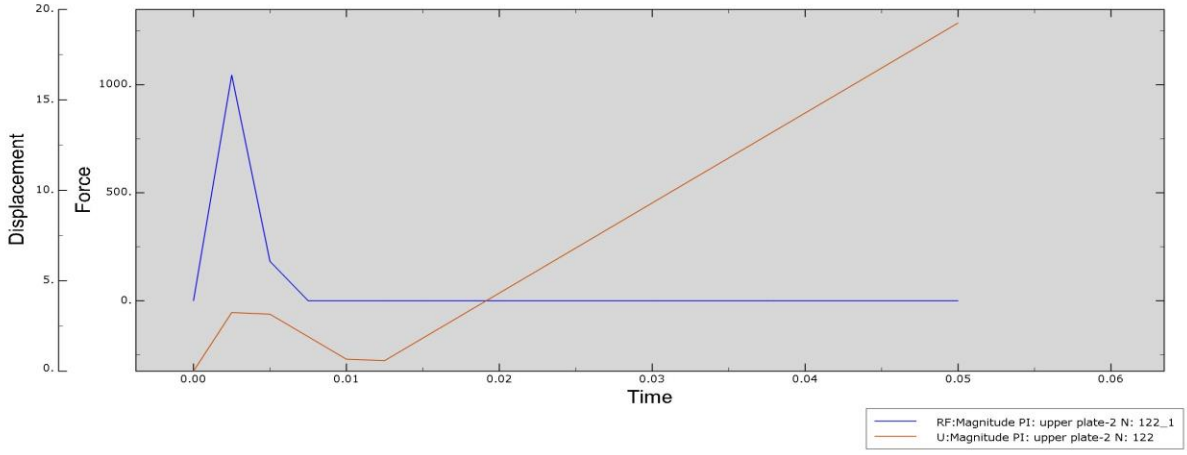

Figure 4.22 Relationship between force and displacement at 7 m/s

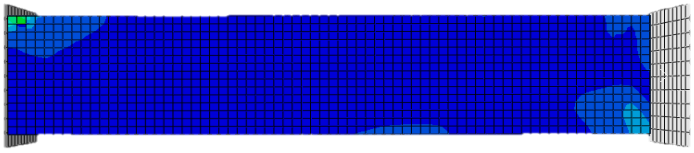

Figure 4.23 Mechanical crash box response at 5 m/s

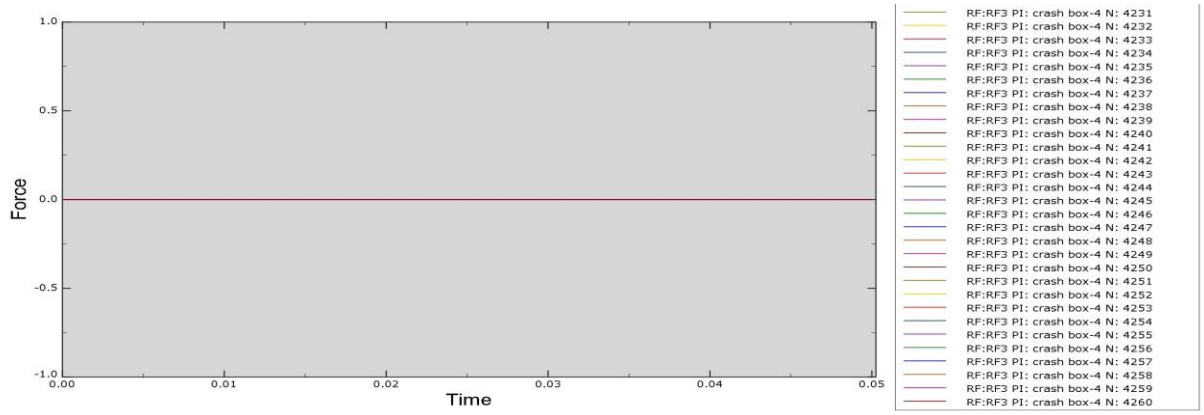

Figure 4.24 Force vs time at 4 m/s

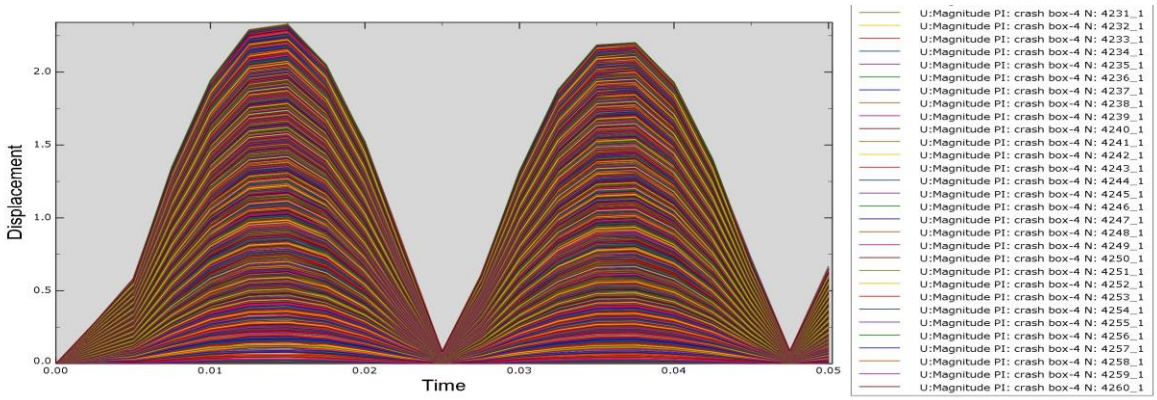

Figure 4.25 Displacement vs time at 4m/s

As the above simulation, the result in figure 4.25 shows the mechanical impact absorber or crash box is effective within a certain range of vehicle speeds. The crash box is simulated at different speed of the car ranging from 4 m/s to 11.94 m/s and the response is shown graphically as the result shown the crash box can able to take low speed impact up to 43 kph, above this the crash loads pass to the front rail of the car frontal structure.

4.4. Electrical simulation result

- Speed of the car is minimum
- The distance between colliding cars minimum

```
front car distance=4cm,  wheel speed=0 Kph     valve open 0.00 percent
front car distance=4cm,  wheel speed=0 Kph     valve open 0.00 percent
front car distance=4cm,  wheel speed=0 Kph     valve open 0.00 percent
front car distance=4cm,  wheel speed=0 Kph     valve open 0.00 percent
front car distance=4cm,  wheel speed=0 Kph     valve open 0.00 percent
front car distance=4cm,  wheel speed=0 Kph     valve open 0.00 percent
front car distance=4cm,  wheel speed=0 Kph     valve open 0.00 percent
front car distance=4cm,  wheel speed=0 Kph     valve open 0.00 percent
front car distance=4cm,  wheel speed=0 Kph     valve open 0.00 percent
front car distance=4cm,  wheel speed=0 Kph     valve open 0.00 percent
front car distance=4cm,  wheel speed=0 Kph     valve open 0.00 percent
front car distance=4cm,  wheel speed=0 Kph     valve open 0.00 percent
front car distance=4cm,  wheel speed=0 Kph     valve open 0.00 percent
front car distance=4cm,  wheel speed=0 Kph     valve open 0.00 percent
front car distance=4cm,  wheel speed=0 Kph     valve open 0.00 percent
front car distance=4cm,  wheel speed=0 Kph     valve open 0.00 percent
front car distance=4cm,  wheel speed=0 Kph     valve open 0.00 percent
front car distance=4cm,  wheel speed=0 Kph     valve open 0.00 percent
front car distance=4cm,  wheel speed=0 Kph     valve open 0.00 percent
front car distance=4cm,  wheel speed=0 Kph     valve open 0.00 percent
front car distance=4cm,  wheel speed=0 Kph     valve open 0.00 percent
front car distance=4cm,  wheel speed=0 Kph     valve open 0.00 percent
front car distance=4cm,  wheel speed=0 Kph     valve open 0.00 percent
```

	Channel A	Channel B	Channel C	Channel D
V/Div	5.00 V	5.00 V	0.00 V	0.00 V
Offset	60.00 V	20.00 V	-20.00 V	-60.00 V
Invert	Normal	Normal	Normal	Normal
Coupling	AC	AC	AC	AC

	Horizontal
Source	Trace
Position	2.00 S
S/Div	200.00 mS

	Trigger
Source	Channel A
Level	-2.00 V
Coupling	DC
Edge	Rising
Mode	Auto

— — *Channel A Pressure*

— *Channel B Distance*

— *Channel C speed*

— · · — *Channel D valve condition*

Figure 4.26 When Speed of the car is minimum and distance is minimum

As indicated in figure 4.26 the data is taken during when the distance between the cars is minimum and the speed is also minimum and the valve is at 0 conditions.

Channel-A is the air spring pressure sensor control circuit reading and it shows that the air pressure at the column or air spring is at the required level.

Logically the pressure sensor has three terminals the first is power the second is the ground and the third one is signal. The pressure sensor functions with the principle of piezoresistance so when the pressure reaches the required level the Piso element emits 5 volts due to the pressure in the piso element. As the above output data indicates the channel A has 5 volts which means the system receives the air pressure inside the air spring is positive.

Channel-B reads the output signal of the ultrasonic sensors mounted at the front end of the car, these ultrasonic sponsors have trigger, echo and signal points as in the digital output indicates the distance between the cars is very low due to that 5volts output received by the microcontroller and the speed is zero that means the car is at zero kilometer per hour and the valve remains closed.

Channel c reads the speed of the car like of the inductive sensors this sensor has three-terminal power, ground, and signal and the signal unit reads zero volts that means the car is not moving.

Channel-D reads the valve condition. The valve needs the pre-condition to trigger. That means the above three channels must read 5 volts or the condition must be in crash condition. The above graph shows the valve is in closed condition.

- When speed of the car is maximum and the distance between colliding cars is also maximum

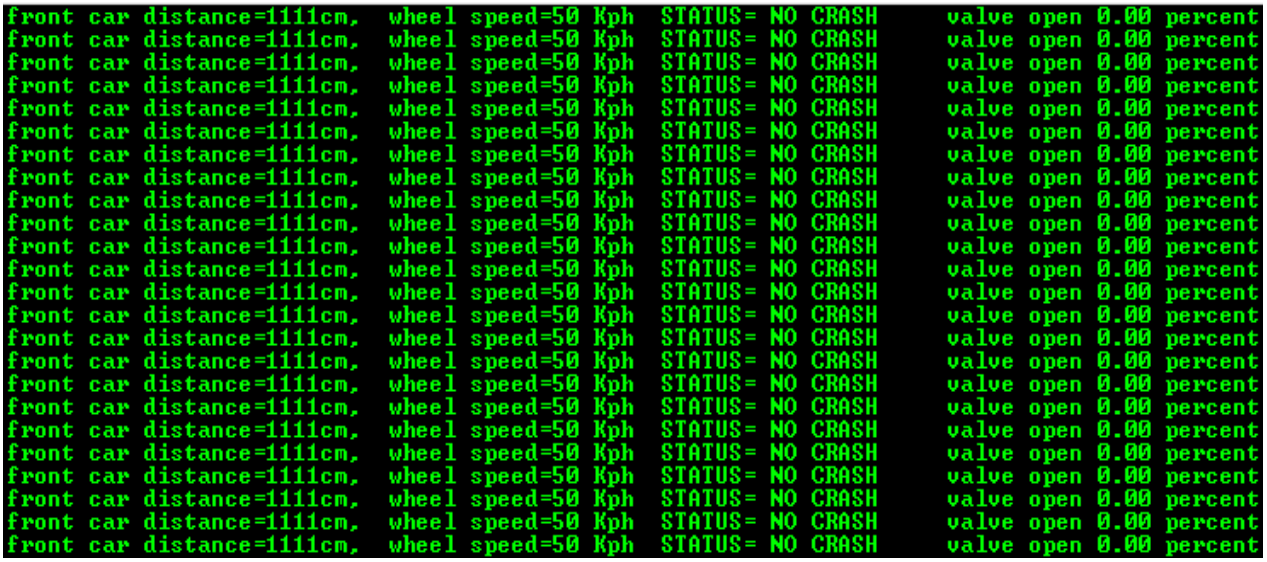

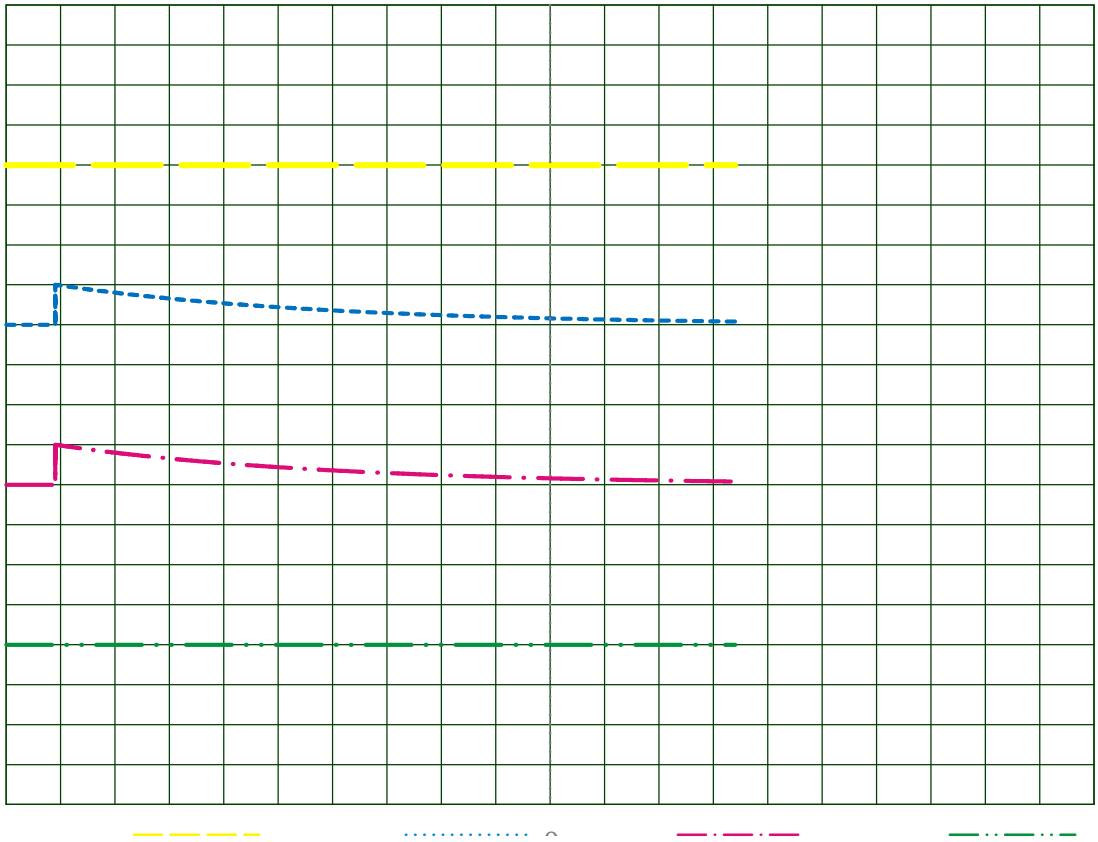

	Channel A	Channel B	Channel C	Channel D
V/Div	5.00 V	5.00 V	5.00 V	0.00 V
Offset	60.00 V	20.00 V	-20.00 V	-60.00 V
Invert	Normal	Normal	Normal	Normal
Coupling	AC	AC	AC	AC

Source	Horizontal		Trigger
Position	Trace	Source	Channel A
S/Div	2.00 S	Level	-2.00 V
	200.00 mS	Coupling	DC
		Edge	Rising
		Mode	Auto

Channel A Pressure
Channel B Distance
Channel C speed
Channel D valve condition

Figure 4.27 When Speed of the car is maximum and distance is maximum

As the above graph in figure 4.27 data shows the vehicle is at maximum speed (means at the top of the low-speed range). Channel c reads 50kph and the distance between the cars is also maximum

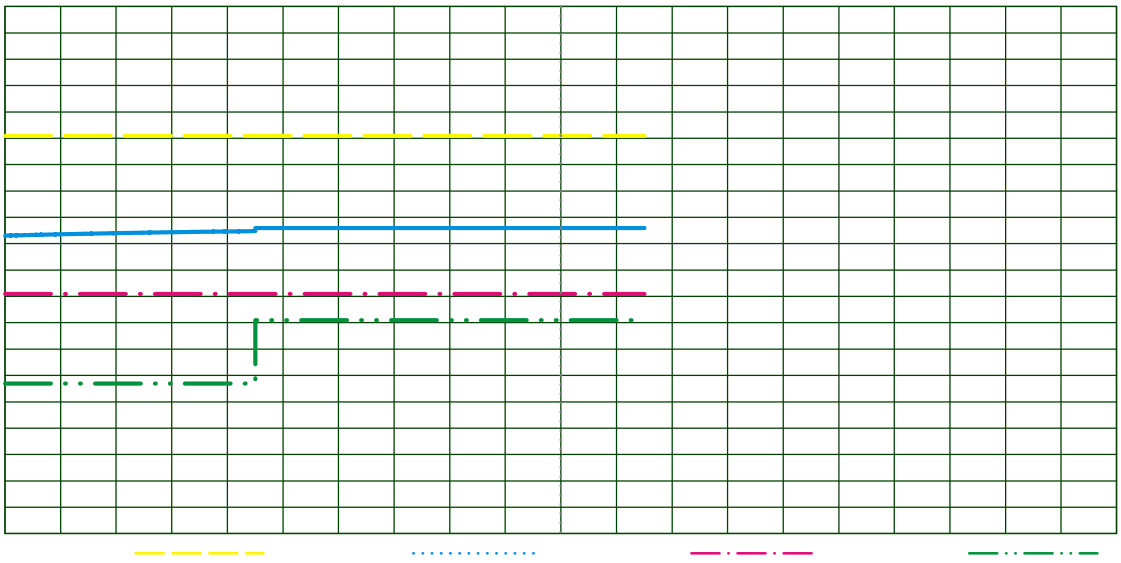

and channel c read 11m gap between the cars, this condition is not enough to trigger the valve so the valve remains closed and the signal voltage reading is 0-volt

- When speed of the car is maximum and the distance between colliding cars is minimum

```
front car distance=4cm,  wheel speed=50 Kph  STATUS= CRASH     valve open 40.00 percent
front car distance=4cm,  wheel speed=50 Kph  STATUS= CRASH     valve open 40.00 percent
front car distance=4cm,  wheel speed=50 Kph  STATUS= CRASH     valve open 40.00 percent
front car distance=4cm,  wheel speed=50 Kph  STATUS= CRASH     valve open 40.00 percent
front car distance=4cm,  wheel speed=50 Kph  STATUS= CRASH     valve open 40.00 percent
front car distance=4cm,  wheel speed=50 Kph  STATUS= CRASH     valve open 40.00 percent
front car distance=4cm,  wheel speed=50 Kph  STATUS= CRASH     valve open 40.00 percent
front car distance=4cm,  wheel speed=50 Kph  STATUS= CRASH     valve open 40.00 percent
front car distance=4cm,  wheel speed=50 Kph  STATUS= CRASH     valve open 40.00 percent
front car distance=4cm,  wheel speed=50 Kph  STATUS= CRASH     valve open 40.00 percent
front car distance=4cm,  wheel speed=50 Kph  STATUS= CRASH     valve open 40.00 percent
front car distance=4cm,  wheel speed=50 Kph  STATUS= CRASH     valve open 40.00 percent
front car distance=4cm,  wheel speed=50 Kph  STATUS= CRASH     valve open 40.00 percent
front car distance=4cm,  wheel speed=50 Kph  STATUS= CRASH     valve open 40.00 percent
front car distance=4cm,  wheel speed=50 Kph  STATUS= CRASH     valve open 40.00 percent
front car distance=4cm,  wheel speed=50 Kph  STATUS= CRASH     valve open 40.00 percent
front car distance=4cm,  wheel speed=50 Kph  STATUS= CRASH     valve open 40.00 percent
front car distance=4cm,  wheel speed=50 Kph  STATUS= CRASH     valve open 40.00 percent
front car distance=4cm,  wheel speed=50 Kph  STATUS= CRASH     valve open 40.00 percent
front car distance=4cm,  wheel speed=50 Kph  STATUS= CRASH     valve open 40.00 percent
front car distance=4cm,  wheel speed=50 Kph  STATUS= CRASH     valve open 40.00 percent
front car distance=4cm,  wheel speed=50 Kph  STATUS= CRASH     valve open 40.00 percent
```

	Channel A	Channel B	Channel C	Channel D
	— — — —	··············	—·—·—	—··—··—
V/Div	5.00 V	5.00 V	5.00 V	5.00 V
Offset	41.00 V	16.00 V	-19.00 V	-43.00 V
Invert	Normal	Normal	Normal	Normal
Coupling	DC	DC	DC	DC

	Horizontal		Trigger
Source	Trace	Source	Channel A
Position	2.00 S	Level	-2.00 V
S/Div	200.00 mS	Coupling	DC
		Edge	Rising
		Mode	Auto

— — *Channel A Pressure*

—— *Channel B Distance*

—— *Channel C speed*

—·· — *Channel D valve condition*

Figure 4.28 When Speed of the car is maximum and distance is minimum

As indicated in the figure 4.28, the vehicle was moving at a constant speed in a straight line and to check the response of the system in cross-traffic condition or sudden obstacle. The system is checked by suddenly decreasing the distance between the car to 4cm, in doing this when we see the channels reading channel A reads the condition of the pressure inside the air spring is at the required level by displaying the pressure sensor signal output which is 5 volts, channel B reads the sudden decrement of the distance between the cars, channel C displays the speed of the car was at a constant speed which is 50kph and channel D shows the response of the control valve, it shows the sudden opening of valve by 40%.

- When speed of the car is minimum and the distance between colliding cars is maximum

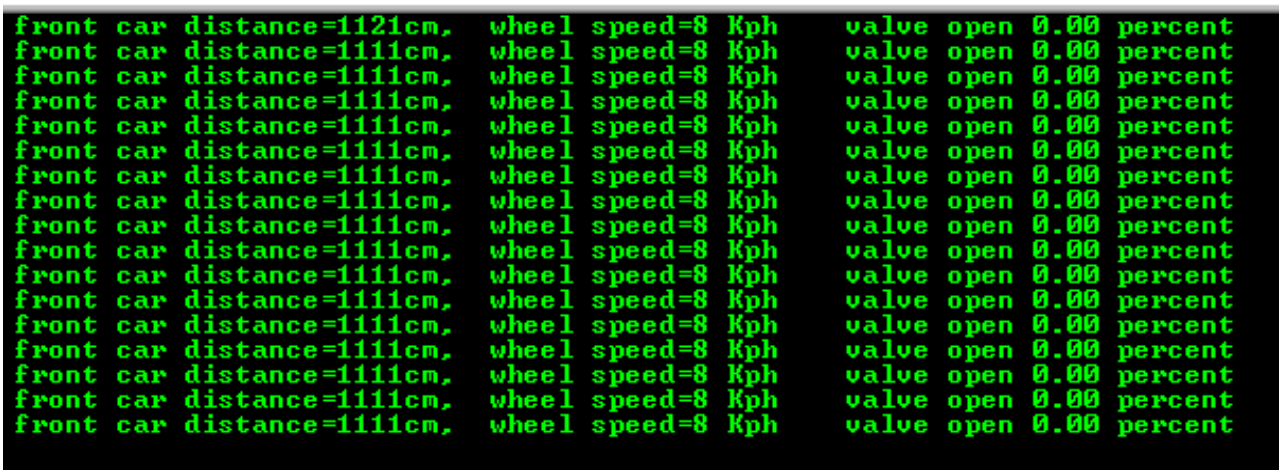

```
front car distance=1121cm,  wheel speed=8 Kph     valve open 0.00 percent
front car distance=1111cm,  wheel speed=8 Kph     valve open 0.00 percent
front car distance=1111cm,  wheel speed=8 Kph     valve open 0.00 percent
front car distance=1111cm,  wheel speed=8 Kph     valve open 0.00 percent
front car distance=1111cm,  wheel speed=8 Kph     valve open 0.00 percent
front car distance=1111cm,  wheel speed=8 Kph     valve open 0.00 percent
front car distance=1111cm,  wheel speed=8 Kph     valve open 0.00 percent
front car distance=1111cm,  wheel speed=8 Kph     valve open 0.00 percent
front car distance=1111cm,  wheel speed=8 Kph     valve open 0.00 percent
front car distance=1111cm,  wheel speed=8 Kph     valve open 0.00 percent
front car distance=1111cm,  wheel speed=8 Kph     valve open 0.00 percent
front car distance=1111cm,  wheel speed=8 Kph     valve open 0.00 percent
front car distance=1111cm,  wheel speed=8 Kph     valve open 0.00 percent
front car distance=1111cm,  wheel speed=8 Kph     valve open 0.00 percent
front car distance=1111cm,  wheel speed=8 Kph     valve open 0.00 percent
front car distance=1111cm,  wheel speed=8 Kph     valve open 0.00 percent
front car distance=1111cm,  wheel speed=8 Kph     valve open 0.00 percent
```

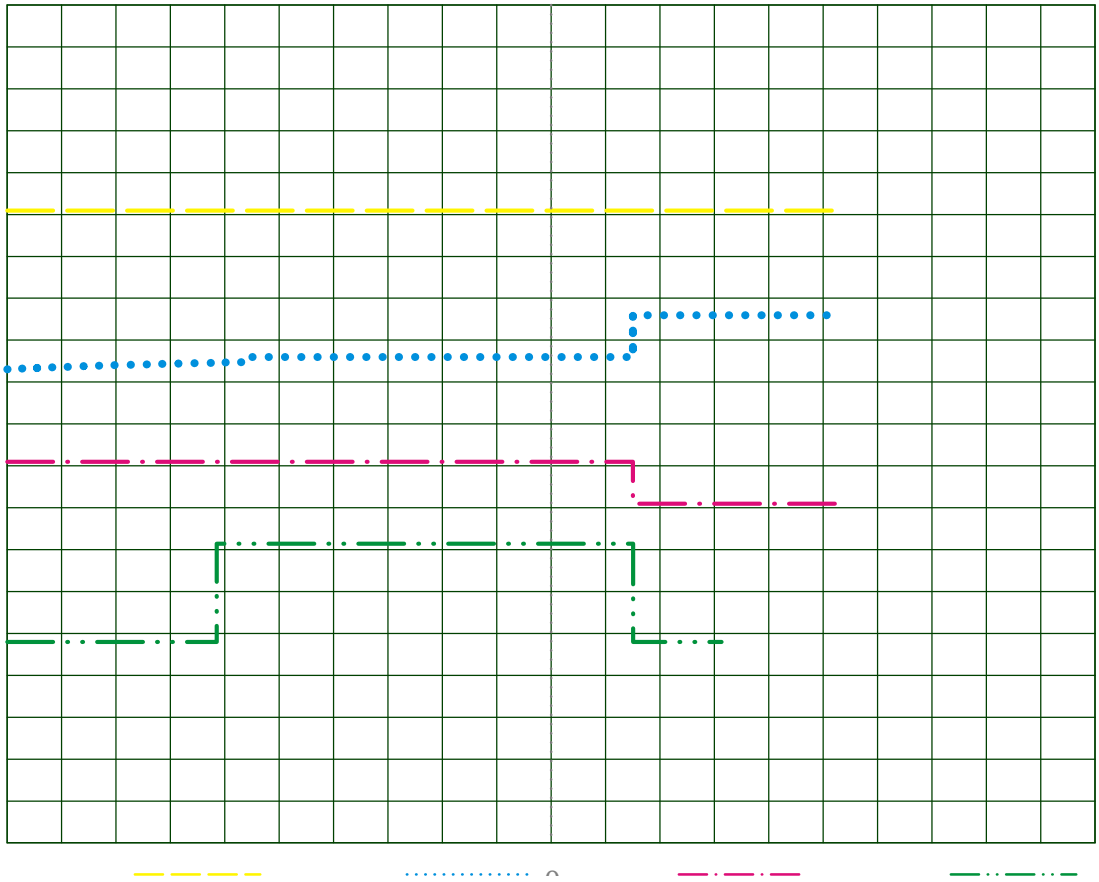

	Channel A	Channel B	Channel C	Channel D
V/Div	5.00 V	5.00 V	5.00 V	0.00 V
Offset	41.00 V	16.00 V	-19.00 V	-53.30 V
Invert	Normal	Normal	Normal	Normal
Coupling	DC	DC	DC	AC
Source	Horizontal		Trigger	
Position	Trace		Source	Channel A
S/Div	2.00 S		Level	-2.00 V
	200.00 mS		Coupling	DC
			Edge	Rising
			Mode	Auto

Channel A Pressure
Channel B Distance
Channel C speed
Channel D valve condition

Figure 4.29 When Speed of the car is minimum and distance is maximum

The response of the system when the vehicle speed is minimum and maximum distance is shown in the figure 4.29. In this extreme condition, the speed of the car suddenly drops to 8kph and the distance between the car rises to 11.1m at this condition the system compares the actual condition and the pre-condition set and maintain the valve condition in the closed state because the vehicle in motion has sufficient distance to bring the vehicle to 0kph. In line with this channel A reads the pressure is at the required level by giving 5 volts signal reading, Channel-B reading shows the ultrasonic sensor reading and indicates the distance is increasing, channel C reads the speed of the car drops to 8kph as the distance increases and speed drops Channel-D receives the command to fully closed the valve.

- When distance is constant and speed varies

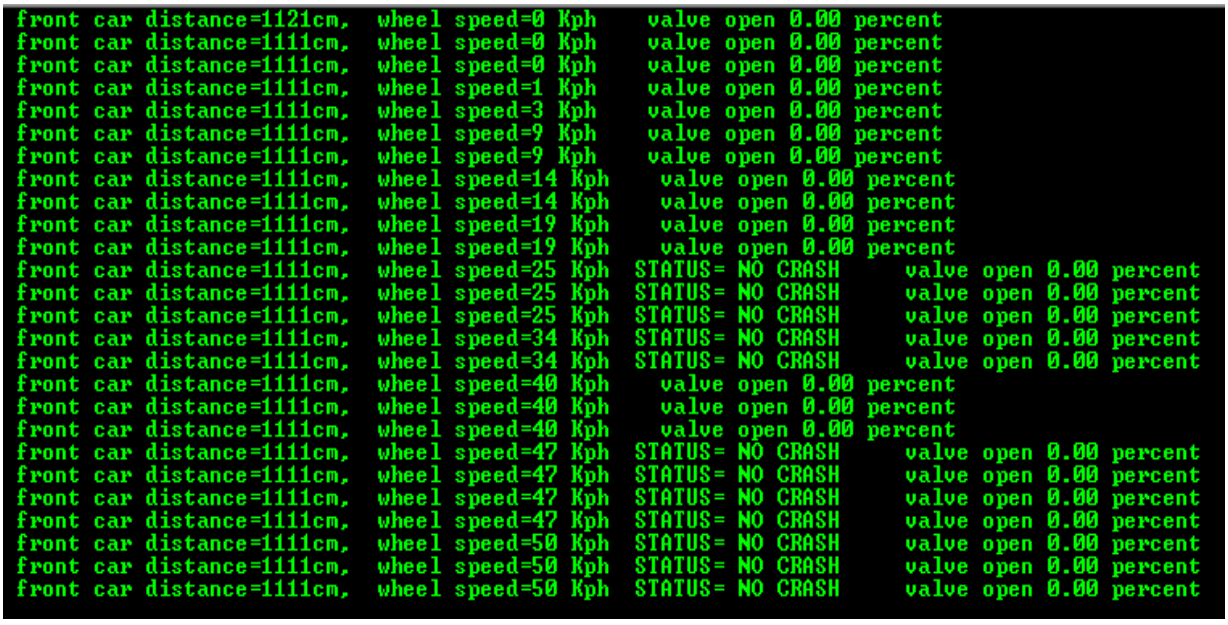

	Channel A	Channel B	Channel C	Channel D
V/Div	5.00 V	5.00 V	5.00 V	0.00 V
Offset	35.00 V	16.00 V	-19.00 V	-185.62 V
Invert	Normal	Normal	Normal	Normal
Coupling	DC	DC	DC	DC

Source	Horizontal	Source	Trigger Channel D
Position	Trace	Level	-8.63 V
S/Div	2.00 S 200.00 mS	Coupling	DC
		Edge	Rising
		Mode	Auto

Channel A Pressure
Channel B Distance
Channel C speed
Channel D valve condition

Figure 4.30 Distance constant but speed varies

Even if the speed of the car is increasing but the distance between the cars is constant or in a safe distance to bring the car to 0kph the valve remains in closed command. Channel A assures the air pressure inside the air spring is at the required level by giving 5volts signal output, channel B shows the distance is constant and 11.1m far, channel C shows the speed of the car is oscillating ranging from 0 to 50kph in line with this channel D shows the valve is in closed condition because of the car is in the safe distance from the colliding car. The response of the system is shown graphically in figure 4.30.

- When speed is constant and distance varies

```
front car distance=4cm,  wheel speed=50 Kph  STATUS= CRASH     valve open 40.00 percent
front car distance=4cm,  wheel speed=50 Kph  STATUS= CRASH     valve open 40.00 percent
front car distance=4cm,  wheel speed=50 Kph  STATUS= CRASH     valve open 40.00 percent
front car distance=4cm,  wheel speed=50 Kph  STATUS= CRASH     valve open 40.00 percent
front car distance=144cm,  wheel speed=50 Kph  STATUS= CRASH     valve open 40.00 percent
front car distance=144cm,  wheel speed=50 Kph  STATUS= CRASH     valve open 40.00 percent
front car distance=144cm,  wheel speed=50 Kph  STATUS= CRASH     valve open 40.00 percent
front car distance=282cm,  wheel speed=50 Kph  STATUS= CRASH     valve open 40.00 percent
front car distance=282cm,  wheel speed=50 Kph  STATUS= CRASH     valve open 40.00 percent
front car distance=283cm,  wheel speed=50 Kph  STATUS= CRASH     valve open 40.00 percent
front car distance=522cm,  wheel speed=50 Kph  STATUS= CRASH     valve open 60.00 percent
front car distance=522cm,  wheel speed=50 Kph  STATUS= CRASH     valve open 60.00 percent
front car distance=523cm,  wheel speed=50 Kph  STATUS= CRASH     valve open 60.00 percent
front car distance=522cm,  wheel speed=50 Kph  STATUS= CRASH     valve open 60.00 percent
front car distance=704cm,  wheel speed=50 Kph  STATUS= CRASH     valve open 90.00 percent
front car distance=704cm,  wheel speed=50 Kph  STATUS= CRASH     valve open 90.00 percent
front car distance=704cm,  wheel speed=50 Kph  STATUS= CRASH     valve open 90.00 percent
front car distance=760cm,  wheel speed=50 Kph  STATUS= CRASH     valve open 90.00 percent
front car distance=760cm,  wheel speed=50 Kph  STATUS= CRASH     valve open 90.00 percent
front car distance=760cm,  wheel speed=50 Kph  STATUS= CRASH     valve open 90.00 percent
front car distance=900cm,  wheel speed=50 Kph  STATUS= NO CRASH     valve open 0.00 percent
front car distance=900cm,  wheel speed=50 Kph  STATUS= NO CRASH     valve open 0.00 percent
front car distance=900cm,  wheel speed=50 Kph  STATUS= NO CRASH     valve open 0.00 percent
front car distance=982cm,  wheel speed=50 Kph  STATUS= NO CRASH     valve open 0.00 percent
front car distance=982cm,  wheel speed=50 Kph  STATUS= NO CRASH     valve open 0.00 percent
front car distance=982cm,  wheel speed=50 Kph  STATUS= NO CRASH     valve open 0.00 percent
front car distance=1111cm,  wheel speed=50 Kph  STATUS= NO CRASH     valve open 0.00 percent
front car distance=1111cm,  wheel speed=50 Kph  STATUS= NO CRASH     valve open 0.00 percent
front car distance=1111cm,  wheel speed=50 Kph  STATUS= NO CRASH     valve open 0.00 percent
front car distance=1111cm,  wheel speed=50 Kph  STATUS= NO CRASH     valve open 0.00 percent
front car distance=1111cm,  wheel speed=50 Kph  STATUS=
```

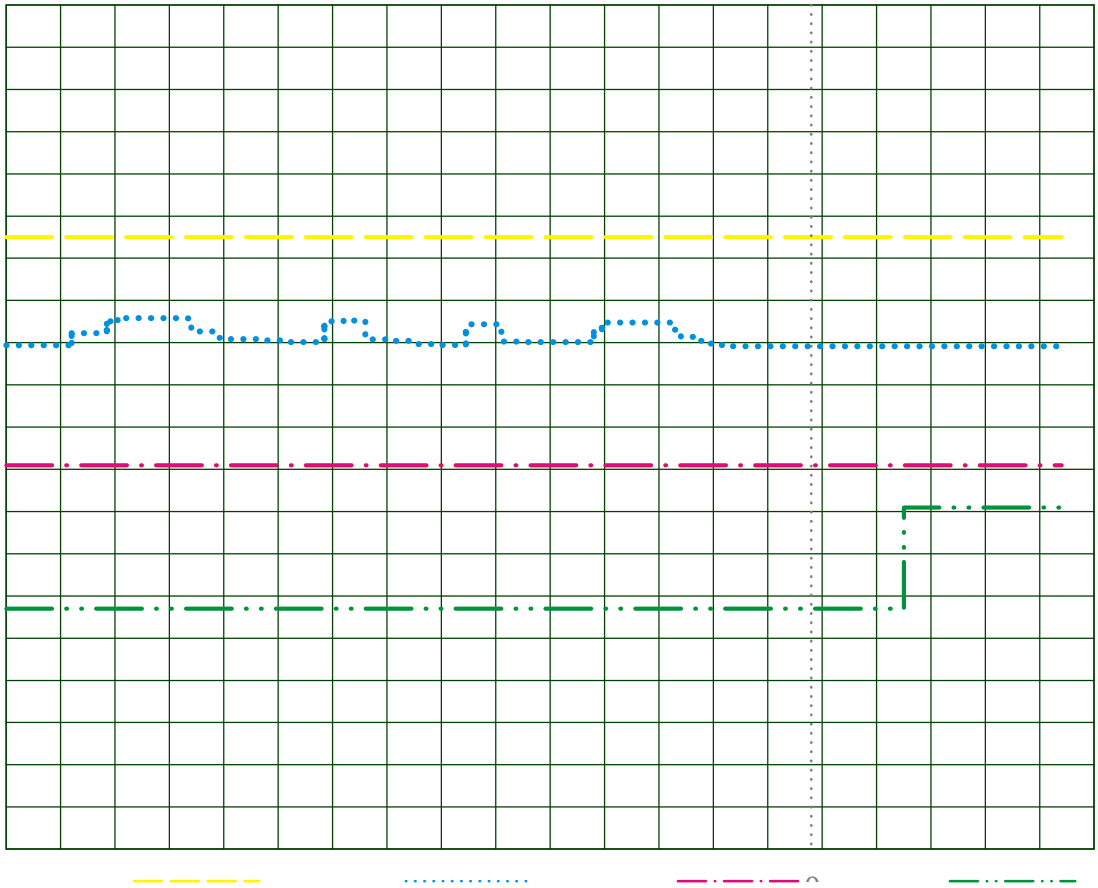

	Channel A	Channel B	Channel C	Channel D
V/Div	5.00 V	5.00 V	5.00 V	0.00 V
Offset	35.00 V	16.00 V	-19.00 V	5.00 V
Invert	Normal	Normal	Normal	-43.00 V
Coupling	DC	DC	DC	Normal
				DC

Source	Horizontal		Trigger
Position	Trace	Source	Channel D
S/Div	1.48 S	Level	-2.00 V
	100.00 mS	Coupling	DC
		Edge	Rising
		Mode	Auto

Channel A Pressure
Channel B Distance
Channel C speed
Channel D valve condition

Figure 4.31 Speed constant but distance varies

In this condition as shown in the figure 4.31 the speed of the car is constant 50kph and the distance between cars in varying from 4 cm to 1111 cm Channel A assures the air pressure inside the air spring is at the required level by giving 5volts signal output, channel B shows the distance oscillating with the above range, C shows the speed of the car is constant that is 50 kph and channel D shows the operation of valve opens up to 90% when the condition is in crash state and closed when the distance is maximum.

- Dynamic operating condition

```
front car distance=1121cm,  wheel speed=50 Kph  STATUS= NO CRASH     valve open 0.00 percent
front car distance=1111cm,  wheel speed=50 Kph  STATUS= NO CRASH     valve open 0.00 percent
front car distance=1111cm,  wheel speed=42 Kph  STATUS= NO CRASH     valve open 0.00 percent
front car distance=922cm,   wheel speed=42 Kph  STATUS= NO CRASH     valve open 0.00 percent
front car distance=922cm,   wheel speed=42 Kph  STATUS= NO CRASH     valve open 0.00 percent
front car distance=352cm,   wheel speed=42 Kph  STATUS= CRASH      valve open 40.00 percent
front car distance=255cm,   wheel speed=42 Kph  STATUS= CRASH      valve open 40.00 percent
front car distance=255cm,   wheel speed=42 Kph  STATUS= CRASH      valve open 40.00 percent
front car distance=255cm,   wheel speed=5 Kph    valve open 0.00 percent
front car distance=255cm,   wheel speed=5 Kph    valve open 0.00 percent
front car distance=255cm,   wheel speed=5 Kph    valve open 0.00 percent
front car distance=255cm,   wheel speed=5 Kph    valve open 0.00 percent
front car distance=255cm,   wheel speed=50 Kph  STATUS= CRASH      valve open 40.00 percent
front car distance=255cm,   wheel speed=50 Kph  STATUS= CRASH      valve open 40.00 percent
front car distance=255cm,   wheel speed=50 Kph  STATUS= CRASH      valve open 40.00 percent
front car distance=255cm,   wheel speed=50 Kph  STATUS= CRASH      valve open 40.00 percent
front car distance=1045cm,  wheel speed=50 Kph  STATUS= NO CRASH     valve open 0.00 percent
front car distance=1045cm,  wheel speed=50 Kph  STATUS= NO CRASH     valve open 0.00 percent
front car distance=1045cm,  wheel speed=21 Kph  STATUS= NO CRASH     valve open 0.00 percent
front car distance=482cm,   wheel speed=21 Kph  STATUS= NO CRASH     valve open 0.00 percent
front car distance=482cm,   wheel speed=21 Kph  STATUS= NO CRASH     valve open 0.00 percent
front car distance=482cm,   wheel speed=21 Kph  STATUS= NO CRASH     valve open 0.00 percent
front car distance=482cm,   wheel speed=21 Kph  STATUS= NO CRASH     valve open 0.00 percent
front car distance=744cm,   wheel speed=37 Kph  STATUS= NO CRASH     valve open 0.00 percent
front car distance=744cm,   wheel speed=37 Kph  STATUS= NO CRASH     valve open 0.00 percent
front car distance=744cm,   wheel speed=37 Kph  STATUS= NO CRASH     valve open 0.00 percent
front car distance=355cm,   wheel speed=37 Kph  STATUS= CRASH      valve open 60.00 percent
front car distance=355cm,   wheel speed=37 Kph  STATUS= CRASH      valve open 60.00 percent
front car distance=355cm,   wheel speed=37 Kph  STATUS= CRASH      valve open 60.00 percent
front car distance=355cm,   wheel speed=37 Kph  STATUS= CRASH      valve open 60.00 percent
front car distance=355cm,   wheel speed=37 Kph  STATUS= CRASH      valve open 60.00 percent
front car distance=355cm,   wheel speed=37 Kph  STATUS= CRASH      valve open 60.00 percent
front car distance=355cm,   wheel speed=12 Kph  STATUS= NO CRASH     valve open 0.00 percent
front car distance=355cm,   wheel speed=12 Kph  STATUS= NO CRASH     valve open 0.00 percent
front car distance=355cm,   wheel speed=12 Kph  STATUS= NO CRASH     valve open 0.00 percent
front car distance=4cm,   wheel speed=12 Kph  STATUS= CRASH      valve open 7.78 percent
front car distance=4cm,   wheel speed=12 Kph  STATUS= CRASH      valve open 7.78 percent
front car distance=4cm,   wheel speed=12 Kph  STATUS= CRASH      valve open 7.78 percent
front car distance=4cm,   wheel speed=0 Kph    valve open 0.00 percent
front car distance=4cm,   wheel speed=0 Kph    valve open 0.00 percent
front car distance=4cm,   wheel speed=0 Kph    valve open 0.00 percent
front car distance=4cm,   wheel speed=0 Kph    valve open 0.00 percent
front car distance=4cm,   wheel speed=0 Kph    valve open 0.00 percent
front car distance=4cm,   wheel speed=48 Kph  STATUS= CRASH      valve open 40.00 percent
front car distance=4cm,   wheel speed=48 Kph  STATUS= CRASH      valve open 40.00 percent
front car distance=4cm,   wheel speed=48 Kph  STATUS= CRASH      valve open 40.00 percent
front car distance=1111cm,  wheel speed=48 Kph  STATUS= NO CRASH     valve open 0.00 percent
front car distance=1111cm,  wheel speed=48 Kph  STATUS= NO CRASH     valve open 0.00 percent
```

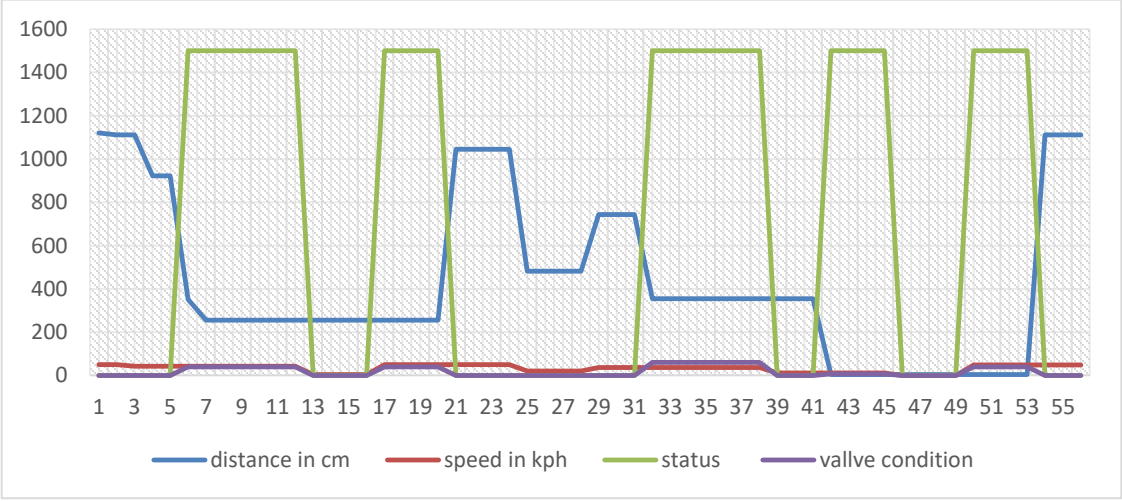

Figure 4.32 Dynamic operating condition

The graph in figure 4.32 clearly shows the random simulation of the above extreme condition with an extended time frame to easily visualize the relationship between valve diameter, speed, and distance in a car dynamic operation. As the graph shows the system compares the distance and the speed of the car to give the command to the valve controlling mechanism.

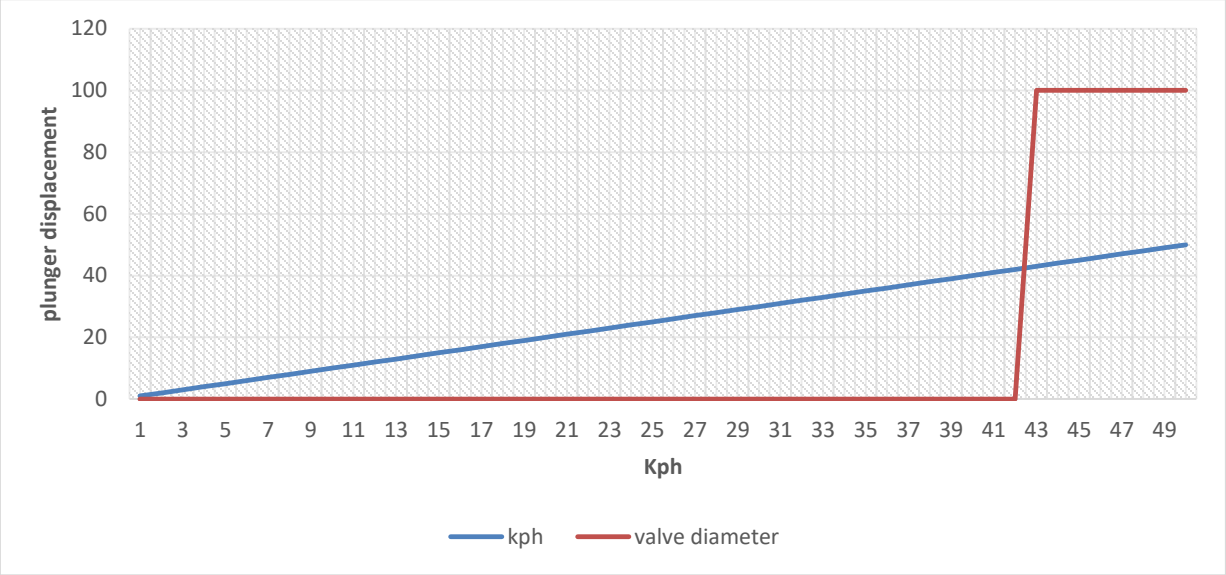

Figure 4.33 Valve control solenoid operation with respect to speed of the car

The above graph in figure 4.33 shows if the distance between the driving car and obstacle car is constant and then the speed of driving a car is constantly increasing, at this time the ultrasonic sensor senses the gap between cars and by this information the microcontroller analyzes the preset condition and ready to open the quick exhaust valve at 100% when the speed reaches about 42kph.

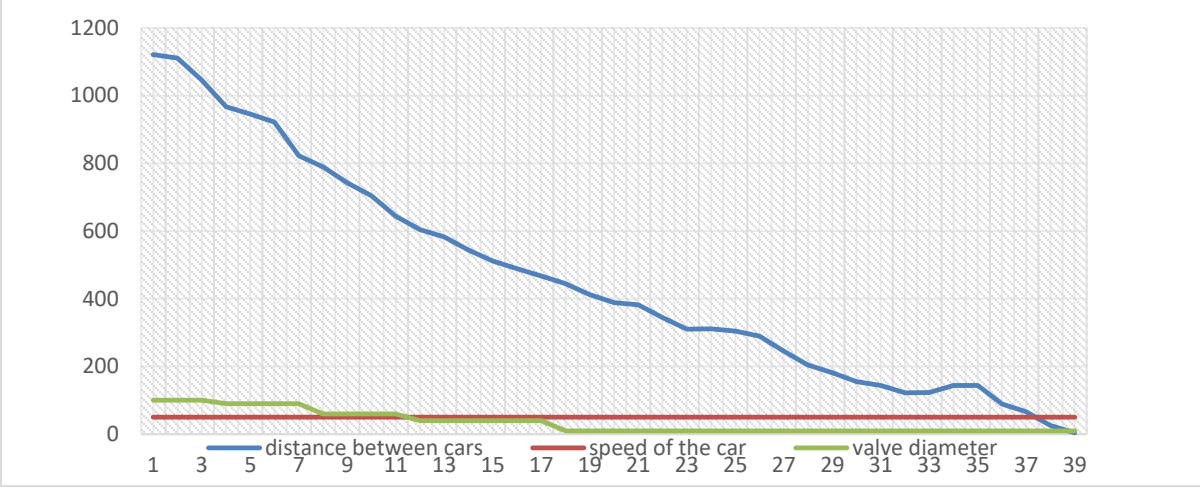

Figure 4.34 The relationship between distance, speed and valve diameter

The above graph in figure 4.34 shows the relation between car speeds, the distance between the car and valve diameter. Even if the speed of the car is constant and the ultrasonic sensor reads the distance between the cars is decreasing the microcontroller compares the real-time situation with the preset values and actuates the quick exhaust valve based on the parameter.

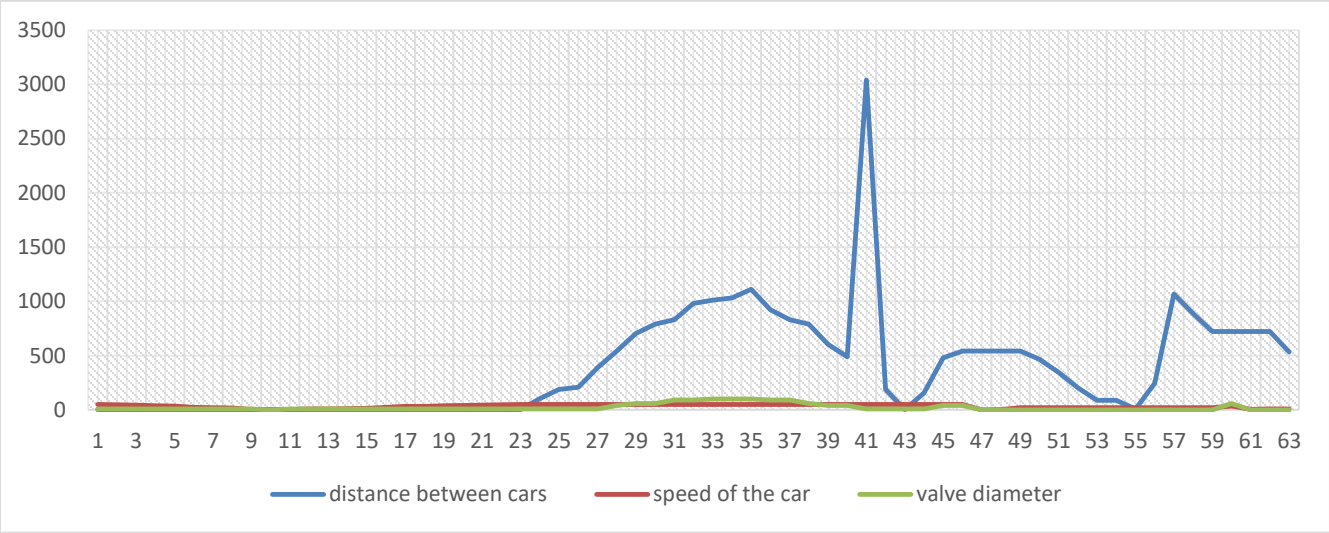

Figure 4.35 Real time behavior of the system

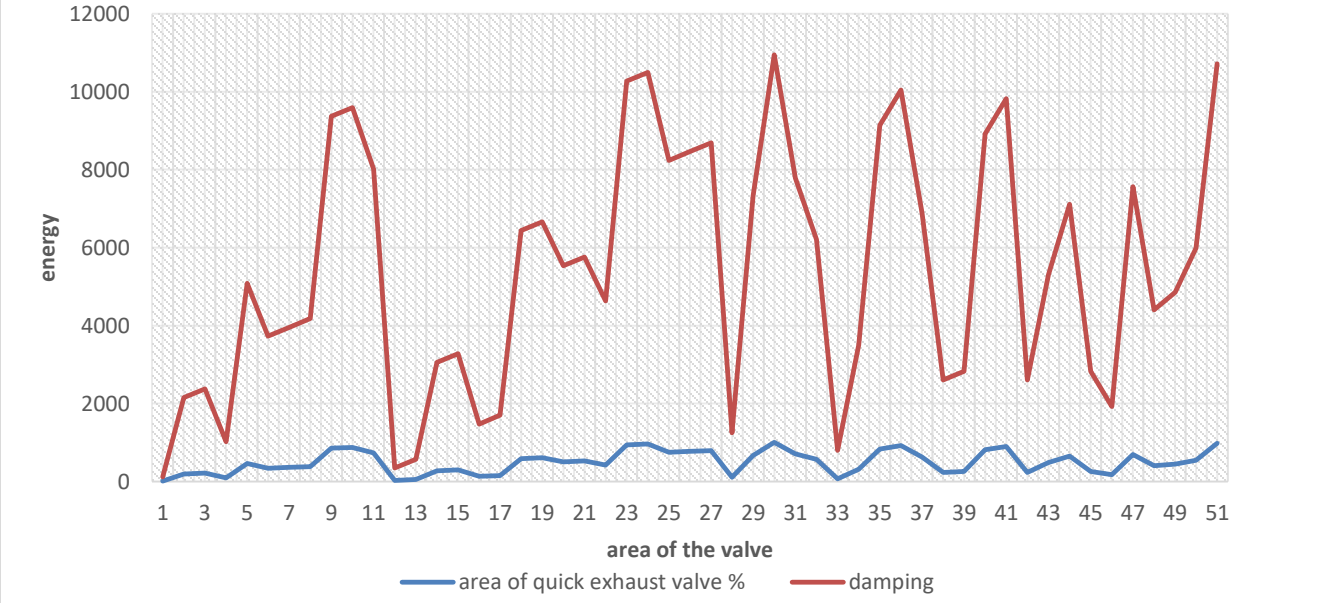

Figure 4.36 Valve diameter vs damping

Beyond simulation of the response and the integration of the system damping the impact during the crash is important as indicated in the graph in figure 4.36 the damping of the crash energy is

achieved by controlling the quick exhaust valve mounted at the bottom plate of the air spring. The diameter of the valve is controlled by a linear motor plunger plugged into the valve port.

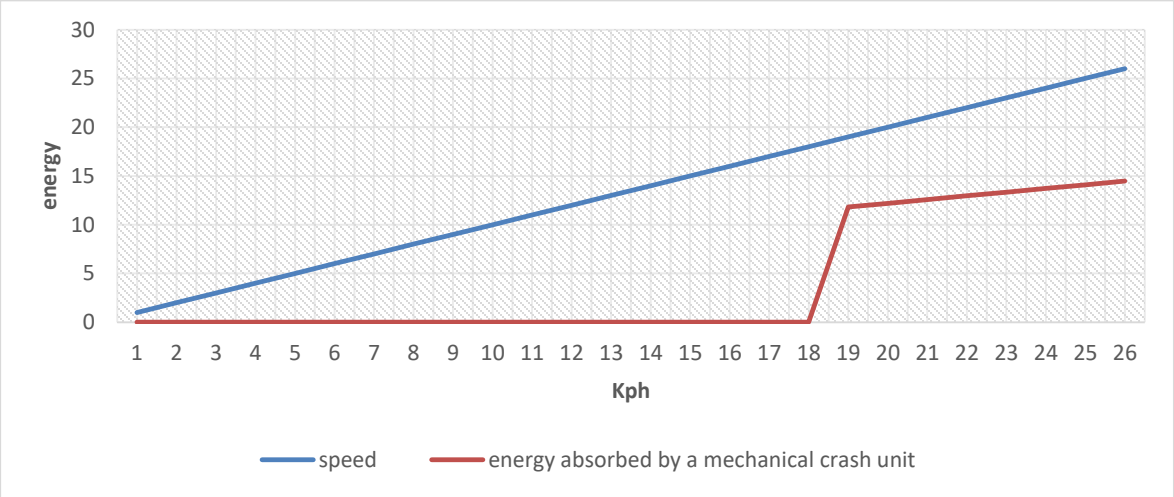

Figure 4.37 Behavior of mechanical cashbox

For comparison the mechanical crash box is capable of absorbing crash energy when the vehicle is above a certain speed, as the above graph in figure 4.37 shows when the vehicle is crash at 18 kph about 11.818 kJ of energy is absorbed, for the crash below 18kph. the crash box didn't absorb impact energy.

Table 4.2 comparison between crash box and adaptive pneumatic impact absorber

	Crash box	Air spring
Upper effective limit	43kph	50kph
Stiffness	Constant	Varying with the severity of the crash
Low effective limit	18kph	1kph

As shown in the table 4.2 the simulation result of the crash box indicates the box effective range is from 18kph of the vehicle up to 43kph, which indicates that the impact below 18kph is absorbed by the additional equipment fitted in the front of the vehicle, and the impact above 43kph passes to the front chassis rail and causes component damage and driver acceleration towards the steering wheel. The air spring operating range is between 4kph up to 50kph which is much better than the crash box range and eliminates the requirements of additional components. As per the rule of national traffic and motor vehicle safety act heavy opponents needs stiffer structure and in case of

lighter opponent less stiff or soft impact absorber is required, to fulfill this requirement the air spring adjusts the stiffness based on the opponent type by controlling the amount of air in the system but, crash box didn’t do so.

CHAPTER FIVE

CONCLUSION AND RECOMMENDATION

5.1. Summary

A low-speed electro-pneumatic frontal-impact absorption system is a system designed to reduce the occupant injuries and vehicle components damaged during the low-speed collision. The system uses a controllable damping element called air spring and controlling element called microcontroller by receiving the input data through sensors and send signals to the actuators.

Air spring is modeled and simulated in ABAQUS software by making the top and bottom plate as a rigid body and fixing the bottom plate for all displacements and free top plate in the y-direction.

First, the air spring is inflated to the pressure equals to P_g and compressed in the negative y-direction, this helps to stimulate the maximum stress condition.

To control the system different electrical sensors, controllers, and actuators are used. At the back of the air spring, the pressure sensor is mounted to control the amount of pressure needed in the air spring, the compressor control system is coded to pre-conditions to maintain the amount of pressure needed and to make idle the control system when the situation is in a crash situation.

At the front end of the bumper, three ultrasonic sensors are mounted to sense the approaching obstacle distance and it works in the principle of releasing sound with frequencies higher than 20 kHz which is not heard by humans and measuring the wave returning duration to the receiver, then the voltage output from the ultrasonic sensor used as a signal to tell whether the obstacle is near to the vehicle or far enough. The microcontroller is coded with the ARDUINO software by studying the real-time scenarios and it uses the input from the ultrasonic sensor as one input to process and decide the amount of quick exhaust valve opening diameter. In line with the ultrasonic sensing, the vehicle speed is sensed, and then the microcontroller compares the distance and the speed of the car and decides whether the car can achieve 0 kph within this distance or not if the distance is not sufficient to bring the car to full stop it considers the situation as the crash situation and if the reverse happens it considers the situation as no crash condition.

If the situation is in a crash situation and the distance is minimum in the range the microcontroller sends the signal to the quick exhaust valve. The valve is controlled by a built-in linear motor

mounted in the port controlling plunger. When the signal from the controller is released it actuates the linear motor to open and close the exhaust port, the amount of opening and closing of the port is directly proportional to the severity of the crash which is decided by the microcontroller based on the input. All the sensing, processing and actuation is performed within 15 micro-seconds.

5.2. Conclusion

To reduce the damage in the vehicle components and occupant injuries adaptive electro-pneumatic system is used, this designed system mounted in the vehicle frontal structure. Then the system operation is animated in Proteus 8 Professional results of electro-pneumatic shows a sufficiently good agreement with the physical parameter taken and the controlled system able to execute and take action within 15micro second which is less than the impact duration for the low-speed frontal crash.

To check the response and operation of the system the following dynamic operation condition is simulated and the result is as follow

When both the Speed and distance between colliding cars are minimum in this condition the probability of a crash between the cars is very low so the valve condition remains closed.

The speed of the car is maximum and the distance between colliding cars maximum in such a scenario the vehicle is at 50 kph and the distance between the cars is 11m apart this condition is not enough to trigger the valve so the valve remains closed and the signal voltage reading is 0-volt.

The speed of the car is maximum and the distance between colliding cars minimum the system is checked by suddenly decreasing the distance between the car to 4cm, and the speed of the car was at a constant speed which is 50kph and quick exhaust valve opens about 40%.

Speed of the car is minimum and the distance between colliding cars maximum in this extreme condition the speed of the car suddenly drops to 8kph and the distance between the car rises to 11.1 m at this condition the system compares the actual condition and the pre-condition set and maintain the valve condition in the closed state because the vehicle in motion has sufficient distance to bring the vehicle to 0kph.

Distance constant but speed varies even if the speed of the car is increasing but the distance between the cars is constant or in a safe distance to bring the car to 0kph the valve remains in closed command.

5.3. Recommendations

In today's world cars creates land mobility, in line with this safety is the major issue, low-speed electro-pneumatic frontal-impact absorption system is a passive safety system so it is important to use the system to reduce the damage to the vehicle component and occupant injuries during a low-speed frontal collision. The following points are recommended points as a future work:

- The system effectiveness is checked for a limited speed range, so more test should be performed to make the system operational for a better range.
- As the result shows the system is effective for crossover vehicles, it is important to adapt for other classes.
- In this work the system effectiveness is checked only for frontal head-on crash, it is recommended to check for different crash scenarios for a better safety improvements of the vehicle.

5.4. Future work

The future of automotive technology is towards electrification and electrical controls, this allows to easily providing advanced and automated active safety system. And the automation development trend shows the coming control system is machine learning, this technology allows loading every crash scenario by machine learning logic and making the system more efficient by making autonomous.

REFERENCES

Balamurugan, and Sekar (2017). Design of Shock Absorber for Car Front Bumper. International Journal of Science Technology & Engineering. Department of Mechanical Engineering Government College of Technology. Coimbatore. India. Issue 09, Volume 3.

David Woo, Seung-Bok Choi, Young Tae Choi and Norman M. Wereley (2007). Frontal Crash Mitigation Using MR Impact Damper for Controllable Bumper Smart Structures and Systems Laboratory. Department of Mechanical Engineering Inha University. Incheon. Korea. Journal of Intelligent Material Systems and Structures. Volume 1.

Devi. B, Krishna.C, and Swaroop (2014). Design Simulation of Crash Box in Car. Mlr Institute of Technology. International Journal of Engineering Research & Technology. Issue 1, volume 3.

G. Nagel and D. Thambiratnam (2002). Energy Absorption and Performance of a Vehicle Impact Protection System Physical Infrastructure Centre. School of Civil Engineering, Queensland University of Technology, Australia. Structures under Shock and Impact. Volume 7.

Ghasemnejad, Hadavinia, Marchant and Aboutorabi (2008). Crashworthiness of Thin-Walled Corrugated Crash Box in Axial Crushing. Structural Durability and Health Monitoring. Volume 098.

Hao Chen, Yali Yang and 'Liangjie Wang (2015). Vehicle Front Structure Energy Absorbing Optimization in Frontal Impact. College of Automotive Engineering, Shanghai University of Engineering Science, Shanghai, China. Mechanical Engineering Journal.

Jain and Sreekumar (2016). The Proof of Concept Design of a Novel 4-Stage Collision Energy Absorption System Mounted in the Front Overhang of Passenger Cars. Indian Institute of Information Technology Design and Manufacturing, Kancheepuram Melakottaiyur. 6th International & 27th All India Manufacturing Technology, Design and Research Conference.

Liuyan Jie,and Ding Lin, (2014). Influence of Material Properties on Automobile Energy-Absorbing Components Crashworthiness. College of Civil Engineering, Heilongjiang University, China. The Open Mechanical Engineering Journal.

Meghana, Ch. Shashikanth, and Kumar (2016). Impact Analysis of Bumper and Car Chassis Frame Due to Frontal Collision for Different Materials Namely Aluminium Alloy (6061), Stainless Steel, Structural Steel and Carbon Epoxy 2. International Journal of Engineering and Management Research, Issue-1 Volume-6, Page Number: 131-135.

Muhammad Nasiruddin S., Hambali A., Rosidah J. and Widodo W.S. and Ahmad M.N (2017). A Review of Energy Absorption of Automotive Bumper Beam. Faculty of Manufacturing Engineering, Universiti Teknikal Malaysia Melaka, International Journal of Applied Engineering Research. Issn 0973-4562, Volume 12.

Nagel and Thambiratnam (2002). Energy Absorption and Performance of a Vehicle Impact Protection System. Physical Infrastructure Centre, School of Civil Engineering, Queensland University of Technology, Australia. Volume 7.

Nasiruddin, Hambali, Rosidah J, Widodo and Ahmad (2017). A Review of Energy Absorption of Automotive Bumper Beam. Faculty of Manufacturing Engineering, University Teknikal Malaysia Melaka. International Journal of Applied Engineering Research ISSN 0973-4562 Volume 12, Number 2.

Nial J. Wykes, Mervgn J. Edwards, C. Adrian Hobbs (2004). Compatibility Requirements for Cars in Frontal and Side Impact. Transport Research Laboratory United Kingdom Paper Number 98-S3-O-04.

Ostrowski, Holnicki-Szulc, and Griskevicius (2007). Adaptive Crashworthiness of Front-End Structure of Motor Vehicles. Kaunas University of Technology. SAE International Journal of Passenger Cars.

Paulius Griskevicius (2007). Adaptive Crashworthiness of Front-End Structure of Motor Vehicles. Kaunas University of Technology. SAE International Journal of Passenger Cars.

Pulkit Sharma, Ram Mohan Telikicherla, Sai Nizampatnam, Viswanathan Parthasarathy (2016). Design Optimization of Vehicle Components for Full Frontal Crash.

R. Balamurugan (2017). Design of Shock Absorber for Car Front Bumper. Department of Mechanical Engineering Government College of Technology, Coimbatore, India, International Journal of Science Technology & Engineering, Volume 3, Issue 09.

Sakhare (2017). Chassis Impact Analysis. Department of Mechanical Engineering, India College of Engineering and Management, Pune Savitribai Phule Pune University, India. International Journal on Theoretical and Applied Research in Mechanical Engineering. Issue-1, Volume -6.

Shashank Jain and Sreekumar M. (2016). The Preliminary Design of a Collision Energy Absorption System. Indian Institute of Information Technology Design and Manufacturing, Kancheepuram Melakottaiyur, Chennai, Tamil Nadu, India.

Sharma, Telikicherla, Nizampatnam, and Parthasarathy (2016). Design Optimization of Vehicle Components for Full Frontal Crash. Advances in Mechanical Engineering, volume 10.

Suraj S Deshmukh and Gareth H Mckinley (2006). Adaptive Energy-Absorbing Materials Using Field-Responsive Fluid-Impregnated Cellular Solids. Department of Mechanical Engineering and Institute of Soldier Nanotechnologies, Massachusetts Institute of Technology, Cambridge. Smart materials and structures.

Tiago Nunes (2017). Multi-Objective Design Optimization of a Frontal Crash Energy Absorption System for A Road-Safe Vehicle, Portugal.

Willem Witteman (1999). Adaptive Frontal Structure Design to Achieve Optimal Deceleration Pulses. The Netherlands Paper Number 05-0243.

APPENDIX A: DRAWING

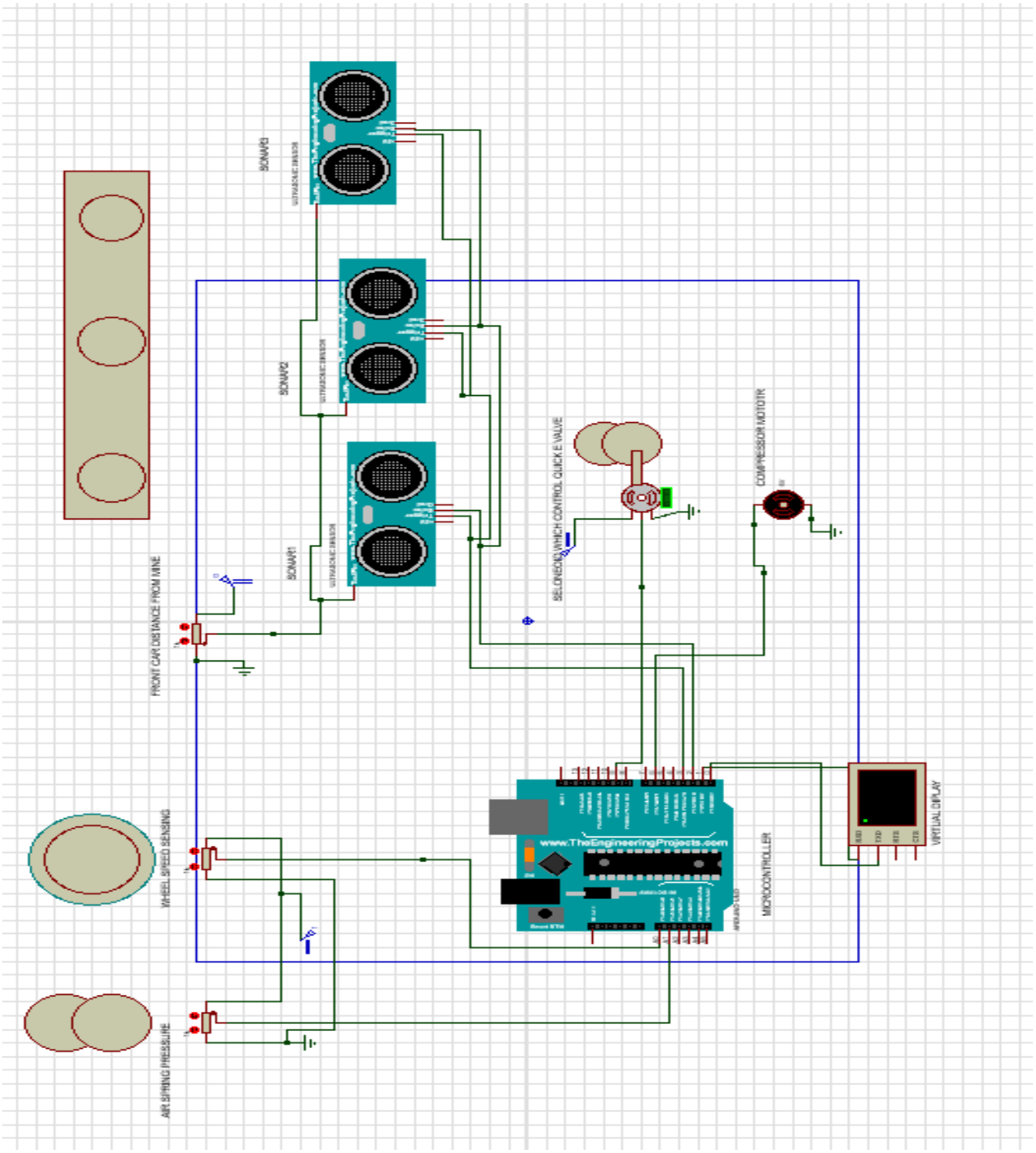

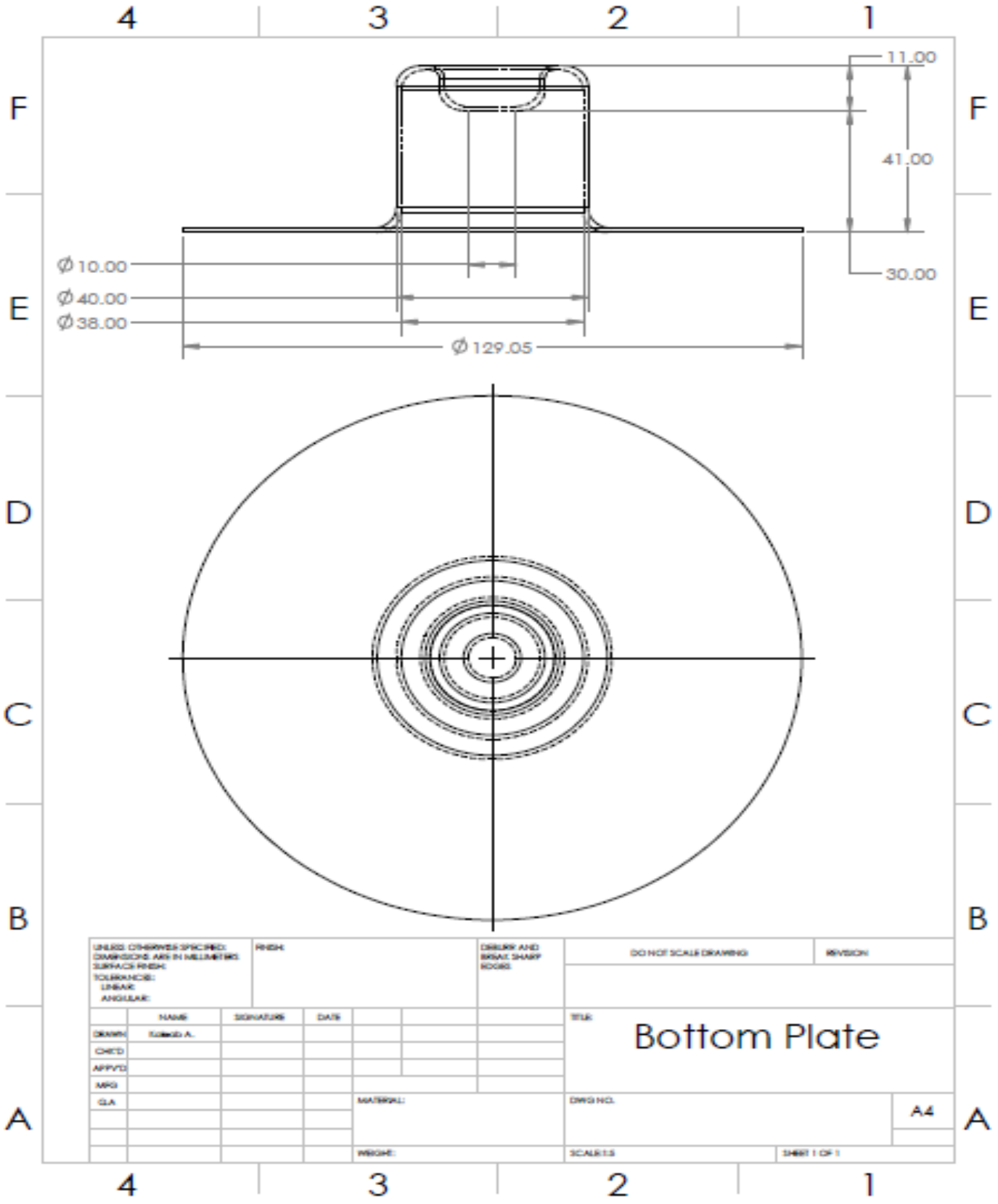
4
3
2
1
F
E
D
C
B
A
11.00
41.00
30.00
Ø 10.00
Ø 40.00
Ø 38.00
Ø 129.05
Bottom Plate
A4

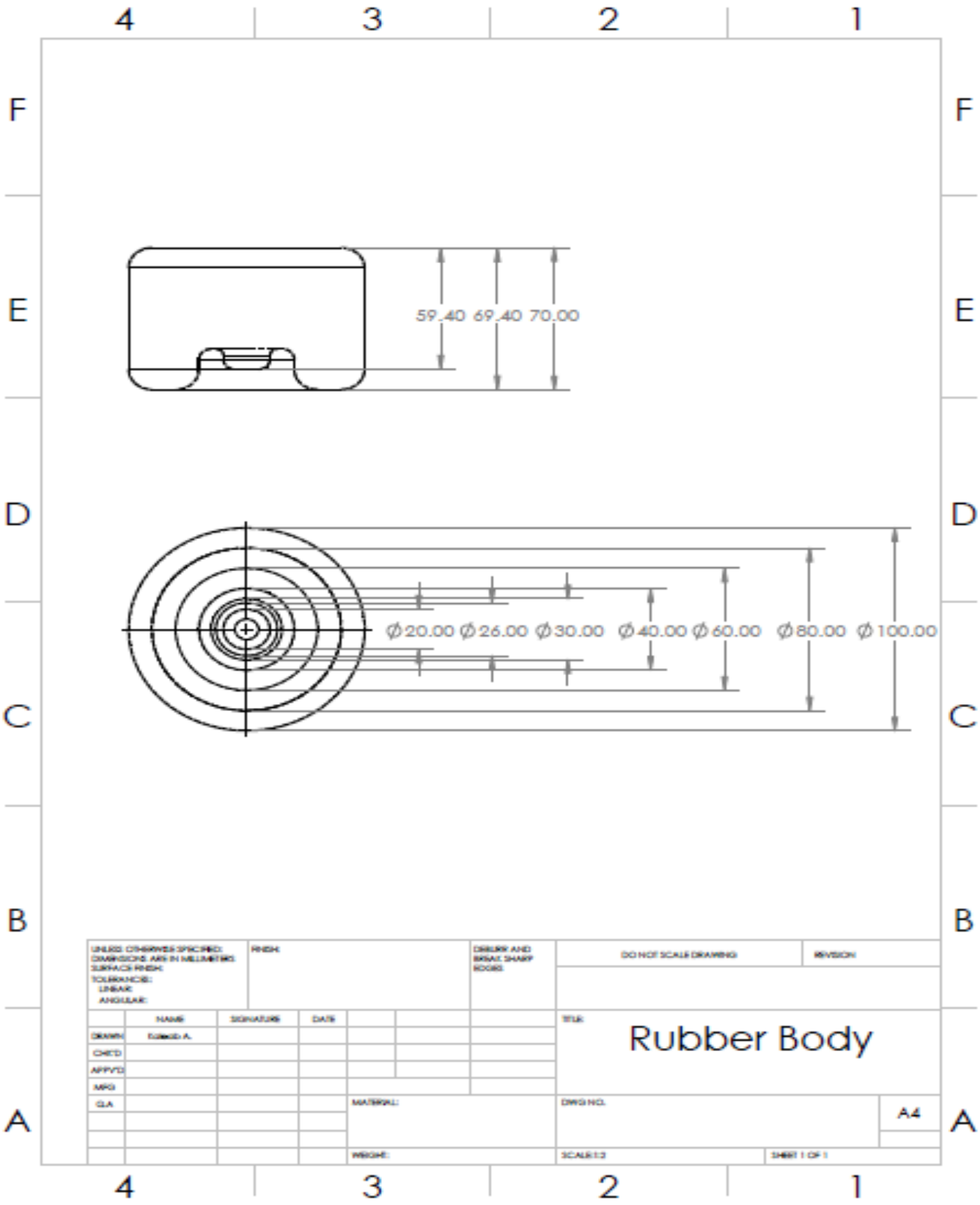
4
3
2
1
F
E
D
C
B
A
59.40 69.40 70.00
Ø20.00 Ø26.00 Ø30.00 Ø40.00 Ø60.00 Ø80.00 Ø100.00
DO NOT SCALE DRAWING
REVISION
TITLE:
Rubber Body
A4
SCALE:1:2

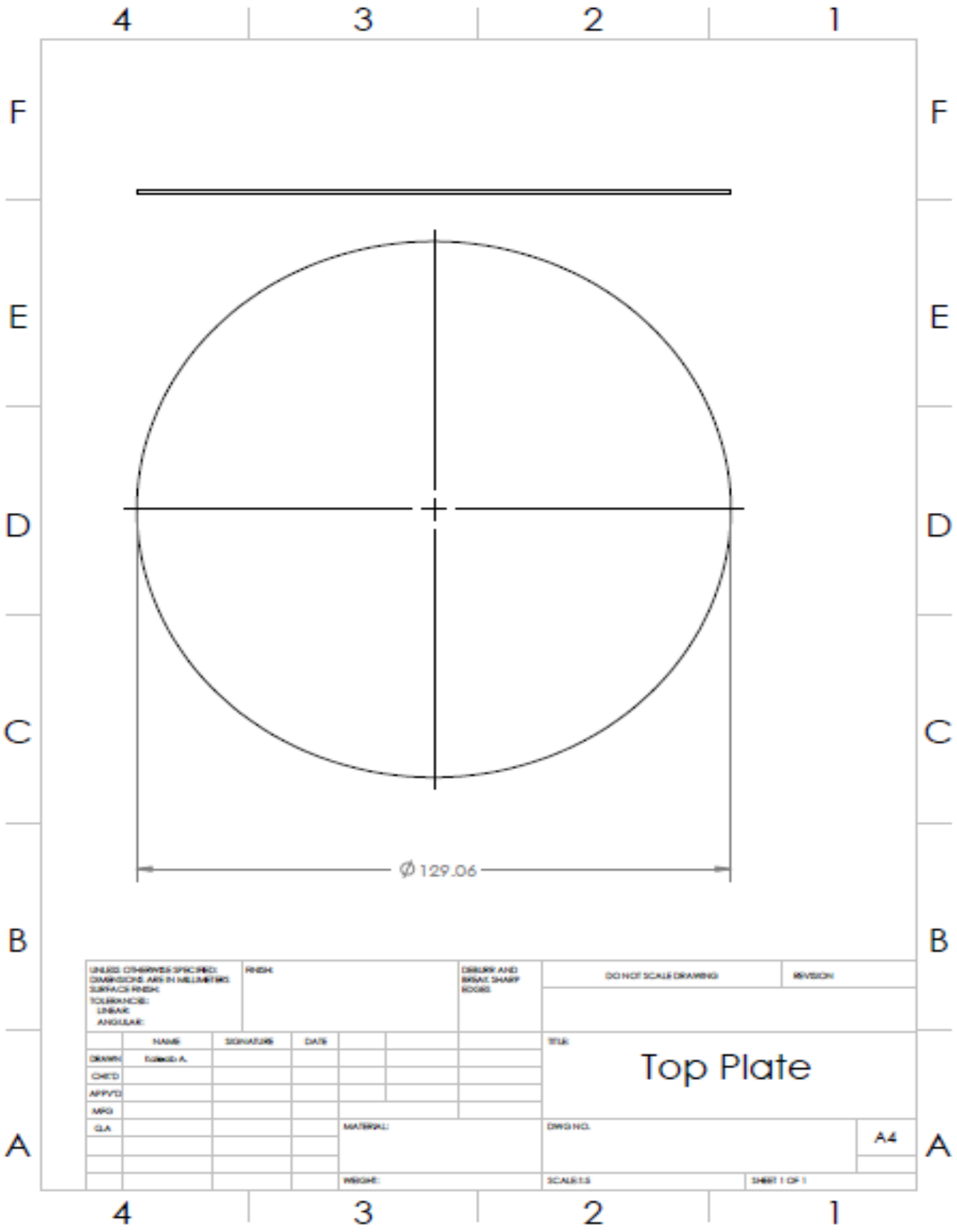
4
3
2
1
F
E
D
C
B
A
Ø 129.06
Top Plate
A4

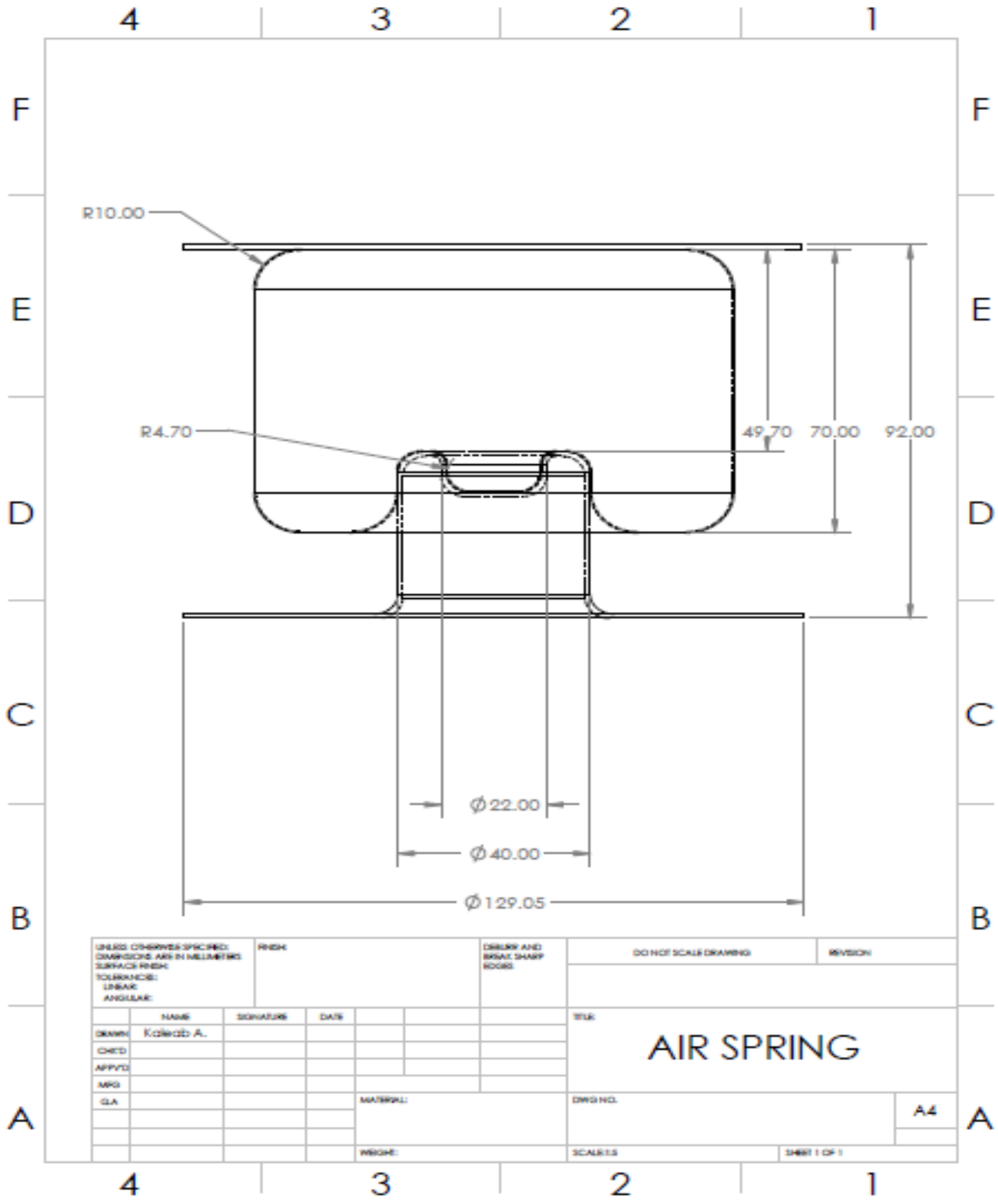
4
3
2
1
F
E
D
C
B
A
R10.00
R4.70
49.70
70.00
92.00
Ø22.00
Ø40.00
Ø129.05
DO NOT SCALE DRAWING
REVISION
Kolecab A.
AIR SPRING
A4

APPENDIX B: MICRO CONTROLLER ARDUINO CODE

```
const int echoPin = 2; // Echo Pin of Ultrasonic Sensor

const int pingPin = 3; // Trigger Pin of Ultrasonic Sensorvoid setup()

int motor =6;

int valvo;

#include <Servo.h>

Servo myservo;  // create servo object to control a servo

 // analog pin used to connect the potentiometer

int val;    // variable to read the value from the analog pin

//-----------------------------------------------------------------------------------------------------------

---

void setup(){

  myservo.attach(9);  // attaches the servo on pin 9 to the servo object

Serial.begin(9600); // Starting Serial Communication

pinMode(pingPin, OUTPUT); // initialising pin 3 as output

pinMode(echoPin, INPUT); // initialising pin 2 as input

pinMode(motor, OUTPUT);

}

//-----------------------------------------------------------------------------------------------------------

----------

void loop(){


long duration, inches, cm;digitalWrite(pingPin, LOW);

delayMicroseconds(2);digitalWrite(pingPin, HIGH);
```

```
delayMicroseconds(10);digitalWrite(pingPin, LOW);duration = pulseIn(echoPin, HIGH); // using pulsin function to determine total time


cm = microsecondsToCentimeters(duration); // calling methodSerial.print(inches);


int speedo=analogRead(A0)/20.46;


Serial.print(" pressure= ");
int pressure=analogRead(A1)/204.6;
Serial.print(pressure);
Serial.print("bar    ");
Serial.print("front car distance=");
Serial.print(cm );
Serial.print("cm, ");
Serial.print(" wheel speed=");
Serial.print(speedo);          // reads the value of the potentiometer (value between 0 and 1023)
Serial.print(" Kph");
if (speedo>40){digitalWrite(motor,LOW);
      if (cm>1000) {valvo=0; Serial.print("  STATUS= NO CRASH ");}
      else if (cm<1000&&cm>800){valvo=0;Serial.print("  STATUS= NO CRASH ");}
      else if (cm<800&&cm>612){valvo=45;Serial.print("  STATUS= CRASH ");}
      else if (cm<612&&cm>450){valvo=30;Serial.print("  STATUS= CRASH ");}
      else if (cm<450){valvo=20;Serial.print("  STATUS= CRASH ");}
   }
```

```
else if (speedo>30&&speedo<40){digitalWrite(motor,LOW);
      if (cm>1000) {valvo=0; Serial.print("  STATUS= NO CRASH ");}
      else if (cm<1000&&cm>800){valvo=0;Serial.print("  STATUS= NO CRASH ");}
      else if (cm<800&&cm>612){valvo=0;Serial.print("  STATUS= NO CRASH ");}
      else if (cm<612&&cm>450){valvo=0;Serial.print("  STATUS= NO CRASH ");}
      else if (cm<450&&cm>312){valvo=30;Serial.print("  STATUS= CRASH ");}
      else if (cm<312){valvo=20;Serial.print("  STATUS= CRASH ");}
    }
else if (speedo>20&&speedo<30){digitalWrite(motor,LOW);
      if (cm>1000) {valvo=0;Serial.print("  STATUS= NO CRASH ");}
      else if (cm<1000&&cm>800){valvo=0;Serial.print("  STATUS= NO CRASH ");}
      else if (cm<800&&cm>612){valvo=0;Serial.print("  STATUS= NO CRASH ");}
      else if (cm<612&&cm>450){valvo=0;Serial.print("  STATUS= NO CRASH ");}
      else if (cm<450&&cm>312){valvo=0;Serial.print("  STATUS= NO CRASH ");}
      else if (cm<312&&cm>200){valvo=10;Serial.print("  STATUS= CRASH ");}
      else if (cm<200){valvo=5;Serial.print("  STATUS= CRASH ");}
    }
else if (speedo>10&&speedo<20){digitalWrite(motor,LOW);
      if (cm>1000) {valvo=0;}
      else if (cm<1000&&cm>800){valvo=0;Serial.print("  STATUS= NO CRASH ");}
      else if (cm<800&&cm>612){valvo=0;Serial.print("  STATUS= NO CRASH ");}
      else if (cm<612&&cm>450){valvo=0;Serial.print("  STATUS= NO CRASH ");}
      else if (cm<450&&cm>312){valvo=0;Serial.print("  STATUS= NO CRASH ");}
      else if (cm<312&&cm>200){valvo=0;Serial.print("  STATUS= NO CRASH ");}
```

```
      else if (cm<200&&cm>112){valvo=7;Serial.print("  STATUS= CRASH ");}
      else if (cm<112){valvo=4.5;Serial.print("  STATUS= CRASH ");}
    }
else if (speedo>5&&speedo<10){digitalWrite(motor,LOW);
      if (cm>1000) {valvo=0;}
      else if (cm<1000&&cm>800){valvo=0;Serial.print("  STATUS= NO CRASH ");}
      else if (cm<800&&cm>612){valvo=0;Serial.print("  STATUS= NO CRASH ");}
      else if (cm<612&&cm>450){valvo=0;Serial.print("  STATUS= NO CRASH ");}
      else if (cm<450&&cm>312){valvo=0;Serial.print("  STATUS= NO CRASH ");}
      else if (cm<312&&cm>200){valvo=0;Serial.print("  STATUS= NO CRASH ");}
      else if (cm<200&&cm>112){valvo=0;Serial.print("  STATUS= NO CRASH ");}
      else if (cm<112&&cm>50){valvo=0;Serial.print("  STATUS= NO CRASH ");}
      else if (cm<50){valvo=4;Serial.print("  STATUS= CRASH ");}
    }
else if (speedo>0&&speedo<5){digitalWrite(motor,LOW);

       if (cm>1000) {valvo=0;}
       else if (cm<1000&&cm>800){valvo=0;Serial.print("  STATUS= NO CRASH ");}
       else if (cm<800&&cm>612){valvo=0;Serial.print("  STATUS= NO CRASH ");}
       else if (cm<612&&cm>450){valvo=0;Serial.print("  STATUS= NO CRASH ");}
       else if (cm<450&&cm>312){valvo=0;Serial.print("  STATUS= NO CRASH ");}
       else if (cm<200&&cm>112){valvo=0;Serial.print("  STATUS= NO CRASH ");}
       else if (cm<112&&cm>50){valvo=0;Serial.print("  STATUS= NO CRASH ");}
       else if (cm<50&&cm>12){valvo=0;Serial.print("  STATUS= NO CRASH ");}
```

```
      else if (cm<12){valvo=3;Serial.print("  STATUS= CRASH ");}
    }


else{ valvo=0;
if (pressure<3){
digitalWrite(motor,HIGH);
Serial.print(" compressor ON ");}
else digitalWrite(motor,LOW);


}


  valvo = map(valvo, 0, 50, 0, 180);     // scale it to use it with the servo (value between 0 and 180)
  Serial.print("    valve open ");
  Serial.print(valvo/1.8);
 Serial.println(" percent");
  myservo.write(valvo);                  // sets the servo position according to the scaled value


  //delay(15);


}long microsecondsToCentimeters(long microseconds) // method to covert microsec to centimeters
{
return microseconds / 29 / 2;
```

}

APPENDIX C: GRAPHS

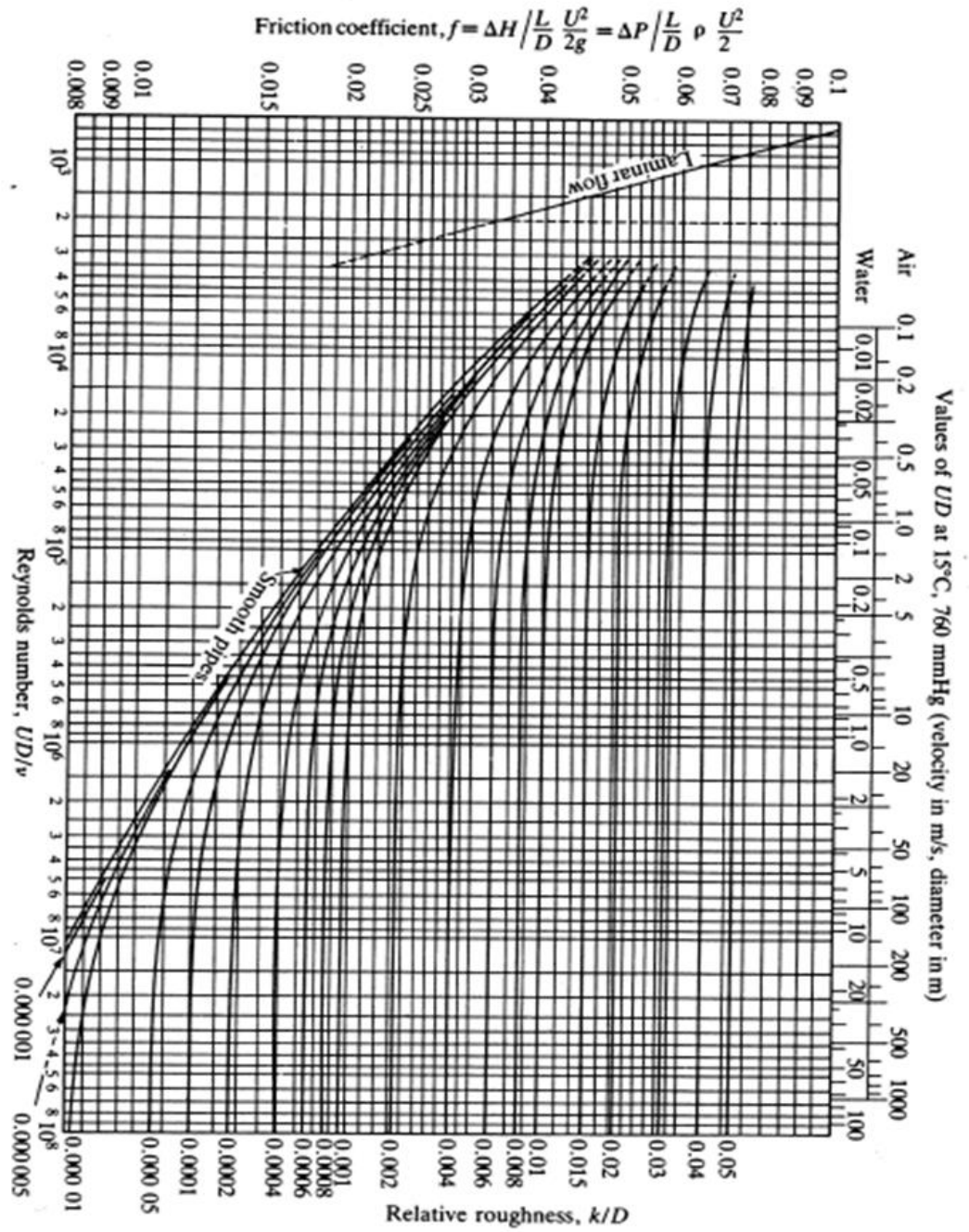

APPENDIX D: VEHICLE SPECIFICATION

DIMENTIONS & WEIGHT Overall length (mm) 4570 Overall width (mm) 1845 Overall height (mm) 1670 (1715 with roof rails) Wheelbase (mm) 2660 Tread Front/Rear (mm) 1570/1570 Ground clearance (mm) 176 Curb weight (kg) 1595-1630 (AT), 1465-1590 (MT), 1500-1615 (CVT) Gross vehicle weight (Kg) 2130 (AT), 2000-2100 (MT), 2050-2110 (CVT)	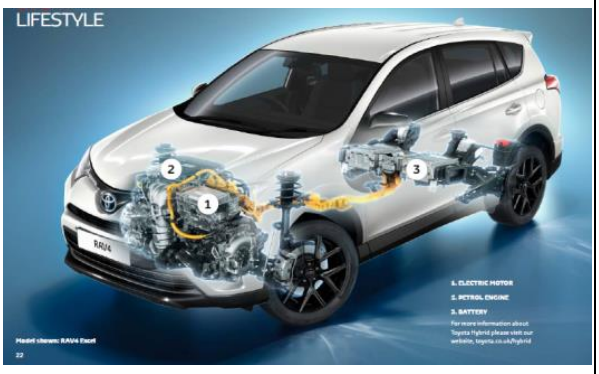
CHASSIS Suspension - Front MacPherson Suspension - Rear Double wishbone Brakes Front/Rear Ventilated disc/Solid disc Minimum turning radius (Tires) (m) 5.3 Fuel tank capacity (liters) 60 Tires 225/65R17H	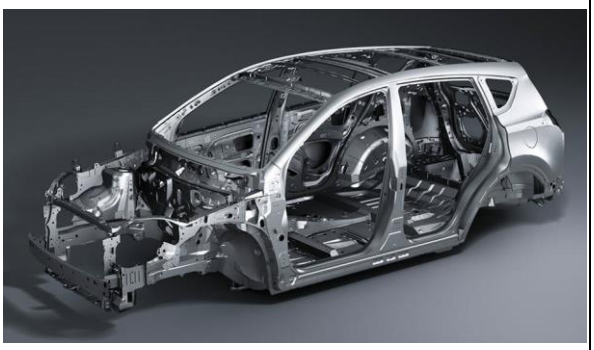

ENGINE Type 16-Valve DOHC with Dual VVT-i Piston displacement (cc) 2494 Max. Output (SAE net) kW/rpm 132/6000 Max. Torque (SAE net) Nm/rpm 233/4100 Fuel system SFI	

Widths shown do not include door mirrors.